

**MRI OF LEG MUSCLE IN WOMEN WITH AND WITHOUT
OSTEOPOROSIS**

**MAGNETIC RESONANCE IMAGING OF LEG MUSCLE
STRUCTURE AND COMPOSITION IN WOMEN WITH AND
WITHOUT OSTEOPOROSIS**

By AMANDA LORBERGS, BSC, MSC

A Thesis Submitted to the School of Graduate Studies
in Partial Fulfillment of the Requirements
for the Degree Doctor of Philosophy

McMaster University
© Copyright by Amanda Lorbergs, August 2014

DOCTOR OF PHILOSOPHY (2014)
(Rehabilitation Science)

McMaster University
Hamilton, Ontario, Canada

TITLE: Magnetic Resonance Imaging of Leg Muscle Structure and
Composition in Women With and Without Osteoporosis

AUTHOR: Amanda Līga Lorbergs, B.Sc. (University of Guelph),
M.Sc. (University of Saskatchewan)

SUPERVISOR: Norma J. MacIntyre, B.Sc. (PT), M.Sc., PhD

NUMBER OF PAGES: xvii, 196

ABSTRACT

Introduction: Bone loss, fractures, and declining physical performance are associated with muscle atrophy and fat infiltration. Muscle structure and composition differences may be apparent between women with and without osteoporosis (OP).

Purpose: To: 1) evaluate the effect of a time period spent in supine on magnetic resonance imaging (MRI) measures of muscle size and diffusion properties in young and older women; 2) assess the feasibility of applying three MRI scanning methods to evaluate macrostructural and microstructural properties of leg muscles in older women; and 3) compare musculoskeletal tissue structure and composition between older women with and without OP, and to determine the relationships between bone, muscle, fat, and physical performance.

Methods: Sixteen young and older women had their legs scanned with MRI at baseline and after 30 and 60 minutes of supine resting. Feasibility of recruitment, participant tolerance to scanning, and image acquisition and analysis protocols were assessed. Thirty-five moderately active, older women with and without OP underwent MRI and peripheral quantitative computed tomography scanning of the leg and performed physical performance tests.

Results: In young and older women, muscle size did not change with time spent supine, but water diffusivity decreased in some muscle regions. It is feasible to perform a single session of three MRI scanning techniques in older women. Women with and without OP had similar musculoskeletal structure that showed fat infiltration is associated with reduced bone strength and slower gait speed.

Conclusions: In young and older women, muscle size is unaffected by a period of supine rest, but time spent in supine may modify water diffusivity measures. It is feasible to use a combination of MRI scanning techniques to evaluate leg muscle structure in older women. MRI improves our understanding of the relationships among muscle, fat, bone, and physical performance.

DECLARATION OF ACADEMIC ACHIEVEMENT

This thesis is prepared as a “sandwich thesis”, which includes three individual projects described in separate manuscripts as prepared for peer-reviewed publication.

For all manuscripts Amanda Lorbergs determined the research questions, provided the overall study design, drafted and handled ethics submissions, spearheaded participant recruitment and scheduling, supervised and/or performed data collection, performed image analyses, conducted statistical analysis and interpretation, composed and submitted the manuscripts for peer-review.

For the first manuscript titled “*Age-related differences in the response of leg muscle cross-sectional area and water diffusivity measures to a period of supine rest*” Dr. Noseworthy developed the MRI image acquisition protocol, provided technical feedback pertaining to MRI acquisition and analysis, consulted on data analysis and interpretation, provided critical review of the manuscript, and approved the final draft. Dr. MacIntyre participated in the conception of the study, assisted with statistical analyses and interpretation, provided critical review of the manuscript, and approved the final draft.

For the second manuscript titled “*Feasibility of magnetic resonance imaging to evaluate leg muscle macrostructural and microstructural properties in older women*” Dr. Noseworthy developed the MRI image acquisition protocol, provided technical feedback pertaining to MRI acquisition and analysis, gave critical review of the manuscript, and

approved the final draft. Dr. MacIntyre participated in the conception of the study, assisted with the interpretation of results, provided critical review of the manuscript, and approved the final draft.

For the third manuscript titled “*Muscle and fat macrostructure and microstructure measured using magnetic resonance imaging are similar in healthy postmenopausal women with and without osteoporosis*” the candidate contacted physicians and obtained participant bone density test results. Dr. Noseworthy developed the MRI protocol, consulted on data analysis and interpretation, gave critical review of the manuscript, and approved the final draft. Prof. Stratford was involved in the conception of the study, consulted on statistical analysis, critically reviewed the manuscript, and approved the final draft. Dr. Holdsworth consulted on the conception of the study and reviewed the manuscript. Dr. Adachi facilitated participant recruitment through his osteoporosis clinic, critically reviewed the manuscript, and approved the final draft. Dr. MacIntyre was involved in the conception of the study, spearheaded funding acquisition, advised on statistical analysis, provided assistance with data interpretation, provided critical review of the manuscript, and approved the final draft.

ACKNOWLEDGEMENTS

The completion of my doctoral dissertation is a testament of the incredible amount of support that I have received from several individuals over the past four years.

First of all, I would like to thank my supervisor Dr. Norma MacIntyre for teaching me to remain positive, patient, and persistent even during academic turbulence. Norma, your willingness to let me explore my research interests was greatly appreciated. Moreover, your encouragement and detailed, constructive feedback kept me motivated to keep moving forward. I'd like to thank you for providing me a diversity of learning opportunities that have enriched my research interests and broadened my collegial network.

Thank you Dr. Michael Noseworthy for sharing your expertise and enthusiasm of medical imaging. Mike, your patience in facilitating my learning was instrumental for my research and I very much appreciated you welcoming me as a visiting student within your lab. Thank you to Prof. Paul Stratford for his timely, valuable, and concise feedback over the past four years. Paul, your positive outlook and statistical expertise are admirable and much appreciated.

Thank you to Dr. Rick Adachi, Dr. Karen Beattie, and all my bone scholar colleagues. Our monthly meetings stimulated thoughtful discussion, helped address research challenges, and were a tremendous source of mentorship over the past four years. Additionally, I'd like to thank Drs. Adachi and Lau for their assistance in recruiting participants from their clinic.

Access to imaging devices and individuals with technical expertise were critical throughout my doctoral research. A special thanks to Dr. Christopher Gordon for access to the pQCT scanner and to Norm Konyer who was always ready to help with MRI data acquisition and analysis. Thank you to all the MRI technologists and the grad students at the Imaging Research Centre for your willingness to explain and assist with aspects of data collection, analyses, and interpretation of engineering concepts in layman's terms.

The research would not have been possible without the generosity of Dr. Jean Wessel's grant from the Arthritis Society. I appreciate the financial support that I received from McMaster University, the Ontario Graduate Scholarship, the Ontario Women's Health Scholar Award, and the CIHR's Strategic Training Program in Musculoskeletal Health Research and Leadership the Joint Motion Program.

To my friends, colleagues, and mentors in the School of Rehabilitation Science: thank you for your unrelenting support. In particular, thanks to Kathryn Sinden who managed to keep my spirits high and never turned down the opportunity to chat over a cup of coffee or glass of beer. Kathryn, thank you for always being there for me and supporting me in my personal and academic endeavours over the past four years.

Kit, thank you for your love, patience, and sense of humour during this PhD journey. You have been there for me as I shed tears of frustration, joy, and exhaustion. Late at night when you would have rather been sleeping, you listened and provided feedback on my presentations. You are always willing to offer a non-judgmental, sympathetic ear and your constant encouragement instills confidence at times when I need it most. Thank you for everything and I hope that I can provide the same support for you as you finish up your PhD.

Finally, I would like to thank my family for their unconditional love, support, and generosity during my many years in school. In particular, thank you to my parents, Modris and Kristine, for always encouraging me to pursue all my goals and for reminding me to aim higher because my education can never be taken away from me. Thank you to my sisters, Aina and Andra, for your most sincere attempt to understand my life over the past few years and for your light-hearted laughter that would make me smile at times when I needed it most. Without all of you, I would not be who or where I am today.

TABLE OF CONTENTS

ABSTRACT	iii
DECLARATION OF ACADEMIC ACHIEVEMENT	v
ACKNOWLEDGEMENTS	vii
TABLE OF CONTENTS	ix
LIST OF FIGURES	xi
LIST OF TABLES	xiv
LIST OF COMMONLY USED ABBREVIATIONS and SYMBOLS	xvi
CHAPTER ONE	1
1.1 MUSCULOSKELETAL AGING	3
1.1.1 Characteristics of aging skeletal muscle.....	3
1.1.2 Characteristics of aging bone	4
1.2 CONDITIONS ASSOCIATED WITH MUSCULOSKELETAL AGING	6
1.2.1 Sarcopenia	6
1.2.2 Osteoporosis	7
1.3 THE MUSCLE-BONE UNIT	13
1.3.1 Fat and the muscle-bone unit.....	15
1.4 MUSCULOSKELETAL IMAGING	16
1.4.1 Dual energy X-ray absorptiometry	17
1.4.2 Computed tomography	18
1.4.3 Peripheral quantitative computed tomography.....	19
1.4.4 Magnetic resonance imaging.....	21
1.5 APPLICATION OF MRI TO EVALUATE LEG MUSCLE STRUCTURE IN WOMEN	27
1.6 SUMMARY OF THESIS OBJECTIVES	35
CHAPTER TWO	36
PREFACE TO CHAPTER TWO	37
2.1 ABSTRACT.....	39
2.2 INTRODUCTION	40
2.3 MATERIALS AND METHODS.....	42
2.4 RESULTS	48
2.5 DISCUSSION.....	56
2.6 ACKNOWLEDGEMENTS.....	63
2.7 REFERENCES	64

CHAPTER THREE	68
PREFACE TO CHAPTER THREE	69
3.1 ABSTRACT.....	71
3.2 INTRODUCTION	72
3.3 METHODS	75
3.4 RESULTS	82
3.5 DISCUSSION.....	89
3.7 ACKNOWLEDGEMENTS.....	98
3.8 REFERENCES	99
CHAPTER FOUR.....	104
PREFACE TO CHAPTER FOUR.....	105
4.1 ABSTRACT.....	107
4.2 INTRODUCTION	109
4.3 METHODS	113
4.4 RESULTS	124
4.5 DISCUSSION.....	135
4.6 ACKNOWLEDGEMENTS.....	143
4.7 REFERENCES	144
CHAPTER FIVE	153
5.1 SUMMARY OF THESIS RESULTS.....	153
5.2 CONTRIBUTIONS OF THE THESIS TO THE LITERATURE	155
5.3 POTENTIAL LIMITATIONS.....	159
5.4 SUMMARY.....	164
REFERENCES.....	165
APPENDIX A	182
APPENDIX B	183
APPENDIX C	190
APPENDIX D	193
APPENDIX E	194
APPENDIX F	195

LIST OF FIGURES

Figure 1.1: pQCT XCT2000 scanner and axial leg images. Standardized positioning for leg image acquisition in the pQCT scanner (A). Axial pQCT leg images at the tibia 4% (B), 14% (C), and 38% (D) sites illustrate bone size and shape at an in-plane resolution of 400 μ m. The colour scale on the left represents low (bottom, dark grey) to high (top, white) tissue volumetric densities (mg/cm³).20

Figure 1.2: Whole body 3T MRI system and axial images of the leg. A woman on the scan bed of the 3T MRI scanner is positioned for imaging with an extremity coil placed around her right leg (A). Axial images of the leg demonstrate how altered sequence parameters can increase the brightness of fat (B) and water (C).....23

Figure 1.3: Ellipsoid representation of a tensor and proposed directions of water molecule diffusion in skeletal muscle. On the left is a schematic arrangement of muscle fibres where orientation is generally similar but not all fibres are parallel, as highlighted by the red lines. On the right is a schematic of proposed diffusion directions characterized by eigenvalues. The largest eigenvalue (λ_1) is oriented along the long axis of a muscle fibre, whereas the second and third eigenvalues (λ_2 and λ_3) represent diffusivity perpendicular to the long axis of the muscle fibres or fascicles.....24

Figure 1.4: Schematic representation of the meaning of fractional anisotropy (FA) values. FA values scaling closer to zero, as illustrated on the left, represent a spherical shape since diffusion would be of the equal magnitude in all directions. Values approaching 1 represent the diffusion primarily in one direction, as in the hypothetical case of an infinitely long cylinder.26

Figure 2.1: Representative leg images from a woman aged 75 years. Proton density (PD) with PURE filter (a), PD water saturated (b), and PD fat saturated (c) axial images of the leg 66% site marked by a fiducial marker. Skeletal muscle and adipose tissue areas of the leg were segmented (d) in contrasting colors from the PD PURE-filtered image.....45

Figure 2.2: Axial image of the leg indicating diffusion tensor imaging regions of interest (ROIs). The analyzed ROIs are indicated by the colored pixels in the anatomical proton density (PD) weighted reference image.....48

Figure 2.3: Individual values for total leg muscle cross sectional area (CSA) plotted as a function of time. Muscle CSA (cm²) for young (A, n = 8) and older (B, n = 8) women at baseline (BL), 30-minute, and 60-minute time points50

Figure 2.4: Individual values for apparent diffusion coefficient (ADC) for leg muscles in young and older women plotted as a function of time. ADC ($\times 10^{-3}$ mm ² /s) for young (left column, n = 8) and older (right column, n = 8) women at baseline (BL), 30 and 60-minute time points for five muscle regions of interest.....	53
Figure 2.5: Individual values for fractional anisotropy (FA) for leg muscles in young and older women plotted as a function of time. FA for young (left column, n = 8) and older (right column, n = 8) women at baseline (BL), 30 and 60-minute time points for five muscle regions of interest	54
Figure 3.1: Sample diffusion tensor projection maps and proton density (PD) reference scan. The first (a), second (b), and third (c) eigenvalues, apparent diffusion coefficient (d), and fractional anisotropy (e) at the 66% site of the leg. The PD-weighted reference scan (f) is shown for the same individual.....	81
Figure 3.2: Flow chart demonstrating the number of individuals exposed, interested, and eligible for the study based on recruitment strategy. The number of volunteers excluded and the reasons for their exclusion are provided.	83
Figure 3.3: Representative axial leg images of a postmenopausal woman with and without the PURE filter application. Images without the PURE filter (a, c) and images with the filter (b, d) are presented as original (a, b) and segmented (c, d) scans. Misrepresentation of intramuscular fat (yellow) with muscle (blue) occurred as a result of signal intensity bands near the subcutaneous fat (c). The PURE post-processing filter applied to the axial PD images of the leg removed the bright signal that was falsely representing intramuscular fat (d).	87
Figure 3.4: Individual values for intramyocellular lipid (IMCL) content. Relative IMCL content was quantified with ¹ H-MRS in the tibialis anterior muscle of nine older women. The dotted horizontal line represents the mean value.	90
Figure 4.1: Representative proton density (PD) weighted images of the leg in a postmenopausal woman with osteoporosis (age = 65y, BMI = 29) before and after segmentation. Each PD image (A) was segmented (B). The tibialis anterior, soleus, and gastrocnemius muscles appear in orange, blue, and red, respectively. The intramuscular fat for each muscle is segmented in yellow, pink, and grey for the tibialis anterior, soleus, and gastrocnemius, respectively. Intermuscular fat (green) is located beneath the muscle fascial plane and surrounding muscle bellies or compartments. The arrow points to the fiducial marker used to visualize the 66% site.	120
Figure 4.2: Diffusion tensor imaging muscle regions of interest (ROIs) and representative projection maps. Muscle ROIs are drawn on the axial proton density reference image of the leg of a woman with osteoporosis (A). Sample fractional anisotropy (B)	

and apparent diffusion coefficient (C) projection maps. The arrow is pointing to the fiducial marker that identified the 66% site of the tibia.....	122
Figure 4.3: Mean values for the apparent diffusion coefficient (ADC) and fractional anisotropy (FA) in leg muscle regions of women with and without osteoporosis. Mean (black dots) and 95% confidence intervals (bars) for (A) ADC and (B) FA in the leg muscles of 35 postmenopausal women with and without osteoporosis.....	130
Figure 4.4: The relationship between tibialis anterior intramyocellular lipid content (mmol/kg ww) and the bone strength index at the 4% tibial site in postmenopausal women (n = 29).....	133
Figure Appendix D1: ¹ H-MRS spectra acquisition screen image.....	193
Figure Appendix D2: Representative spectra fitting using LCModel software	193
Figure Appendix E1: Flow chart demonstrating the number of individuals screened and enrolled for the study.	195

LIST OF TABLES

Table 1.1: WHO thresholds guiding clinical diagnosis of osteopenia and osteoporosis	8
Table 1.2: Advantages and disadvantages of employing DXA as a clinical and research imaging tool	18
Table 1.3: Signal intensities of musculoskeletal tissues on T1- and T2-weighted images	22
Table 1.4: Description of study designs, study population characteristics, and magnetic resonance imaging acquisition methods	30
Table 1.5: Description of primary objectives, muscle and fat measures, and results of studies measuring leg muscle in women with magnetic resonance imaging (MRI)..	31
Table 2.1: Participant descriptive characteristics.....	49
Table 2.2: Fractional anisotropy (FA) and apparent diffusion coefficient (ADC, $\times 10^{-3}$ mm ² /s) represented at three time points (baseline, 30 minutes , 60 minutes) of supine lying for five leg muscle regions of interest (ROIs) for the groups of young and older women. All measures are presented as mean (SD).....	51
Table 2.3: Eigenvalues ($\times 10^{-3}$ mm ² /s) represented at three time points (baseline, 30 minutes, 60 minutes) of supine lying for five leg muscle regions of interest for the groups of young and older women. All measures are presented as mean (SD).....	55
Table 3.1: Participant characteristics (N = 9)	84
Table 3.2: Variability in proton density imaging, diffusion tensor imaging, and proton magnetic resonance spectroscopy muscle and fat outcomes in the leg muscle regions of interest (ROIs). All values presented as mean (SD) with 95% confidence interval (CI).....	88
Table 3.3: Examples of sample size calculations for prospective studies to determine the effect of increased physical activity level on leg muscle structure using the apparent diffusion coefficient (ADC) in older women.....	95
Table 4.1: Descriptive statistics of women with and without osteoporosis*	125
Table 4.2: pQCT bone and muscle outcomes for the total sample and groups of women with and without osteoporosis, presented as mean (SD). Bone area and content and muscle cross-sectional area measures are adjusted for tibia length	127

Table 4.3: MRI derived muscle and fat volumes normalized to tibia length for the total sample and groups of women with and without osteoporosis, presented as mean (SD)	128
Table 4.4: Microstructural measures of muscle and intramyocellular lipid (IMCL) content of the leg muscle regions of interest (ROIs) for the total sample and groups of women with and without osteoporosis, presented as mean (SD).....	129
Table 4.5: Correlation coefficients for bone structure and strength outcomes with individual muscle volumes in postmenopausal women with and without osteoporosis (n = 35). Pearson correlation coefficients equal to or greater than 0.4 are presented with their 95% confidence intervals	132
Table 4.6: Mean (SD) self-reported physical activity levels and performance-based physical performance for the total sample and groups of women with and without osteoporosis.....	134
Table Appendix C1. Correlations between measures of leg muscle and fat macrostructure with bone structure and strength adjusted for tibia length in postmenopausal women with and without osteoporosis (n = 35).....	190
Table Appendix C2. Correlations between muscle and fat microstructure and bone structure and strength adjusted for tibia length in postmenopausal women with and without osteoporosis (n = 35)	191
Table Appendix C3. Correlations between muscle and fat macrostructure and microstructure and measures of physical performance and self-reported physical activity levels in postmenopausal women with and without osteoporosis (n = 35).	192
Table Appendix E1: Reliability of Fractional Anisotropy	194
Table Appendix E2: Reliability of muscle cross-sectional area	194

LIST OF COMMONLY USED ABBREVIATIONS and SYMBOLS

30-CST	30 Second Chair Stand Test
95% CI	95% Confidence Interval
λ	Eigenvalue
AAS	Adjusted Activity Score
aBMD	Areal bone mineral density
ADC	Apparent diffusion coefficient
BMD	Bone mineral density
BMI	Body mass index
BSI	Bone Strength Index
CSA	Cross-sectional area
CoA	Cortical area
CoC	Cortical content
CoD	Cortical density
DTI	Diffusion tensor imaging
DXA	Dual energy X-ray absorptiometry
EDL	Extensor digitorum longus
EHL	Extensor hallicus longus
EMCL	Extramyocellular lipid
FA	Fractional anisotropy
FOV	Field of view
FWHM	Full width half maximum
GC	Gastrocnemius
¹ H-MRS	Proton magnetic resonance spectroscopy
HAP	Human Activity Profile
HU	Hounsfield units
ICC	Intraclass correlation coefficient
IMAT	Intermuscular adipose tissue
IMCL	Intramyocellular lipid
IMF	Intermuscular fat
LG	Lateral head of gastrocnemius
MAS	Maximum Activity Score
MG	Medial head of gastrocnemius
MRI	Magnetic resonance imaging
pQCT	Peripheral quantitative computed tomography
QCT	Quantitative computed tomography
RAPA	Rapid Assessment of Physical Activity

RF	Radiofrequency
ROI	Region of interest
SD	Standard deviation
SOL	Soleus
SNR	Signal to noise ratio
SSI	Strength Strain Index
T1	Longitudinal relaxation time
T2	Transverse relaxation time
T2D	Type 2 diabetes
TE	Echo time
TibA	Tibialis anterior
TibP	Tibialis posterior
ToA	Total bone area
ToC	Total bone content
ToD	Total bone density
TR	Transverse relaxation time
TrA	Trabecular bone area
TrC	Trabecular bone content
TrD	Trabecular bone density
vBMD	Volumetric bone mineral density
WHO	World Health Organization

CHAPTER ONE

INTRODUCTION TO THE THESIS

The overall goal of this doctoral thesis has been to determine whether women with and without osteoporosis exhibit differences in leg muscle structure and composition, as measured by advanced magnetic resonance imaging (MRI) scanning methods.

As a component of the candidate's PhD degree requirements in the School of Rehabilitation Science at McMaster University, this sandwich thesis consists of an introductory chapter, three interrelated manuscripts, and a general discussion. The introduction (Chapter One) provides the background to the thesis and introduces the reader to: characteristics of the healthy and pathologic aging musculoskeletal system, interrelationships between musculoskeletal tissues, pharmacologic and non-pharmacologic treatment strategies for osteoporosis, and medical imaging techniques for measuring musculoskeletal structure and composition. Furthermore, the introduction reviews literature describing the application of MRI methods to evaluate leg muscle structure and composition in women and presents the purpose of the thesis and specific objectives underpinning the design and conduct of each thesis study. Each study is presented as an independent chapter in manuscript format compliant with instructions for submission to target peer review journals. Chapters Two and Three describe protocol development and feasibility assessment, respectively. Chapter Four describes the final cross-sectional observational study of postmenopausal women in which the MRI-based

musculoskeletal outcomes, bone outcomes, and physical performance outcomes are assessed. The final chapter (Chapter Five) summarizes the extent to which the thesis study results address the goal to determine whether women with and without osteoporosis exhibit differences in skeletal muscle structure and composition. The scientific contribution and future research directions based on the findings are highlighted in the final chapter.

1.1 MUSCULOSKELETAL AGING

The aging process is associated with progressive decline in muscle mass and bone mineral density, and concomitant increases in fat mass. These changes may lead to musculoskeletal conditions that predispose older adults to mobility impairments, falls, fractures, and frailty. To mitigate the increasing public health burden of musculoskeletal conditions, prevention and rehabilitation strategies require a greater understanding of their determinants. This section describes characteristics of aging skeletal muscle and bone, with an emphasis on the lower extremity and the effect of female hormone changes accompanying the menopausal transition.

1.1.1 Characteristics of aging skeletal muscle

Muscle function is an important predictor of mobility, independence, hospitalization, and mortality [1-3]. Age-related declines in physical function are attributed to both macrostructural (e.g., muscle mass) and microstructural (e.g., fibre size) changes in skeletal muscle. Reduced muscle mass is the most noticeable and unavoidable consequence of the aging process [4]. Muscle mass begins to decrease in mid-adulthood, however it generally becomes noticeable in women around the time of menopause [5]. After menopause, the involuntary loss of muscle mass is approximately 0.6% annually [6]. As muscle mass is lost, muscle weakness ensues [1]; however, the two processes have different trajectories. In adults aged over 70y, muscle weakness occurs at a faster rate than the rate of loss of muscle mass [7] and both decline more rapidly in the lower extremities than in the upper extremities [8]. The mechanism of muscle strength loss is complex. Muscle strength is an independent predictor of mobility impairments, which is

evident in women as young as 55y of age [1, 8]. Although muscle macrostructure, measured as cross-sectional area (CSA), density, and volume, are considered adequate surrogates of muscle force [9-13], there are several microstructural alterations in skeletal muscle that also contribute to the age-related decline in physical performance.

Several characteristics of muscle microstructure are considered to be important determinants of physical functioning. A large body of research has characterized muscle fibre changes with aging using histological staining techniques from biopsy specimens. In general, aged muscle has fewer total numbers of fibres and motor units [14, 15]. While type I (i.e., slow-twitch) fibre size remains unchanged, the overall proportion of type I fibres increases with age [16, 17]. Conversely, type II (i.e., fast-twitch) fibre area is reduced and fibre atrophy becomes evident in type II fibres [16, 17]. As muscle fibre size, number, and activation is reduced, there is a gradual infiltration of non-contractile tissue within skeletal muscle. The non-contractile tissue in aging muscle is typically characterized as fat or fascia that reduces the proportion of contractile tissue available for activation by alpha motoneurons. This reduces the magnitude of force produced by activated muscles [18]. An accumulation of fat within and around muscle fibres adversely affects metabolism and physical function, evidenced by poor insulin sensitivity, slower gait speed, and longer stair ascent and descent times [19-21].

1.1.2 Characteristics of aging bone

Bone turnover in adulthood is attributed to remodeling. Beginning at the age of 40y, bone formation by osteoblasts and resorption by osteoclasts becomes progressively imbalanced as the reduction in osteoblast vitality exceeds that of the osteoclasts. A net

loss of bone mass and density is a normal consequence of aging. The rate of bone loss in women is accelerated due to cessation of menstruation and decline in ovarian hormone production, or menopause, around the age of 51y. During the ten-year menopausal transition women can lose 2.5 to 3% of their bone mass annually [22, 23]. After the menopausal transition, women and men lose bone mass at a similar rate, but women never recover bone lost during menopause and a significant deficit in bone mass persists thereafter. Thus, women can lose up to 25% of their total bone mineral between the onset of menopause and the age of 75y [24].

In the absence of estrogen, the rate of bone remodeling is accelerated by the increased recruitment and activation of osteoclasts [25]. Both trabecular and cortical bone compartments are affected by estrogen depletion, but trabecular bone has a larger metabolically active surface area and, consequently, greater bone loss is observed in that bone compartment. The trabecular bone compartment loses mineral mass and density due to thinning of bone plates and rods comprising the trabecular network and increased perforations enlarge marrow pore sizes after menopause [26]. Cortical bone also becomes increasingly porous [27, 28] and sustains a significant amount of resorption on the endosteal surface [29] described as trabecularization. Since bone strength is a product of mineral density, size, and mineral content, an increased amount of periosteal apposition in the long bone of the skeleton of postmenopausal women increases the bone size to preserve its strength [29]. Reductions in bone mineral density (BMD), which primarily occur within the perimenopausal years, are reported to be of similar magnitude in the upper and lower extremities [27, 30, 31]. Thus, reduced BMD, cortical thinning,

and compromised microarchitecture associated with the menopausal transition are major contributing factors to bone fragility and fracture.

1.2 CONDITIONS ASSOCIATED WITH MUSCULOSKELETAL AGING

1.2.1 Sarcopenia

Irwin Rosenberg is credited with coining the term “sarcopenia” from the Greek meaning “poverty of flesh” [32]. Based on a recent international consensus, the definition of sarcopenia has evolved and is defined as “the age-associated loss of skeletal muscle mass and function. Sarcopenia is a complex syndrome that is associated with muscle mass loss alone or in conjunction with increased fat mass” [33]. While sarcopenia is an inevitable consequence of aging, it lacks standardized assessment methods and a clinically accepted clinical definition. According to the International Working Group on Sarcopenia, older adults should be evaluated for sarcopenia if they present with: obvious declines in physical performance (i.e., mobility difficulty, strength loss), recurrent falls, unintentional weight loss of >5%, recent hospitalization or extended immobilization, or chronic conditions associated with muscle loss (e.g., Type II diabetes (T2D), chronic heart failure, chronic kidney disease) [33].

The etiology of sarcopenia is attributed to muscle atrophy and the loss of Type II muscle fibres [34]. The decline in muscle function associated with sarcopenia is attributed to structural changes in muscle associated with age-related atrophy. With aging, functional deficits are associated with reduced recruitment and activation of motor units, reduced insulin sensitivity, and dysfunctional mitochondria [33, 35, 36]. Reduced

levels of physical activity contribute to muscle atrophy and the concomitant reduction in muscle quality due to the infiltration of fat and other connective tissue [37]. Several systemic and local factors are also recognized for their influence on the sarcopenic muscle phenotype, including oxidative stress, reduced endocrine function, and inflammation [38]. Common components among criteria employed to diagnose sarcopenia include the ratio of low appendicular fat-free lean mass to height squared and a gait speed of less than 1m/s [33]. It is worth noting that the prevalence of sarcopenia varies greatly depending on the diagnostic criteria applied. Using the fat-free lean mass ratio definition above, the prevalence of sarcopenia is largely underestimated [39]. Still, based on this definition, sarcopenia affects as many as 30% of all adults aged over 60y and 50% of adults over 80y [40]. The costs associated with sarcopenia are remarkable. In the United States \$18.5 billion in healthcare expenditures was spent on sarcopenia in 2000 [41]. As the number and proportion of older adults continues to rise, the estimated direct healthcare costs attributable to sarcopenia will also increase substantially.

1.2.2 Osteoporosis

Osteoporosis (OP) is defined as a systemic skeletal disorder that is characterized by low bone mass and deterioration of bone microarchitecture that increases one's risk of fracture [42]. The clinical diagnosis of OP is based on areal BMD (aBMD) measurement performed using dual energy X-ray absorptiometry (DXA). In 2002, the WHO defined BMD thresholds by which an individual's bone status could be classified. Normal bone mass, low bone mass (i.e., osteopenia), and pathological bone loss (i.e., OP) are defined based on standard deviation score (T-score) determined for aBMD measured at the hip

and spine as compared to aBMD values for healthy gender-matched young adults [43].

Table 1.1 presents the WHO BMD T-score thresholds for clinical diagnosis of bone health. In Canada, an individual's 10-year absolute fracture risk is estimated based on the BMD results at the femoral neck in combination with sex, age and clinical risk factors [44]. Based on the WHO definition, 1.4 million Canadians have OP and the majority are women over the age of 65y [45].

Table 1.1: WHO thresholds guiding clinical diagnosis of osteopenia and osteoporosis

STATUS	T-SCORE
Normal	> -1.0
Osteopenia	Between -1.0 and -2.5
Osteoporosis	< -2.5
Severe (established) osteoporosis	≤ -2.5 + fragility fracture

Women are more likely to develop OP than men because men gain more bone mass during puberty and lose less during aging since they do not experience the rapid loss associated with perimenopause and the abrupt loss of estrogen. The most serious consequence of OP is a fragility fracture. Fracture risk is greater for women than men, with predicted incidences at 1 in 3 and 1 in 5, respectively [45]. The most common fragility fracture sites are the hip, spine, and wrist [46]. Of these fragility fracture sites, hip fractures are the most debilitating whereas fractures at the distal radius and vertebrae are most common [45]. The distal radius and vertebra are predominantly trabecular bone sites and thus the incidence of fracture at these sites coincides with the rapid loss of bone

mineral attributed to the early perimenopausal transition [26, 47]. Vertebral fractures are especially critical to identify clinically because they are the hallmark of OP and predict future fragility fractures, including hip fractures [48]. Depending on fracture site and severity, the consequences of osteoporotic fracture include pain, mobility impairments, poor quality of life, and mortality [49, 50]. Fractures also contribute to an enormous economic burden. In Canada, it is estimated that acute healthcare costs associated with osteoporotic fractures are \$1.2 billion annually, yet this estimate rises to nearly \$4 billion when outpatient treatment, prescriptions, and long-term care costs are included [51].

1.2.2.1 Non-pharmacologic treatment of osteoporosis

The specific treatment approach for individuals with OP is dependent largely upon the nature of the decrease in BMD and the presence of clinical risk factors. Non-pharmacologic treatment options are generally viewed as healthy lifestyle habits that can mitigate BMD decline and help prevent fragility fractures. The 2010 Canadian Clinical Practice Guidelines for OP recommend that all adults aged 50y and older have an adequate daily intake of calcium (1200 mg) and vitamin D (800–2000 IU), regularly engage in active weight-bearing exercise, and partake in fall-prevention strategies [52].

Combined calcium and vitamin D are known to have a protective effect on bone aBMD [53]. A meta-analysis suggested that there is an 18% decrease in the relative risk of non-vertebral fracture associated with calcium and vitamin D supplementation [54]. In adults aged over 65y, vitamin D deficiency is associated with increased fat infiltration in thigh muscles, impaired balance, and slower gait [55]. A minimum of 800 IU/day of

vitamin D has been shown to significantly improve body sway and lower extremity strength, thus decreasing the likelihood of falls [56].

Physical activity and exercise are also recommended for preventing bone loss, falls, and fractures [45, 52, 57]. Weight-bearing exercise results in modest improvements for BMD at the spine [58] and cortical bone geometry at the tibia [59]. Based on the Grading of Recommendations Assessment, Development, and Evaluation method, an international consensus process recently published a statement that strongly recommends that individuals with OP engage in a multicomponent exercise program that includes resistance training in combination with balance training [57]. Thus, in addition to mechanical benefits of weight-bearing on bone remodeling, combination exercise programs focus on muscle strengthening and balance exercises to reduce the likelihood of falls [60]. Since bone tissue is less responsive to mechanical stimuli with advancing age, the goal of exercise is to slow the loss of bone [61]. A potential explanation for the lack of efficacy of exercises aiming to increase bone strength in postmenopausal women with OP may be impairment at the level of the muscle which prevents the generation of dynamic bone strains above the critical threshold for maintaining bone strength.

1.2.2.2 Pharmacologic treatment of osteoporosis

The clinical practice guidelines indicate that individuals with OP or high fracture risk are candidates for pharmacological treatment to improve bone resistance to fracture [52]. The drug therapies for OP are classified as either anti-resorptive or anabolic, depending on their mechanism of action. From there, they are categorized into four classes: bisphosphonates, Selective Estrogen Receptor Modulators (SERMs), parathyroid

hormone (PTH), and denosumab. Parathyroid hormone therapy is the only anabolic pharmacologic treatment currently approved for clinical use in North America. Very little evidence is available that directly compares treatments in trials, and there are no direct comparisons available with fracture incidence as primary outcome. As such, identifying the ‘best-choice treatment’ for an individual depends on indirect drug comparisons and a variety of factors such as drug characteristics, patient medical history, and individual preferences. Individual preferences are critical, since poor patient adherence to osteoporosis drugs limits treatment efficacy [62] and results in an increased incidence of osteoporotic fractures [63].

Bisphosphonates are synthetic compounds that have a high affinity for bone mineral that permits binding to skeletal surfaces at active remodeling sites. As bisphosphonates become embedded in the bone surface they generate metabolites that inhibit mature osteoclast activity and induce osteoclast apoptosis, thereby effectively reducing the rate of bone turnover within three to six months of initiating treatment [64, 65]. Bisphosphonates preserve, but do not rebuild, trabecular and cortical architecture and are thought to reduce the rate of osteocyte apoptosis [64, 65]. Bone balance remains positive over long-term bisphosphonate use because the compounds remain embedded in bone for several years, with some studies observing positive results up to a decade following introduction of therapy [66, 67]. There are four bisphosphonates currently approved for use in Canada: alendronate (Fosamax®), etidronate (Didrocal®), risedronate (Actonel®) and zoledronate (Aclasta®). Daily doses of alendronate [68], risedronate

[69], and zoledronate [70] reduce the risk of hip fracture. All four bisphosphonates increase BMD and reduce the risk of vertebral fractures by 35 to 65% [68, 70-72].

Raloxifene (Evista®) is an estrogen agonist/antagonist from a family of non-hormonal drugs called SERMs. SERMs bind with estrogen receptors to activate estrogen pathways in some tissues, including bones, while blocking pathways in others, including breast tissue [73]. No effect of raloxifene is documented for reducing the incidence of hip and non-vertebral fractures [74]. Raloxifene is a potent anti-resorptive agent prescribed for postmenopausal women with low BMD specifically for preventing vertebral fractures [75].

Women at high risk for osteoporotic fractures or who demonstrate suboptimal response to previous anti-resorptive agents are good candidates for PTH. Teriparatide (Forteo®) is the biochemically-synthesized form of the intact human PTH molecule. In contrast to all other anti-osteoporosis drugs, Teriparatide is the only anabolic bone therapy approved by Health Canada. Teriparatide increases aBMD, restores trabecular connectivity and increases cortical thickness by activating osteoblasts to secrete new bone [65, 76-78]. As a monotherapy and in combination with anti-resorptives, vertebral and non-vertebral fracture risk is reduced in postmenopausal women taking Teriparatide [79, 80].

Denosumab (Prolia®) is the newest class of osteoporosis treatments approved by Health Canada. It is a fully human monoclonal antibody that is a potent inhibitor of bone resorption. Denosumab binds to receptor activator of nuclear factors K-B ligand (RANKL) to prevent binding to its receptor RANK on immature osteoclasts, thereby

inhibiting their proliferation, maturation, activation, and survival [81]. In postmenopausal women, denosumab injected twice annually reduces the risk of hip, vertebral, and non-vertebral fractures [82, 83]; however, bone turnover levels return to baseline nine months after treatment cessation and aBMD gains from therapy are diminished shortly thereafter [84, 85].

1.3 THE MUSCLE-BONE UNIT

The potential benefits of preventing the onset and consequences of musculoskeletal conditions associated with aging are significant. Thus, there is considerable interest in understanding the relationship between skeletal muscle loss and bone loss. A vast body of literature has investigated the interactions between the tissues using numerous measurement techniques. The evidence suggests that muscle and bone are intricately related through mechanical, biochemical, and genetic factors. To-date, there are two prevailing theories that attempt to explain the coordinated structural adaptations of muscle and bone.

The Mechanostat is the most established and widely recognized theory for explaining the adaptations of bone mass and architecture to mechanical loading [86]. The fundamental assumption of Frost's Mechanostat theory is that mechanical factors dominate the mechanisms that control bone mass in individuals with 'normal' health status, and that bone mass in persons of 'normal' status are only minimally influenced by non-mechanical factors such as hormones and nutrition. Further, Frost proposed that bone tissue maintains strain levels within an acceptable range using a regulatory feedback

loop that controls communication between bone mass and tissue strain [86]. Support for the Mechanostat theory is evident in athletes who demonstrate dramatic bone structure and strength adaptations in response to sport-specific loading characteristics [87, 88]. The osteogenic effect of mechanical factors is affected by, but not limited to, factors such as the magnitude, rate, and distribution of strains [65, 89]. Conversely, in instances of bed-rest immobilization where musculoskeletal forces are reduced there is diminished bone structure, microarchitecture and strength [90, 91]. The important role of muscle contractions is documented in studies that have showed that resistance training in healthy adults can mitigate bone loss during immobilization and recover bone lost after immobilization [92, 93].

The second theory of bone and muscle interactions extends beyond the mechanical response and suggests a role for molecular signaling and crosstalk between muscle and bone tissues. The finding of a positive influence of muscle on bone healing in the absence of contractile muscle forces [94, 95] led to the identification of several cytokines, which influence the action of cells in an autocrine, paracrine, and endocrine manner. When produced by muscle cells, cytokines are called myokines. Myokines such as insulin-like growth factor-1 and basic fibroblast growth factor are highly expressed with muscle contractions and bind to receptor proteins on the periosteal bone surface [96, 97]. On the other hand, myostatin is a negative regulator of muscle growth and has a direct effect on bone metabolism. Myostatin expression and secretion in muscle is stimulated by glucocorticoids, which contribute to muscle atrophy and inhibit bone formation [98, 99]. Thus, depending on the state of muscle activity, (i.e., hypertrophy,

injury, disuse) myokines can have an anabolic or catabolic effect on bone metabolism [99, 100].

1.3.1 Fat and the muscle-bone unit

The relationship between fat and muscle and bone is complex, yet understanding the associations between the tissues is a growing concern given the increasing prevalence of obesity and growing proportion of older adults in whom fat impairs muscle metabolism, bone formation, and physical functioning [101, 102]. Bone, muscle, and fat are derived from the same mesenchymal stem cells (MSCs) whose differentiation is partly influenced by environmental conditions. For instance, the increased adiposity observed in postmenopausal women is attributed, in part, to estrogen, which promotes MSC differentiation into osteoblasts rather than adipocytes [103].

The spatial distribution of adipose tissue storage has important structural and biochemical implications for neighbouring bone and muscle. In the extremities, subcutaneous fat is associated with metabolic syndrome [104]. Ectopic fat, which is fat deposited in locations that are predominantly not associated with fat storage (e.g., within or around organs, skeletal muscle), is more harmful than subcutaneous fat [102]. With aging, subcutaneous fat is increasingly redistributed as ectopic fat and poses significant health burdens for individuals and healthcare systems [3, 105]. With respect to fat accumulated in and around skeletal muscle, negative health outcomes include muscle weakness, mobility limitations, and increased risk of hip fracture [1, 20, 106-108]. This has fostered an interest in distinguishing fat situated within muscles from fat that is situated between muscles and muscle compartments. It is hypothesized that effects of

these fat depots may have implications for mobility, bone adaptation, and muscle metabolism [109]. Intramuscular fat, defined as the fat located within muscle and external to the muscle cells, increases with advancing age and inactivity and is associated with poor physical performance [21, 110-113]. On the other hand, intermuscular fat is the fat situated within the fascial envelopes surrounding muscles and muscle compartments. Intermuscular fat is associated with adverse metabolic effects and poor muscle strength that contribute to an increased risk of mobility limitations [20, 114, 115]. Despite the consequences of intramuscular and intermuscular fat on muscle force production and physical performance, there is a paucity of literature describing the effect of spatial distribution of ectopic fat in skeletal muscle on bone structure and strength.

1.4 MUSCULOSKELETAL IMAGING

Non-invasive assessment of musculoskeletal tissues *in vivo* is achieved using a broad range of medical imaging devices. The most appropriate imaging device to use to answer a clinical or research question depends on a number of factors, such as access to the technology and expertise related to image acquisition and analysis, characteristics of the population and anatomic site of interest, and the desired level of structural detail or image resolution. Moreover, the potential risks to the patient, feasibility of image acquisition and analysis protocols, and the relative importance of its measurements to clinical risk factors and health outcomes also should be considered. Four medical imaging modalities are frequently discussed within this thesis. This section introduces

each of these non-invasive imaging techniques and discusses their noteworthy advantages and limitations.

1.4.1 Dual energy X-ray absorptiometry

Dual energy X-ray absorptiometry (DXA) is a widely available imaging tool for quantifying aBMD. Image acquisition with DXA involves passing two photon energies through the body, from which radiologically distinct materials (e.g., bone mineral and soft tissue; lean tissue and fat) are separated based on the energy attenuation. From an assessment of the total projected area of the bone under investigation, aBMD is calculated as the ratio of bone mineral content (BMC, or mass of mineral) to unit projected area (g/cm^2) with minimal radiation exposure to the patient (0.5-5 μSv) [116]. Commercially available DXA software enables skeletal assessment of the whole body, as well as hip, spine, and forearm regions independently. Identification and quantification of vertebral fractures and their severity is also possible with DXA [117]. Precision of DXA BMD measures is excellent and coefficients of variation are typically reported between 1 and 1.5% at the hip and spine [118]. As presented in Table 1.2, there are several advantages to DXA that has popularized its clinical and research application worldwide. Despite its application to the WHO osteoporosis definition and absolute fracture risk algorithm (FRAX), an inherent limitation of DXA is its planar image projection. This is a significant disadvantage of the device, since it precludes any adjustment or interpretation for bone size or shape and quantification of volumetric BMD.

Table 1.2: Advantages and disadvantages of employing DXA as a clinical and research imaging tool

Advantages	Disadvantages
Widely available	Software assumes homogenous soft tissue distribution
Quick and easy patient positioning; Short scan time; Low radiation exposure	Degenerative diseases affect BMD measurements at spine
Good precision; Reliable reference ranges	BMD and T-scores only interpreted in terms of osteoporosis
BMD predicts fracture risk	Fracture and non-fracture population curves overlap
Effectively monitors treatment response	Unable to monitor bone size or structure changes

1.4.2 Computed tomography

Computed tomography (CT) acquires anatomical images by capturing X-rays emitted from a rotating source and multi-detector row. The photon energy is quantified as the tissue-specific linear attenuation coefficient detected after passing through the body calibrated to Hounsfield units (HU). Relative to water (0 HU), fat tissue is characterized by negative HU values and HU values for muscle tissue are positive [104, 119]. Using a hydroxyapatite calibration standard, HU are converted to three dimensional, volumetric BMD (νBMD ; g/cm^3) and this is referred to as quantitative computed tomography (QCT). Lower attenuation coefficients (lower HU) suggest a greater degree of fat infiltration within the muscle. The resolution of spiral CT scans ranges from 100 to 300 μm for peripheral and central anatomic sites, respectively. Several slices can be acquired very quickly, but the radiation exposure associated with image acquisition is the principle limitation of this technique (1.0-3.0mSv at the hip, 1.5-2.3mSv at the spine) [116]. Nevertheless, QCT is used for clinical and research applications because precision errors

for vBMD, while somewhat higher than DXA areal BMD, can be minimized using the multi-slice acquisition and automated placement of a volume of interest.

1.4.3 Peripheral quantitative computed tomography

Peripheral quantitative computed tomography (pQCT) is a compact QCT scanner that is used to acquire axial images of appendicular body regions. Similar to QCT, the device's X-ray source and detectors rotate 180 degrees around the gantry to obtain images from several angles. In contrast to QCT, the calibration phantom for pQCT assumes calibration remains standard over time and the device converts all attenuation coefficients to density values. The highest *in vivo* in-plane resolution achieved by the XCT2000 scanner is 200 μ m. This device is advantageous because its operation costs are far less and the radiation exposure is considerably reduced as compared with QCT scanners. The effective dose of a single tomographic pQCT slice is approximately 1 μ Sv [116].

As a research tool, the primary application of pQCT has been to explore and monitor changes in bone shape and mineral distribution in cortical and trabecular compartments during various stages of development, aging, or in response to treatment. As illustrated in Figure 1.1 (panel A), measurement sites are limited to appendicular regions because the small gantry diameter (140mm for the XCT2000 device). For bone imaging, pQCT is advantageous because it facilitates separation of cortical and trabecular bone compartments. Figure 1.1 (panels B, C, D) depicts the dense cortical bone, which can be visualized and quantified separately from the trabecular bone because their variation in vBMD. A drawback of pQCT lies in soft tissue imaging because the resolution does not permit individual muscles or muscle compartments to be

distinguished, nor does it allow isolation of intramuscular versus intermuscular fat.

Interest in the muscle-bone unit has resulted in pQCT being increasingly applied to obtain measurements of muscle cross-sectional area and density as measures of general size, estimated strength, and amount of dense muscle proteins. Although Canadian normative data are becoming increasingly available, pQCT remains a research tool because there is no cost-recovery mechanism in place to attract clinical utility.

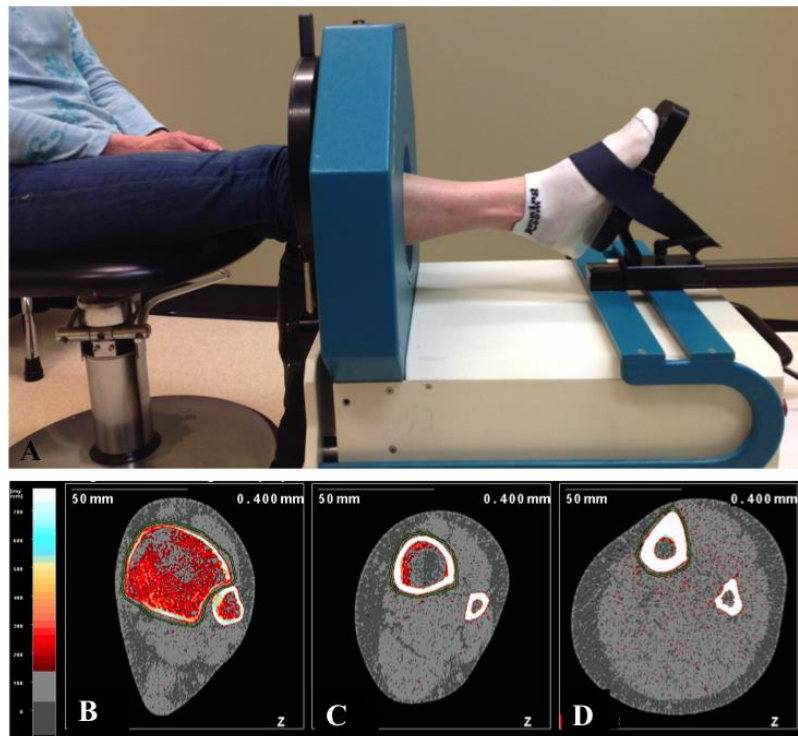


Figure 1.1: pQCT XCT2000 scanner and axial leg images. Standardized positioning for leg image acquisition in the pQCT scanner (A). Axial pQCT leg images at the tibia 4% (B), 14% (C), and 38% (D) sites illustrate bone size and shape at an in-plane resolution of 400µm. The colour scale on the left represents low (bottom, dark grey) to high (top, white) tissue volumetric densities (mg/cm^3).

1.4.4 Magnetic resonance imaging

Magnetic resonance imaging (MRI) provides excellent soft tissue contrast and, therefore, is considered the gold standard for clinical imaging of the neurological, cardiovascular, reproductive, and musculoskeletal systems. Specifically, musculoskeletal imaging would be indicated for joint derangement, infection, tumour, inflammation, post-trauma, and vascular pathologies. Image acquisition with MRI is achieved by using the signal of the protons from the nuclei of hydrogen atoms. In the absence of a magnetic field, hydrogen nuclei spin about axes that are randomly arranged. In the presence of a magnetic field, the spins of hydrogen atoms align parallel to the magnetic field and undergo precession. Precession is the wobbling motion of a spinning object that occurs in the presence of an external magnetic field. The rate at which precession occurs is called the Larmor frequency, which is directly proportional to the strength of the magnetic field. When the transmitter coil applies a radiofrequency (RF) pulse, the longitudinal magnetization is tipped by 90 degrees into the transverse plane. The rotating transverse magnetization gives rise to the MR signal in the receiver coil. Hydrogen atom spins eventually relax in the longitudinal direction due to spin-lattice interaction and in the transverse direction due to spin-spin interactions. Since longitudinal (T1) and transverse (T2) relaxation times vary by tissue type, as presented in Table 1.3, adjustment of the pulse sequence timing and duration will govern the degree of tissue contrast. In general, T1 weighted MRI sequences represent the current gold standard for measuring muscle morphology [120].

Table 1.3: Signal intensities of musculoskeletal tissues on T1- and T2-weighted images

Tissue	T1	T2
Muscle	Dark	Dark
Fat	Bright	Bright
Bone (cortical)	Dark	Dark
Inflammatory Tissue	Dark	Bright

A clear advantage of MRI over DXA, QCT, and pQCT, is the ability to modify pulse sequence specifications to enhance the contrast of tissue(s) of interest. An example of fat and water images is shown in Figure 1.2. High resolution, noninvasive imaging in the absence of ionizing radiation is another clear advantage of MRI. Whole-body MRI scanners, as shown in Figure 1.2, provide a means of examining the whole body or any body region with excellent image resolution. This section will describe two advanced MRI techniques that are able to provide greater detail about the structure and composition of skeletal muscle.

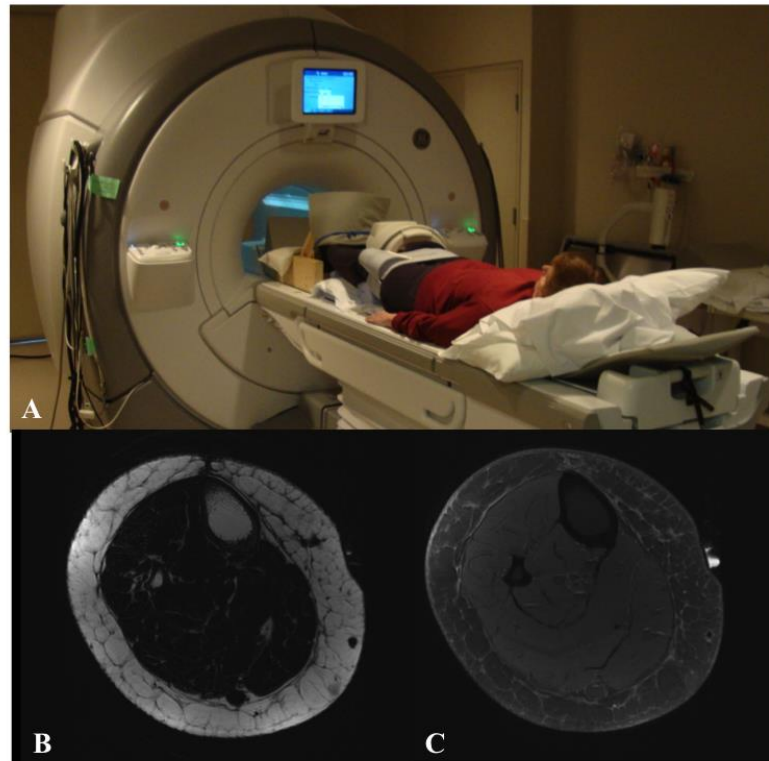


Figure 1.2: Whole body 3T MRI system and axial images of the leg. A woman on the scan bed of the 3T MRI scanner is positioned for imaging with an extremity coil placed around her right leg (A). Axial images of the leg demonstrate how altered sequence parameters can increase the brightness of fat (B) and water (C).

1.4.4.1 Diffusion tensor imaging

Diffusion tensor imaging (DTI) is an advanced MRI technique that calculates the random and multidirectional movement of water molecules. Diffusion tensor imaging has been widely applied to study ordered biological tissue, such as the brain, but its ability to characterize anisotropic tissue structure has been more recently extended to understand skeletal muscle structure. In anisotropic tissues, water diffusion is greater in some directions than others. Diffusion tensors are encoded in at least six directions, or three orthogonal planes, and can be visualized as an ellipse. Figure 1.3 illustrates the diffusion

ellipsoid. Thus, diffusion encoding is not confounded by muscle fibre orientation and information about the direction and shape of diffusivity can be calculated and reported as eigenvectors and eigenvalues, respectively [121].

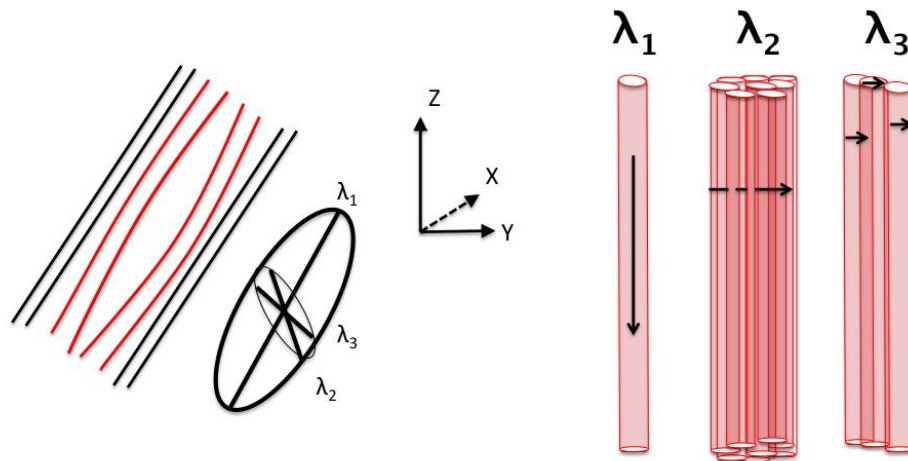


Figure 1.3: Ellipsoid representation of a tensor and proposed directions of water molecule diffusion in skeletal muscle. On the left is a schematic arrangement of muscle fibres where orientation is generally similar but not all fibres are parallel, as highlighted by the red lines. On the right is a schematic of proposed diffusion directions characterized by eigenvalues. The largest eigenvalue (λ_1) is oriented along the long axis of a muscle fibre, whereas the second and third eigenvalues (λ_2 and λ_3) represent diffusivity perpendicular to the long axis of the muscle fibres or fascicles.

Although muscle fibres are aligned in the same orientation, they are not always aligned in parallel. Thus, the diffusion ellipsoid is used to visualize eigenvalues and the three largest diffusion directions that they represent. The first eigenvalues (λ_1) is thought to represent water diffusivity along the long axis, or length, of the myofibre. The second and third eigenvalues (λ_2 and λ_3) represent water diffusivity in the direction perpendicular to muscle fibres or across muscle fascicles [122]. The apparent diffusion coefficient (ADC), also known as the mean diffusivity, represents the average rate of water diffusion

in a region of interest (ROI). The DTI measure that provides a summary of tissue structure is fractional anisotropy (FA). As presented in Figure 1.4, FA scales from 0 to 1 and is used to describe tissue as more isotropic with diffusion strength equal in all directions or anisotropic with diffusion in primarily one direction [123]. The ADC and FA are the diffusion tensor values often reported in skeletal muscle research and are calculated as follows:

$$ADC = \frac{\lambda_1 + \lambda_2 + \lambda_3}{3}$$

$$FA = \sqrt{\frac{3}{2}} \sqrt{\frac{(\lambda_1 - ADC)^2 + (\lambda_2 - ADC)^2 + (\lambda_3 - ADC)^2}{\lambda_1^2 + \lambda_2^2 + \lambda_3^2}}$$

The eigenvalues and their proposed diffusivity directions are validated with myocardial muscle using an automated software analysis [124]. Recently, DTI measures in a chick embryo were associated with muscle fibre formation and growth, as tracked using histological staining [125]. In humans, leg muscle λ_3 is correlated with physiological CSA of muscle fibres [126, 127] that has led to characterizing muscle fibre types using water diffusivity measures [128]. Interpretation of DTI measures must consider cell membranes, submembrane barriers (e.g., mitochondria, lipids, and morphological changes to muscle fibres) as potential modifiers of the magnitude and direction of water diffusivity. In attempt to confirm ‘proof of concept’ of the measures based on water diffusivity, DTI has been validated with respect to muscle aging [129], injury [130], and exercise physiology [131].



Figure 1.4: Schematic representation of the meaning of fractional anisotropy (FA) values. FA values scaling closer to zero, as illustrated on the left, represent a spherical shape since diffusion would be of the equal magnitude in all directions. Values approaching 1 represent the diffusion primarily in one direction, as in the hypothetical case of an infinitely long cylinder.

1.4.4.2 Proton magnetic resonance spectroscopy

Proton magnetic resonance spectroscopy ($^1\text{H-MRS}$) quantifies fat infiltration on a microscopic scale. Proton MRS is the only non-invasive method that differentiates two distinct lipid depots in muscle tissue: intramyocellular lipid (IMCL) and extramyocellular lipid (EMCL). IMCL is stored within the cytoplasm of muscle cells in spherical droplets, whereas EMCL is nestled along the muscle fibre bundles or fasciae [132]. Spectral fitting is highly dependent upon separation of the IMCL and EMCL peaks [133]. The greatest separation of the peaks is demonstrated in muscle fibres that are aligned perpendicular to the magnetic field [134].

Prior to the development of $^1\text{H-MRS}$, quantification of IMCL *in vivo* could only be performed by invasive biopsy techniques requiring painful muscle specimen extraction and the same muscle site could not be assessed over time. The evaluation of IMCL was

popularized upon discovering the inverse relationship between the amount of IMCL and insulin sensitivity [19]. Since then, several metabolic factors have been identified to influence the spectroscopic measurement of IMCL content, such as nutrition [135], age [136], sex [137], training status [138], obesity [139, 140], and muscle group [141].

1.5 APPLICATION OF MAGNETIC RESONANCE IMAGING TO EVALUATE LEG MUSCLE STRUCTURE IN WOMEN

This section describes the results of a scoping review that aimed to gather information about the extent to which various MRI techniques have been applied to evaluate leg muscle macrostructure, microstructure, and composition in women across the lifespan. In line with this aim, only articles that reported separate results for muscle of the leg in women were included. Articles were excluded if they measured clinical populations, for example stroke survivors, women with spinal cord injury or congenital muscle disease, without a control group for comparison.

The comprehensive literature search and study selection, described in Appendix A, yielded a total of seventeen eligible publications that matched the predetermined review criteria. Each eligible publication was obtained in full text and pertinent information was extracted by two reviewers independently. Extracted data included the study design, population characteristics, study objectives, MRI techniques employed, primary outcomes and results. Table 1.4 summarizes the study design, population, and MRI techniques described in each article eligible for inclusion. Research originated from North America (n = 7) [109, 110, 142-146], Europe (n = 8) [112, 147-153], and Asia (n =

2) [154, 155]. None of the articles were Canadian. The study designs were predominantly cross-sectional (n = 14), but also included one case study [152], one prospective cohort [151], and one single-blind randomized cross over study [143]. Of the cross-sectional studies, comparisons were made for: sex (n = 7) [112, 147-150, 153, 154], age (n = 2) [110, 145], ethnicity (n = 1) [144], training status (n = 2) [142, 155] and health status (n = 2) [109, 146].

The most commonly reported outcomes were leg muscle CSA and volume, as measured from T1 and T2 weighted axial images using commercially available and custom software. Alizai et al. (2012) incorporated a clinical semi-quantitative scoring system for fatty infiltration along with a fat fraction calculated using magnetic resonance (MR) chemical shift-based water/fat separation. Three articles applied DTI to leg muscle ROIs and two studies reported IMCL content using ¹H-MRS (Table 1.4). Two articles used MRI-based images to validate DXA-based measurements of lean mass [142, 148]. Until recently, the majority of MRI publications that examined leg muscle size and structure were performed in healthy premenopausal women. The summary of primary study objectives, primary muscle and fat measures, and results are presented in Table 1.5.

Overall, there was consensus among the publications that older women have less muscle mass and greater fat infiltration compared to older men [110, 112, 145, 147]. Articles that specifically recruited postmenopausal women were interested in measuring fat infiltration, however the studies were focused on women with or at risk of type 2 diabetes (T2D) [109, 145, 146]. Despite the established importance of skeletal muscle structure and composition for optimal functioning, most of the literature reviewed did not

investigate the relationship between non-invasive muscle and fat outcomes and clinically validated measures of physical performance. Indeed, Kent-Braun et al. (2000) reported that fat infiltration in the anterior compartment of the leg was lower in a subset of postmenopausal women who recorded higher levels of physical activity measured by accelerometry over a seven-day period ($n = 10$, $r = -0.69$, $p = 0.03$). Additionally, Boettcher et al. (2009) found that aerobic fitness, as measured by an incremental test performed to maximal exhaustion, was inversely associated with intermuscular fat content in the leg of middle-aged women at risk for T2D ($n = 152$, $r = -0.41$, $p < 0.001$).

Postmenopausal women were underrepresented in the MRI literature reviewed. For instance, non-invasive muscle microstructural outcomes have never been reported in postmenopausal women. Given the combination of shifting population demographics to a larger proportion of older adults and an increasing prevalence of musculoskeletal disability with aging [156], there is a pivotal role for MRI as a non-invasive imaging tool for assessing and monitoring musculoskeletal macrostructure and microstructure. Since DTI and $^1\text{H-MRS}$ can determine skeletal muscle microstructure and composition, there is a tremendous opportunity to apply these novel outcomes to explore the connection between muscle structure and bone loss in postmenopausal women.

Table 1.4: Description of study designs, study population characteristics, and magnetic resonance imaging acquisition methods

Citation	Design	Population	MRI method(s)
Fuller et al. 1999 [147]	Cross-sectional	N = 16 (n = 8 W); healthy; aged 41 to 60y	T2
Kent-Braun et al. 2000 [110]	Cross-sectional	N = 23 (n = 11 W); healthy, sedentary; aged 29(4)y <i>and</i> N = 21 (n = 10 W); healthy, sedentary; aged 73(6)y	T1
Bamman et al. 2000 [142]	Cross-sectional	N = 7 W; healthy, endurance trained, preM; aged 34(5)y <i>and</i> N = 32 W; healthy, untrained preM; aged 37(8)y	T1
Larson-Meyer et al. 2002 [143]	Single-blind cross-over	N = 7 W; healthy, endurance trained, preM; aged 35(8)y	¹ H-MRS
Holmback et al. 2002 [148]	Cross-sectional	N = 30 (n = 15 W); healthy; aged 23(3)y	T1
Holmback et al. 2003 [149]	Cross-sectional	N = 30 (n = 15 W); healthy; aged 23(3)y	T1
Galban et al. 2005 [150]	Cross-sectional	N = 24 (n = 12 W); healthy, untrained; aged 29(1)y	DTI
Trappe et al. 2007 [151]	Prospective cohort	N = 24 W; healthy; aged 33(1)y	PD
Ruan et al. 2007 [144]	Cross-sectional	N = 142 (n = 103 W); ambulatory, weight-stable, sedentary, community-dwelling; aged 42(15)y	T1
Grosset et al. 2008 [152]	Case study	N = 1 W; healthy, moderately active; aged 29y	T1
Rana et al. 2008 [154]	Cross-sectional	N = 17 (n = 9 W); healthy, non-smokers; aged 20, 35y	T1
Deux et al. 2008 [153]	Cross-sectional	N = 20 (n = 10 W); normal; aged 27(2)y	T1, DTI
Boettcher et al. 2009 [112]	Cross-sectional	N = 249 (n = 152 W); at high risk of T2D; aged 46(11)y	¹ H-MRS
Hasson et al. 2011 [145]	Cross-sectional	N = 12 (n = 6 W); healthy; aged 26(3)y <i>and</i> N = 12 (n = 6 W); healthy; aged 70(5)y	T1
Alizai et al. 2012 [146]	Cross-sectional	N = 27 W; postM, with T2D; aged 63(5)y <i>and</i> N = 35 W; postM, without T2D; aged 63(6)y	T1
Karampinos et al. 2012 [109]	Cross-sectional	N = 27 W; postM, with T2D; aged 63(5)y <i>and</i> N = 35 W; postM, without T2D; aged 63(6)y	T2
Okamoto et al. 2012 [155]	Cross-sectional	N = 12 W; healthy, trained athletes; aged 20(1)y <i>and</i> N = 11 W; healthy, untrained; aged 22(1)y	T1, DTI

W = women, preM = premenopausal, postM = postmenopausal, T2D = type 2 diabetes, age described as mean (SD) or (min, max) years, DTI = diffusion tensor imaging, MRS = magnetic resonance spectroscopy, PD = proton density weighted, T1 = T1-weighted images, T2 = T2-weighted images

Table 1.5: Description of primary objectives, muscle and fat measures, and results of studies measuring leg muscle in women with magnetic resonance imaging (MRI)

Citation	Objectives	MRI Muscle and Fat Measures	Findings (as they relate to MRI muscle and fat measures in the leg)
Fuller et al. 1999 [147]	To validate estimates of DXA leg and thigh soft tissue modeling methods using MRI	Tissue volume (To, Mu, AT), Proportion AT in calf	Mu volume was greater in men than women. Proportion AT was lower in men than women, but absolute AT volumes was similar between groups.
Kent-Braun et al. 2000 [110]	To determine the effect of age, gender, and physical activity level on Con and Non-Con tissue area in the leg.	AC ToCSA, ConCSA, Non-ConCSA, % Non-ConCSA	Compared to older adults, young adults had greater ConCSA, less Non-ConCSA, and % Non-ConCSA. Men had larger AC To, Con, and Non-ConCSA than women. Men and women had similar % Non-ConCSA. Habitual physical activity was inversely related to Non-ConCSA in older, but not young adults.
Bamman et al. 2000 [142]	To determine whether DXA estimated muscle size predicts PF MVC and could be used in lieu of MRI.	ACSA, PCSA, volume of SOL and GC	All MRI-based muscle size indices were sig related to isometric PF MVC (ACSA > PCSA > muscle volume; explained 42.2-53.7% of the variance in MVC). Trained preM women had greater ACSA, PCSA, volume, and PF MVC vs untrained preM women.
Larson-Meyer et al. 2002 [143]	To evaluate the effect of a 2 hour treadmill run and recovery diet on IMCL content in the leg of trained endurance runners.	IMCL and EMCL content in SOL	IMCL content was reduced by ~25% during the run. Recovery of IMCL levels to baseline was quicker with moderate-fat diet vs extremely low-fat diet.
Holmback et al. 2002 [148]	To determine the intra-rater test-retest and inter-rater reliability of MRI measures of ConCSA and Non-ConCSA in ankle DF.	ACSA, ConCSA, Non-ConCSA, % Non-ConCSA in DF	Intra-rater reliability of ConCSA (ICC>0.99) and Non-ConCSA was (ICC>0.94) was excellent for both raters. Inter-rater reliability of ConCSA was excellent (ICC>0.99). Inter-rater reliability of Non-ConCSA was good on occasion 1 (ICC=0.82) and excellent on occasion 2 (ICC=0.94). ACSA and ConCSA were larger in men vs women, but sexes were similar in Non-ConCSA and % Non-ConCSA.

Holmback et al. 2003 [149]	To determine the relationship between of ankle DF muscle strength, size, and fibre type composition and the influence of sex.	ACSA, ConCSA, non-ConCSA, %Non-ConCSA in DF	ConCSA was a major determinant of Con and Ecc DF peak torque. Body wt and fibre areas were major determinants of ConCSA. Men had larger ConCSA and fibre areas than women.
Galban et al. 2005 [150]	To determine if water diffusion within skeletal mu differs between sexes.	λ_1 , λ_2 , λ_3 , FA, trace of the diffusion tensor, Ellipsoid eccentricity for ROIs in SOL, LG, MG, TibA, TibP, EDL, PL.	Compared to men, women had higher eigenvalues and trace of the diffusion tensor. The differences were significant for all muscles, except λ_1 in SOL, λ_2 in PL, and λ_3 in TibA and PL. Women had lower FA and ellipsoid eccentricity than men, but these differences were only significant in SOL, LG, and MG.
Trappe et al. 2007 [151]	To test exercise and nutrition as countermeasures to muscle volume and strength loss during 60 days of simulated weightlessness.	Mu volume in SOL and GC	SOL and GC muscle volumes decreased similarly in control ($-29 \pm 1\%$) and nutrition ($-28 \pm 1\%$) groups. Mu volume loss was attenuated in exercise group ($-8 \pm 2\%$).
Ruan et al. 2007 [144]	To determine the predictive value of each slice location and which slice locations provide the best estimates of whole body IMAT.	Mass and volume of Mu, SAT, IMAT in calf	Highest correlations between single-slice IMAT and total body IMAT volumes were at the midcalf for Asian women. Adding two more sites improved the predictive strength. Calf IMAT was positively correlated with body weight in all ethnicities.
Grosset et al. 2008 [152]	To determine the changes in mu volume and shape associated with total ankle immobilization with cast, using the quadriceps, hamstring, and TS muscles as models of atrophy.	ACSA and volume of SOL and GC, SAT volume	Mu volume loss was -0.78% per day, with total -21.9% SOL and GC volume reduction. These deficits persisted after 2 months of recovery. GC most affected by immobilization, but also showed greatest improvement after 2 months recovery. SAT volume decreased 10.2% and was equal along length of leg.
Rana et al. 2008 [154]	To estimate and compare measures of working mu oxidative capacity in young men and women.	Peak area of PCr, Oxidative capacity, [PCr] at rest	No gender differences in rate of PCr depletion or recovery or in oxidative capacity in response to PF exercise intervention.

Deux et al. 2008 [153]	To determine whether water diffusion changes can be detected during contraction and rest of calf mu in normal volunteers.	λ_1 , λ_2 , λ_3 , ADC, FA in SOL and MG	At rest, λ_1 , λ_2 , and ADC of MG were higher than in TA. Plantarflexion did not change MG DTI measures. Dorsiflexion resulted in ADC increase in TA.
Boettcher et al. 2009 [112]	1) To quantify IMAT and investigate its association with other lipid depots. 2) To determine whether anthropometric data correlate with the amount of IMAT.	CSA of leg IMAT, non-AT and SAT, VAT, total AT, IMCL of TibA	IMAT was correlated with total AT, lower extremity AT, SAT, and VAT in men and women. Women have more IMAT and less non-AT in leg vs men, but IMCL was similar between sexes. Body wt and BMI had positive associations with IMAT. IMCL was associated with insulin sensitivity in women ($r=-0.44$, $p<0.001$) but not men.
Hasson et al. 2011 [145]	1) To quantify the volume, proportion, and longitudinal distribution of Con and Non-Con volumes in the DF and PF mu of young and older adults. 2) To determine whether Con volumes can be accurately estimated from MRI models of tissue distribution.	Ankle DF (TibA, EHL, EDL, PT) and ankle PF (MG, LG, SOL) CSA and volume, predicted mu volume from CSA_{max} , CSA at 30% site, and avg CSA_{max} using 3, 5, or 10 slices	Compared to young adults, the older adults had smaller cCSA and volume. Older adults had 3.6x more nCSA in DF and PF . Proportion of non-conCSA varied along the length of the leg, with lowest proportions near the center of the mu belly and a tendency to increase distally. Single-slice conCSA measures predicted volume with an avg error of about 8–11% for young and older adults. Using multiple slices improved estimates by ~50%, with avg errors of ~ 3–4%.
Alizai et al. 2012 [146]	To assess the reproducibility of the semi-quantitative Goutallier classification and validate this system with quantitative mu to fat fraction derived from a MRI chemical shift-based water/fat separation technique.	Semi-quantitative Goutallier grades of fat infiltration, fat fractions	Intra-observer reproducibility of intramuscular fat was 2.7%. Intra-observer and inter-observer agreement were excellent ($\kappa=0.81-0.83$). Fat fractions were correlated with Goutallier grades. Mean fat fraction differed among the 5 clinical grades in each ROI. Women with and without T2D had similar Goutallier grades.

Karampinos et al. 2012 [109]	To demonstrate the feasibility of assessing the spatial distribution of mu AT using chemical shift-based water/fat separation and to characterize differences in calf IMAT compartmentalization in patients with T2D compared to healthy age-matched controls.	SAT, TAT, non-AT, Intra-muscular AT and IMAT volumes in DP, AC, and LC and SOL, MG, LG	DP compartment and AC contributed relatively more to the IMAT volume in T2D group than in control group. Women with T2D had a less SAT and TAT volumes compared to controls. Intramuscular AT, IMAT, and non-AT were similar between groups.
Okamoto et al. 2012 [155]	To compare the differences in diffusion properties leg musculature in athletically trained vs untrained young women.	$\lambda_1, \lambda_2, \lambda_3$, ADC, FA in LG, MG, SOL, and TibA	Trained women had lower values for $\lambda_1, \lambda_2, \lambda_3$, and ADC than untrained women in all muscle ROIs. FA was similar in trained and untrained groups.

AC = anterior compartment

ACSA = anatomical cross-sectional area

ADC = apparent diffusion coefficient

AT = adipose tissue

Avg = average

BMI = body mass index

CSA = cross-sectional area

Con = concentric contraction

ConCSA = contractile tissue cross-sectional area

DF = dorsiflexors

DP = deep posterior

DXA = dual energy X-ray absorptiometry

Ecc = eccentric contraction

EDL = extensor digitorum longus

EHL = extensor hallicus longus

EMCL = extramyocellular lipid

FA = fractional anisotropy

GC = gastrocnemius

ICC = intraclass correlation coefficient

IMAT = intermuscular adipose tissue

IMCL = intramyocellular lipid

LC = lateral compartment

LG = lateral head of gastrocnemius

MG = medial head of gastrocnemius

Mu = muscle

MVC = maximum voluntary contraction

MRI = magnetic resonance imaging

Non-AT = non-adipose tissue (represents lean tissue)

Non-ConCSA = non-contractile tissue cross-sectional area

PCr = phosphocreatine

PCSA = physiological cross-sectional area

PF = plantarflexors

PostM = postmenopausal

PreM = premenopausal

PT = peroneus tertius

ROI = region of interest

SAT = subcutaneous adipose tissue

SOL = soleus

T2D = type 2 diabetes

TibA = tibialis anterior

TibP = tibialis posterior

TAT = total adipose tissue

To = total

TS = triceps surae (soleus and gastrocnemius muscles)

VAT = visceral adipose tissue

Wt = weight

$\lambda_1, \lambda_2, \lambda_3$ = first, second, third eigenvalues

1.6 SUMMARY OF THESIS OBJECTIVES

As a first step toward the overall thesis goal of determining differences in MRI-derived skeletal muscle structure and composition between women with and without OP, two studies were conducted to address methodological factors pertaining to protocol development and feasibility. Chapter Two is the protocol development study that assessed whether muscle CSA and water diffusion properties of leg muscles in young and older women changed over a period of time spent in supine rest. Chapter Three describes and evaluates the feasibility of applying three MRI scanning methods (PD-weighted imaging, DTI, and ¹H-MRS) to evaluate macrostructural and microstructural properties of leg muscles in older women. The third study (Chapter Four) applied the three MRI techniques described in Chapters Two and Three to determine whether postmenopausal women with and without OP are different in bone structure, muscle structure and muscle composition. Additionally, Chapter Four explored the associations between bone structure and strength outcomes and muscle structure and composition, and physical outcomes in older women. Overall, the studies in this dissertation aimed to apply MRI to assess musculoskeletal tissue structure and composition in women with and without OP.

CHAPTER TWO

AGE-RELATED DIFFERENCES IN THE RESPONSE OF LEG MUSCLE CROSS-SECTIONAL AREA AND WATER DIFFUSIVITY MEASURES TO A PERIOD OF SUPINE REST

PREFACE TO CHAPTER TWO

Authors: Amanda L. Lorbergs, Michael D. Noseworthy, Norma J. MacIntyre

Publication status: This manuscript was submitted to the journal *MAGMA Magnetic Resonance Materials in Physics, Biology and Medicine*. The manuscript received conditional acceptance (pending major revisions) in February 2014. The version of the manuscript included in the dissertation incorporates the peer-review feedback; however, the manuscript has not been accepted for publication in its current form. Upon final acceptance, a request will be made to the publisher of the journal to obtain permission to include copyright material.

Summary: This study evaluates the effect of a period of time spent in supine on skeletal muscle cross-sectional area (CSA) and water diffusivity in the leg of healthy young and older women. Leg muscle CSA and water diffusivity variables changed similarly over a period of time spent in supine in young and older women. The findings suggest that MRI scan acquisition protocols can be performed within 60 minutes of supine resting without a significant effect on muscle CSA and water diffusivity in the leg. This study demonstrates an important first step to developing a MRI scanning protocol for leg musculature in older women.

Age-related differences in the response of leg muscle cross-sectional area and water diffusivity measures to a period of supine rest

Authors: Lorbergs, Amanda L.
School of Rehabilitation Science
McMaster University, IAHS 403
1400 Main St. W., Hamilton, ON, L8S 1C7, Canada

Noseworthy, Michael D.
Department of Electrical and Computer Engineering
School of Biomedical Engineering
McMaster University, ITB building
1280 Main St. W., Hamilton, ON, L8S 4K1, Canada

MacIntyre, Norma J.
School of Rehabilitation Science
McMaster University, IAHS 403
1400 Main St. W., Hamilton, ON, L8S 1C7, Canada

Corresponding author: Amanda L. Lorbergs
Email: lorberal@mcmaster.ca
Telephone: +1 (905) 525-9140 ext: 26410
Fax: +1 (905) 524-0069

Word counts: Abstract: 190
Text: 4376

Number of figures: 5

Number of tables: 3

Number of references: 37

2.1 ABSTRACT

Object: To assess whether cross-sectional area (CSA) and water diffusion properties of leg muscles in young and older women change with increased time spent in supine rest.

Materials and Methods: Healthy young (n = 9, aged 20-30y) and older (n = 9, aged 65-75y) women underwent MRI scanning of the right leg at baseline, 30 and 60 minutes of supine rest. Muscle CSA was derived from proton density images. Water diffusion properties (apparent diffusion coefficient (ADC) and fractional anisotropy (FA) of the tibialis anterior, tibialis posterior, soleus, and medial and lateral heads of gastrocnemius) were derived from diffusion tensor imaging (DTI). Repeated measures ANOVAs and Bonferroni post-hoc tests determined the effects of time and group on each muscle outcome.

Results: In both groups, muscle CSA and FA did not change significantly over time whereas ADC significantly decreased. A greater decline at 30min for young women was only observed in medial gastrocnemius ADC.

Conclusion: Regardless of age, ADC values decreased with fluid shift associated with time spent supine, whereas CSA and FA were not affected. For leg muscle assessment in young and older women, DTI scanning protocols should consider the amount of time spent in a recumbent position.

KEYWORDS: women, aging, skeletal muscle size, diffusion tensor imaging (DTI), posture

2.2 INTRODUCTION

Magnetic resonance imaging (MRI) techniques permit noninvasive visualization and evaluation of body tissues. There is growing interest in applying MRI to better understand changes in tissue size, distribution, and structure associated with injury [1], disuse [2], disease [3], and aging [4]. Given the rising proportion of older adults, MRI is a promising modality for identifying and monitoring age-related changes in skeletal muscle structure and function. Studies evaluating leg muscles in older adults have revealed that muscle size and fat infiltration are related to mobility and physical function [5, 6]. Despite the fact that both men and women lose muscle mass [7] and accumulate fat within and around muscle with aging [8], the prevalence of physical disability is greater among older women [9]. The application of MRI to study muscle structure in older women could inform efforts to prevent and treat musculoskeletal conditions for optimal physical functioning with aging.

Advanced MRI scanning permits muscle evaluation beyond quantification of tissue cross-sectional area (CSA). For example, the application of MRI diffusion encoding gradients provides information about muscle microstructure on a smaller scale than the typical image resolution. Diffusion tensor imaging (DTI) calculates three eigenvalues ($\lambda_1, \lambda_2, \lambda_3$) representing the magnitude of diffusion in three orthogonal directions, with λ_1 corresponding to water diffusion along the length of muscle fibres and λ_2 and λ_3 representing perpendicular water diffusion either across fibres or across muscle fascicles [10]. Measures calculated from the DTI eigenvalues include apparent diffusion coefficient (ADC; the mean of the three eigenvalues) and fractional anisotropy (FA; a

function of the three eigenvalues). Although a number of studies have quantified muscle and fat content in the leg of older women [5, 6, 8, 11], there are no published reports of muscle microstructure as measured by DTI in this population. Compared to men, young women have less muscle mass, lower FA values and higher eigenvalues in the leg muscles [8, 12, 13]. A study of age-related changes in DTI measures found lower eigenvalues and reduced FA in the tibialis anterior in older men [14], but there are no studies that have directly compared noninvasive measures of muscle CSA and microstructure in the leg of young and older women.

Prior to applying MRI techniques to skeletal muscle examination in older women, it is important to consider the effect of postural changes on body fluid distribution and evaluate whether this differs from young women. The leg muscles are thought to be an important compartmental reservoir for fluid redistribution associated with changes in body posture [15]. Gravity-induced shifts in vascular fluids result from a net increase of intravascular fluid from the interstitial space [16]. Acute fluid shifts in the leg have been reported in response to changes in posture: from standing to sitting [16] and from standing to supine lying [2]. In healthy young adults, body fluid volumes in the leg and muscle CSA are decreased in response to these changes in posture [2, 15, 16]. More recently, significant reductions in muscle DTI measures were observed in young adults (30% female) 34 minutes after lying supine on the MRI table [17, 18]. It is unknown whether changes in CSA and diffusion properties of leg muscles occur or differ between young or older women with increased time spent in supine lying.

A number of age-related adaptations in skeletal muscle may influence the effect of changes in posture on fluid shifts in the lower extremity. For example, with advancing age skeletal muscle fibres are fewer in number and smaller in size [19], cross-sectional geometry deforms [20], and intramuscular fat accumulates [8]. Further, the autonomic nervous system is less responsive in older adults and that may subsequently attenuate fluid shifts following postural change from standing to supine [21]. As MRI becomes increasingly available to research musculoskeletal aging and disability, a first step in protocol development is to assess whether fluid shifts significantly affect muscle size and microstructure measurements in older women. The primary objective of this study is to assess whether leg muscle CSA and water diffusion properties (ADC, FA) in young and older women change with increased time spent in supine rest and differ with age.

2.3 MATERIALS AND METHODS

This cross-sectional study was approved by our institutional research ethics board (Appendix B). Written informed consent was provided by all subjects and MRI safety screening was performed with each participant prior to initiating the study.

2.3.1 Subjects and recruitment

Eighteen women were recruited using poster and email advertisements, presentations to a community group and university students, and mailed letter invitations to past study participants. Young women were aged between 20 and 30 years and older women were aged between 65 and 75 years. Prior to enrolment, all interested volunteers were screened by telephone. Women who reported moderate physical activity levels, but

did not train specifically in any sport or exercise program, were eligible. Volunteers taking medications that would alter body composition (e.g. steroids) were excluded. Exclusion criteria were: diabetes, chronic obstructive pulmonary disorder, stroke, cancer in the past five years, smoking cigarettes in the past two years, surgery in the past six weeks, any neurologic or musculoskeletal condition affecting the back or lower limbs, or any MRI incompatibility.

2.3.2 Anthropometry

Height was measured to the nearest 0.1 cm using a wall-mounted stadiometer and weight was measured to the nearest 0.1 kg using a calibrated scale. Body mass index (BMI; kg/m^2) was derived from height and weight as an anthropometric estimate of adiposity. Right tibial length was measured from the base of the medial malleolus to the superior margin of the medial epicondyle [22]. The 66% site (from the distal end) was calculated from the total tibia length and identified with a fiducial marker.

2.3.3 Image acquisition

A 3.0T MRI scanner and an 8-channel phased array RF knee coil (General Electric Healthcare Discovery MR 750, Milwaukee, WI) were used for all imaging. Participants were positioned supine with knees extended and both feet immobilized in a custom standardized positioning rig comprised of wooden footrests that supported the ankle joints in neutral and suspended the calf muscles above the scan bed to prevent muscle distortion in the image [18]. The right leg was placed in the RF coil with the fiducial marker (66% site) centered in the coil prior to advancing the participant feet first into the magnet bore. The scanning protocol was repeated three times. Participants were

not repositioned between the three sets of scans and were instructed not move for approximately 75 minutes. An accredited MRI technologist conducted all scanning.

The scanning protocol began with the acquisition of a three-plane localizer scan (31s duration). Axial proton density (PD) weighted images were acquired with the following parameters: 30 contiguous slices (FRFSE-XL, 15th slice was centred in the middle of the fiducial marker), TE/TR = 30/2344ms, field-of view (FOV) = 16cm, matrix = 320x320mm, slice thickness = 4mm (0mm skip), resolution = 0.5x0.5x4mm, scan time = 6min 30s. The phased array uniformity enhancement (PURE) post-processing filter was applied to PD images to correct for field inhomogeneity and reduce edge blurring, as shown in Figure 2.1. The baseline PD scans were performed three minutes after the localizer scan was initiated. The PD scans were repeated 30 and 60 minutes after the baseline PD scanning, which corresponded to minutes 33 and 63 of the scan acquisition protocol.

Apart from in-plane resolution, DTI scans were acquired with identical geometry as the PD scans. DTI scans were acquired using a dual spin-echo planar imaging (EPI) pulse sequence with the following parameters: 30 slices, 4mm thick, 0 skip, 15 optimized diffusion encoding gradients [18], one $b = 0$ s/mm², b -value = 350 s/mm², TE/TR = 68.3/6000ms, number of excitations (NEX) = 4, matrix size = 64x64mm, total time per average = 1min 42s, total scan time = 6min 48s. Each average was collected separately to correct for eddy currents and motion prior to merging and subsequent calculation of the diffusion tensor. DTI scans were acquired immediately following PD image acquisitions at baseline (10 minutes after localizer scan initiation) and were repeated at 40 minutes and

70 minutes of the scan acquisition protocol. For convenience, the three PD and DTI acquisition time points are referred to as baseline, 30 and 60 minutes of supine rest throughout the manuscript.

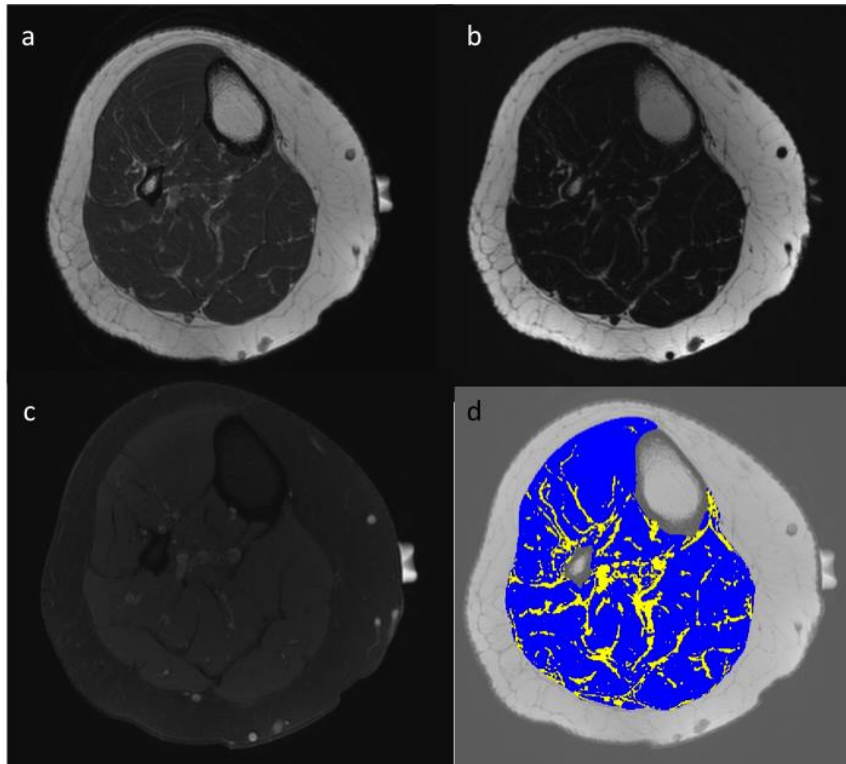


Figure 2.1: Representative leg images from a woman aged 75 years. Proton density (PD) with PURE filter (a), PD water saturated (b), and PD fat saturated (c) axial images of the leg 66% site marked by a fiducial marker. Skeletal muscle and adipose tissue areas of the leg were segmented (d) in contrasting colors from the PD PURE-filtered image.

2.3.4 Image processing and analyses protocols

Prior to processing and analyses, axial PD images were visually inspected by an accredited technologist to screen for potential subclinical pathology. The PURE-filtered PD images acquired at each time point were exported to a separate PC workstation where SliceOmatic v4.3 software (TomoVision, Montreal, Canada) was used to analyse the

images. Total muscle CSA was calculated from three contiguous axial images nearest to the site with the largest leg muscle CSA. The semi-automated segmentation process involved two stages. First, all pixels representing soft tissue below the subcutaneous fascia were tagged using the morphological mode; and second, all pixels representing inter- and intra-muscular adipose tissue (bright pixels situated beneath the subcutaneous fascia, between the intermuscular fascia or within intramuscular fascia) were tagged in a contrasting colour using the region growing mode. The software generated a histogram of the pixel intensity distribution within each image. To segment the pixels representing adipose depots the separation threshold was defined as the (brighter) pixel intensities to the right of the muscle peak where the slope approached zero. Sample PD and segmented images are presented in Figure 2.1. Manual editing by visual inspection was performed to make small adjustments as needed. Muscle CSA was calculated as the quotient of muscle volume and total thickness of the three slices analysed.

DTI outcomes were calculated for five regions of interest (ROIs) defined within four leg muscles: tibialis anterior (TibA), tibialis posterior (TibP), soleus (SOL), medial head of gastrocnemius (MG) and lateral head of gastrocnemius (LG). Tensor calculation and subsequent analysis was performed using a combination of home-developed Bourne-Again Shell (BASH) scripts, FSL [23] and Diffusion Toolkit (DTK) [24]. To correct for eddy current distortion the FSL *eddy_current* function was employed. This function is based on a previously developed image registration tool [25] and was also used for motion correction. The reference for eddy current and motion correction was the $b = 0$ s/mm² image of the first NEX. Following tensor calculation, the five ROIs were

manually drawn on five contiguous images around the site with the largest leg muscle CSA using Analysis of Functional Neuroimaging (AFNI) software [26]. As shown in Figure 2.2, large ROIs were drawn for each muscle. Visible vessels, fat and fascia were identified and excluded from the ROI using the corresponding PD images for anatomical reference. Analysis of each ROI in the image stack yielded mean λ_1 , λ_2 , λ_3 , ADC and FA values. The DTI outcomes of interest were ADC and FA, which were calculated as follows [27]:

$$ADC = \frac{\lambda_1 + \lambda_2 + \lambda_3}{3} \quad (1)$$

$$FA = \sqrt{\frac{3}{2}} \sqrt{\frac{(\lambda_1 - (\lambda))^2 + (\lambda_2 - (\lambda))^2 + (\lambda_3 - (\lambda))^2}{\lambda_1^2 + \lambda_2^2 + \lambda_3^2}} \quad (2)$$

where (λ) represents the mean of all three eigenvalues.

2.3.5 Statistical analysis

All data were visually inspected and statistically assessed with the Kolmogorov-Smirnov test for violations of normality. Data are described as mean and standard deviation (SD). One-way analysis of variance (ANOVA) was used to compare baseline characteristics of the groups of young and older women. To address our study objectives, we applied a repeated measures ANOVA with one between-person factor at two levels (age group: young, older) and one within-person factor at three levels (occasion: baseline, 30 minutes, 60 minutes) to the outcomes muscle CSA, ADC, and FA. If the within-person F-value was significant, differences between baseline, 30-minute, and 60-minute occasions were subsequently tested using pairwise comparisons with a Bonferroni adjustment set at $p < 0.05$ for all comparisons. If the sphericity assumption was not met,

the Greenhouse Geisser adjusted F-value was reported. All statistical analyses were performed with SPSS V.20 (Statistical Package for the Social Sciences Inc., Chicago, IL, USA).

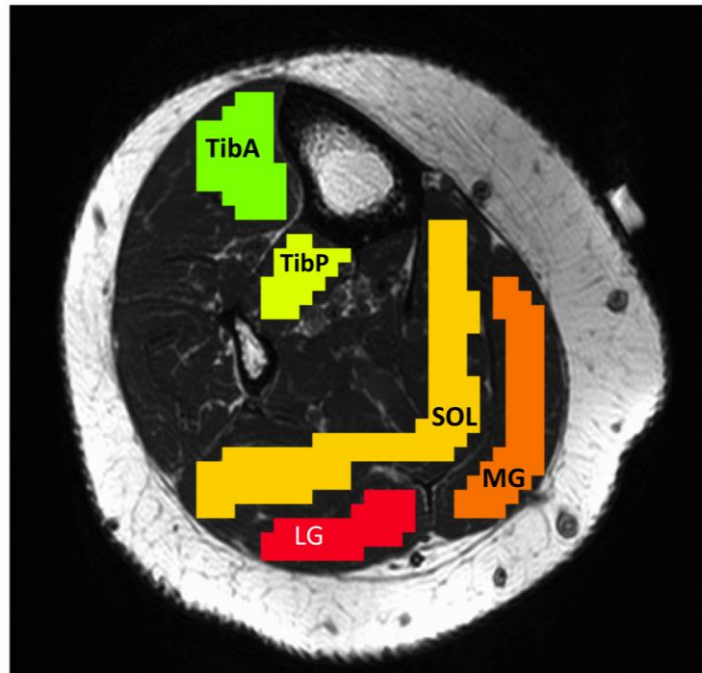


Figure 2.2: Axial image of the leg indicating diffusion tensor imaging regions of interest (ROIs). The analyzed ROIs are indicated by the colored pixels in the anatomical proton density (PD) weighted reference image. TibA = tibialis anterior, TibP = tibialis posterior, SOL = soleus, MG = gastrocnemius medial head, LG = gastrocnemius lateral head

2.4 RESULTS

Nine young and nine older women participated in the study. Descriptive and anthropometric characteristics of the participants are summarized in Table 2.1. The groups were statistically similar in height ($p = 0.19$), weight ($p = 0.20$), and BMI ($p =$

0.88). Data for two participants, one from each group, were excluded from analyses due to operator error during scan acquisition (young) or image artifact (older).

Table 2.1: Participant descriptive characteristics

Characteristic	Young (n = 9)		Older (n = 9)	
	Min, Max	Mean (SD)	Min, Max	Mean (SD)
Age (y)	22, 30	25.8 (3.4)	65, 75	71.0 (3.8)
Height (cm)	155, 185	169.8 (11.1)	155, 169	160.9 (5.1)
Weight (kg)	54, 86	68.0 (11.7)	47, 82	60.9 (10.0)
Body mass index (kg/m ²)	19, 33	23.7 (4.6)	19, 29	23.4 (3.1)

Max = maximum; Min = minimum

2.4.1 Effect of supine rest on muscle CSA

Leg muscle CSA for young and older women at baseline, 30 minutes and 60 minutes of resting supine are illustrated in Figure 2.3. There was no significant effect of time spent supine on muscle CSA in young or older women. Since muscle CSA remained stable over time for the young and older women, the intraclass correlation coefficient and standard error of the measurement were calculated (Appendix E).

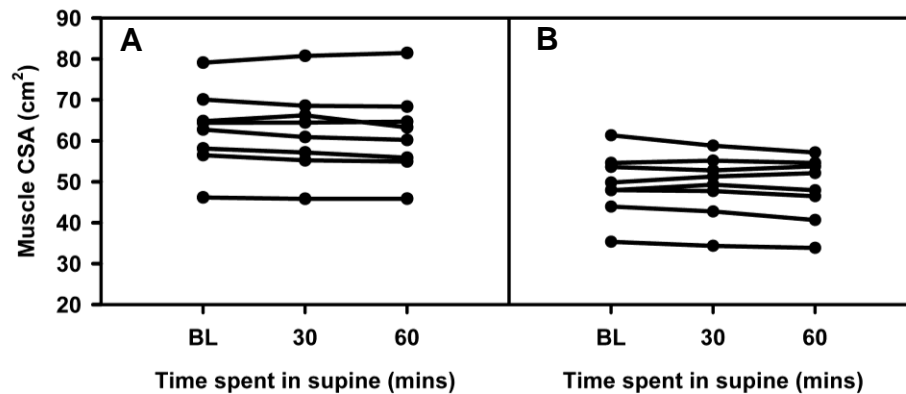


Figure 2.3: Individual values for total leg muscle cross sectional area (CSA) plotted as a function of time. Muscle CSA (cm²) for young (A, n = 8) and older (B, n = 8) women at baseline (BL), 30-minute, and 60-minute time points

2.4.2 Effect of supine rest on muscle DTI

Table 2.2 provides the mean ADC and FA values for each muscle ROI for each group at baseline, and after 30 and 60 minutes spent in supine position. Figure 2.4 illustrates the ADC values in the leg muscle ROIs at each time point for each young and older woman. Between baseline and 30 minutes spent supine, ADC was significantly reduced in the TibA ($p = 0.003$), SOL ($p = 0.005$), MG ($p < 0.001$), and LG ($p = 0.001$) for both young and older women. Between 30 and 60 minutes of supine lying, MG and LG continued to decrease in the young and older women and these changes were significant (MG: $p < 0.001$; LG: $p = 0.02$). Compared to the older women, the decline in MG ADC was significantly greater in the young women between baseline and 30 minutes in supine ($F_{GG}(1.44, 20.17) = 4.12, p = 0.043$).

Table 2.2: Fractional anisotropy (FA) and apparent diffusion coefficient (ADC, $\times 10^{-3} \text{ mm}^2/\text{s}$) represented at three time points (baseline, 30 minutes, 60 minutes) of supine lying for five leg muscle regions of interest (ROIs) for the groups of young and older women. All measures are presented as mean (SD)

ROI		Young (n = 8)			Older (n = 8)		
		BL	30min	60min	BL	30min	60min
TibA	FA	0.22 (0.02)	0.22 (0.01)	0.23 (0.01)	0.23 (0.02)	0.23 (0.02)	0.24 (0.02)
	ADC	1.72 (0.04)	1.66 (0.05)	1.66 (0.04)	1.74 (0.08)	1.68 (0.09)	1.67 (0.07)
TibP	FA	0.24 (0.03)	0.23 (0.03)	0.23 (0.03)	0.27 (0.04)	0.28 (0.03)	0.28 (0.04)
	ADC	1.74 (0.07)	1.74 (0.08)	1.73 (0.06)	1.86 (0.17)	1.78 (0.11)	1.74 (0.09)
SOL	FA	0.24 (0.01)	0.23 (0.01)	0.23 (0.01)	0.25 (0.02)	0.24 (0.02)	0.24 (0.02)
	ADC	1.70 (0.07)	1.67 (0.06)	1.66 (0.08)	1.72 (0.11)	1.67 (0.10)	1.65 (0.09)
MG	FA	0.27 (0.02)	0.26 (0.01)	0.26 (0.01)	0.28 (0.03)	0.27 (0.02)	0.27 (0.02)
	ADC	1.63 (0.11)	1.56 (0.11)	1.54 (0.10)	1.70 (0.12)	1.67 (0.13)	1.65 (0.12)
LG	FA	0.28 (0.04)	0.28 (0.03)	0.27 (0.03)	0.27 (0.02)	0.27 (0.03)	0.27 (0.03)
	ADC	1.67 (0.12)	1.63 (0.11)	1.60 (0.10)	1.67 (0.12)	1.62 (0.13)	1.58 (0.12)

BL = baseline, TibA = tibialis anterior, TibP = tibialis posterior, SOL = soleus, MG = medial gastrocnemius, LG = lateral gastrocnemius.

Figure 2.5 illustrates the FA values in the leg muscle ROIs at each time point for each young and older woman. There were no differences in FA over time between young and older women at any muscle ROI. In the SOL, young and older women had significant decreases in FA between baseline and 30 minutes ($p = 0.026$) without any detectable change thereafter ($p = 0.52$). Since FA remained stable over time for the young and older women, intraclass correlation coefficients for each muscle ROI were calculated (Appendix E).

2.4.3 Group comparisons

Young women had larger muscle CSA compared to older women ($F(1,14) = 9.3, p = 0.009$). Table 2.3 provides the mean $\lambda_1, \lambda_2,$ and λ_3 for each muscle ROI for each group at baseline, and after 30 and 60 minutes spent in supine position. Mean values of $\lambda_1, \lambda_2,$ and λ_3 were generally larger for older women than young women; however, there were no statistically significant differences for any muscle ROI (all $p \geq 0.13$), with the exception of TibP λ_1 ($F(1,14) = 6.5, p = 0.02$). ADC for all ROIs was similar between groups. Older women had higher FA values for all ROIs, however the difference was only significant at the TibP ($F(1,14) = 5.51, p = 0.034$).

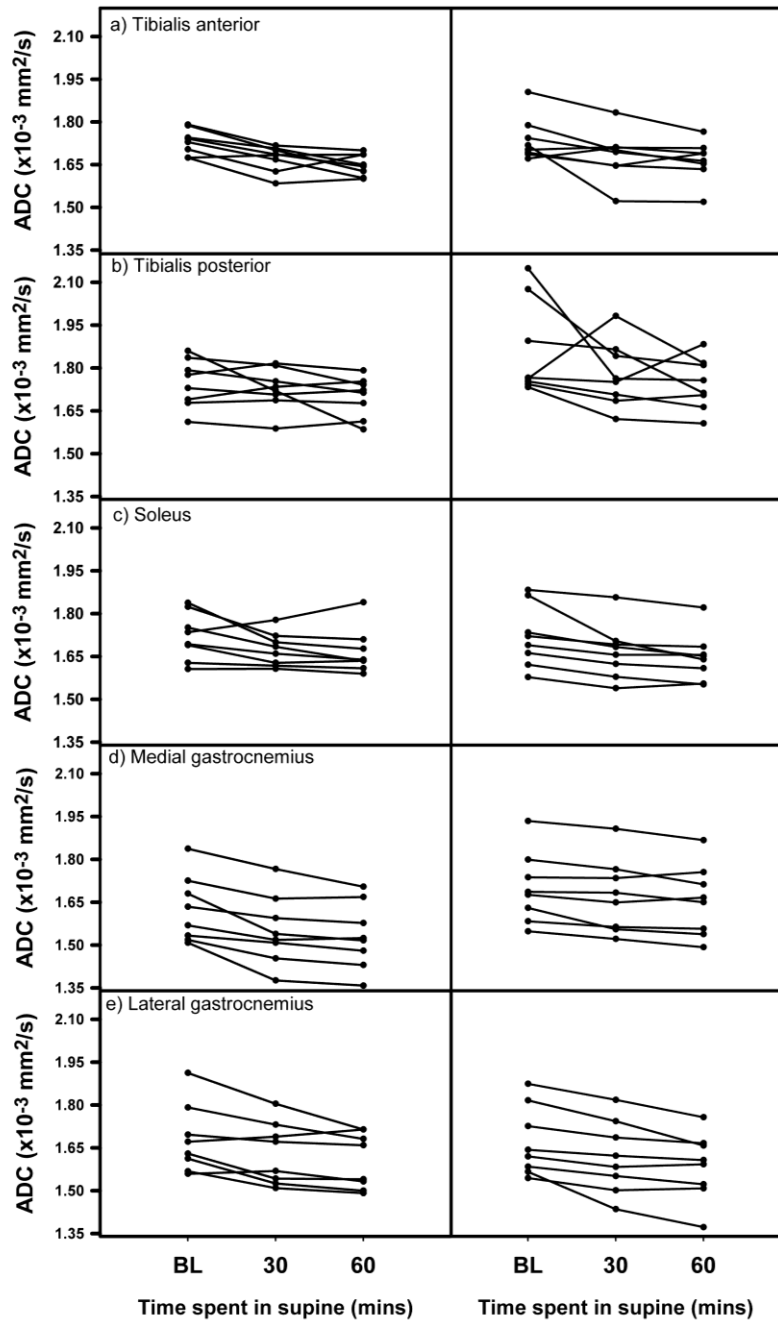


Figure 2.4: Individual values for apparent diffusion coefficient (ADC) for leg muscles in young and older women plotted as a function of time. ADC ($\times 10^{-3} \text{ mm}^2/\text{s}$) for young (left column, $n = 8$) and older (right column, $n = 8$) women at baseline (BL), 30 and 60-minute time points for five muscle regions of interest.

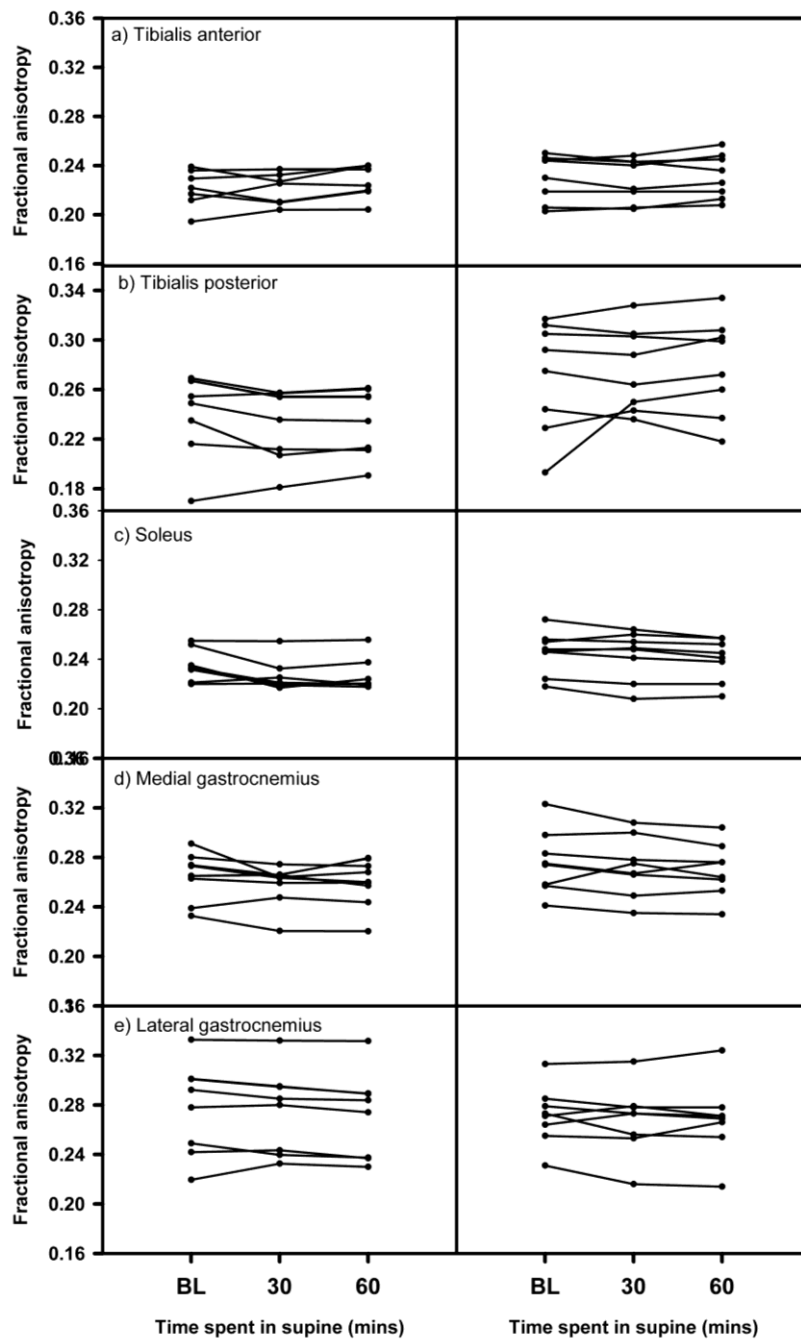


Figure 2.5: Individual values for fractional anisotropy (FA) for leg muscles in young and older women plotted as a function of time. FA for young (left column, n = 8) and older (right column, n = 8) women at baseline (BL), 30 and 60-minute time points for five muscle regions of interest

Table 2.3: Eigenvalues ($\times 10^{-3}$ mm²/s) represented at three time points (baseline, 30 minutes, 60 minutes) of supine lying for five leg muscle regions of interest for the groups of young and older women. All measures are presented as mean (SD)

ROI		Young (n = 8)			Older (n = 8)		
		BL	30min	60min	BL	30min	60min
TibA	λ_1	2.14 (0.07)	2.07 (0.05)	2.08 (0.05)	2.19 (0.07)	2.12 (0.09)	2.09 (0.08)
	λ_2	1.61 (0.04)	1.56 (0.05)	1.55 (0.04)	1.61 (0.10)	1.56 (0.09)	1.52 (0.07)
	λ_3	1.41 (0.03)	1.35 (0.05)	1.35 (0.04)	1.45 (0.13)	1.38 (0.09)	1.35 (0.08)
TibP	λ_1	2.20 (0.14)	2.19 (0.12)	2.18 (0.09)	2.41 (0.19)	2.32 (0.15)	2.28 (0.12)
	λ_2	1.63 (0.07)	1.63 (0.08)	1.61 (0.07)	1.73 (0.17)	1.65 (0.15)	1.62 (0.11)
	λ_3	1.38 (0.06)	1.40 (0.07)	1.38 (0.06)	1.48 (0.18)	1.37 (0.07)	1.33 (0.09)
SOL	λ_1	2.15 (0.07)	2.09 (0.06)	2.08 (0.08)	2.19 (0.15)	2.12 (0.13)	2.09 (0.12)
	λ_2	1.58 (0.08)	1.55 (0.08)	1.56 (0.10)	1.59 (0.11)	1.55 (0.10)	1.54 (0.09)
	λ_3	1.38 (0.07)	1.36 (0.05)	1.35 (0.06)	1.40 (0.10)	1.33 (0.07)	1.32 (0.06)
MG	λ_1	2.13 (0.14)	2.03 (0.13)	2.01 (0.11)	2.24 (0.18)	2.19 (0.18)	2.16 (0.17)
	λ_2	1.45 (0.13)	1.40 (0.12)	1.38 (0.11)	1.53 (0.11)	1.51 (0.12)	1.50 (0.12)
	λ_3	1.30 (0.08)	1.25 (0.08)	1.23 (0.09)	1.37 (0.11)	1.31 (0.10)	1.30 (0.10)
LG	λ_1	2.19 (0.12)	2.13 (0.11)	2.09 (0.08)	2.17 (0.18)	2.10 (0.19)	2.06 (0.18)
	λ_2	1.55 (0.16)	1.51 (0.14)	1.48 (0.13)	1.58 (0.13)	1.53 (0.12)	1.49 (0.10)
	λ_3	1.28 (0.12)	1.25 (0.11)	1.23 (0.11)	1.30 (0.12)	1.23 (0.09)	1.21 (0.10)

ROI = region of interest, BL = baseline, TibA = tibialis anterior, TibP = tibialis posterior, SOL = soleus, MG = medial gastrocnemius, LG = lateral gastrocnemius

2.5 DISCUSSION

This study evaluated the influence of a period of time spent in supine lying on leg muscle CSA, ADC, and FA in young and older women. We obtained repeated measures of CSA and water diffusion properties in the leg muscle of healthy young and older women after they were positioned in supine lying to evaluate whether these measures change as a function of the amount of time spent in a recumbent posture. For both young and older women, 60 minutes of supine rest did not significantly alter muscle CSA. ADC declined significantly and similarly between baseline and 30 minutes for all women in most muscles, with only the rate of decline in MG ADC differing between groups. In both groups, FA in most muscles was not detected with 30 or 60 minutes of supine rest. Compared to older women, the young women had larger leg muscle CSA and lower TibP FA values. Taking into account the effect of time, our findings suggest that young and older women have similar DTI measures in leg muscles that change similarly over 30 and 60 minutes of supine rest. MRI scanning for muscle CSA and most DTI measures can be performed without delay in young and older women.

The current investigation was motivated by previous studies that reported that muscle CSA and diffusivity properties (eigenvalues and ADC) were significantly reduced in young adults within half an hour of assuming supine lying for baseline scanning [17, 18]. Muscle CSA was reduced on average (SD) by 3.2 (1.0)% and 4.9 (1.2)% following just 34 and 64 minutes of supine rest, respectively, in healthy young adults (mean age 26.8 years) [17]. To assess if time spent in supine influences muscle CSA and water diffusivity properties differ in older women, we replicated a previously reported image

acquisition protocol performed in our laboratory [17, 18]. Contrary to the previous study, our findings suggest that leg muscle CSA in healthy young women does not decrease significantly after 30 or 60 minutes of supine rest. Interestingly, we made the same observation for muscle CSA in older women. This suggests that any fluid shifts resulting from a short duration of supine rest do not significantly alter leg muscle CSA. The effect of supine rest on lower extremity fluid shifts and subsequent changes in muscle CSA are reported by others as well [2, 15, 16]. Berg (1993) used computed tomography to study CSA changes in the thigh and calf of eight healthy males with a mean age of 27 years. They demonstrated that after 60 minutes of supine rest muscle CSA was reduced by a mean (SD) of 5.5 (2.7%) compared to baseline [2]. These findings were supported by a study that measured leg muscle CSA with MRI in healthy college students and reported a mean (SD) decrease of 8 (2.0)% in response to 12 hours of resting supine [15]. A possible reason for the discordance of our findings in the young women can be explained by differences in participant characteristics, namely sex and training status. Previous studies examined athletes [2, 16] or a mixed sample of men and women of unknown training status [17, 18]. Athletes and men typically exhibit larger muscle CSA [8] and improved microvascular fluid filtration [28, 29]. It is possible that athletically trained individuals may demonstrate better awareness of their hydration levels. These training-related factors are potentially related to muscle CSA response to supine rest, since an increased amount of lean tissue and fluid volume, combined with a greater microvascular filtration capacity would present a higher likelihood of experiencing fluid shifts in response to 30 or 60 minutes resting supine. Our recruitment strategy focused on

enrolling women, both young and older, with moderate physical activity levels.

However, by doing so, we excluded participants that would be more likely to demonstrate fluid shifts detectable with MRI in 60 minutes or less. Advanced age and sex [19] also contribute to the observation of smaller muscle CSA, which may partially explain the non-significant decreases in our sample compared to earlier studies combining data for young men and young women [2, 15-18].

Aging is associated with atrophy and fatty infiltration of muscle tissue. Peripheral blood vessel compliance also declines with age and has been implicated in slower vascular responses to gravitational stresses [30, 31]. The loss of muscle mass and accumulation of non-contractile tissue within the muscle result in a smaller volume of vasculature and contractile tissue that would be affected by fluid shifts in response to postural changes. Blood pressure in the leg increases in an erect posture. In contracting muscle, increased blood flow to skeletal muscle in response to a greater level of physical exertion required to walk from the bus stop or parking lot to our imaging suite may have affected the muscle CSA values obtained at baseline, particularly for older women. However, the absence of muscle CSA change between imaging time points suggests that the muscle contractions required to walk the distance to our imaging suite were insufficient to cause a large fluid shift response.

This is the first study to compare the influence of time spent in supine on leg muscle DTI measures in young and older women. Our findings of ADC change over time are generally in agreement with Elzibak et al. (2013) who found young adult leg muscle ADC values significantly decreased within 34 minutes of supine rest, without significant

change in FA over that same time period [18]. Despite our best efforts to replicate the image acquisition protocol, differences in DTI analysis may account for the lack of change in TibP ADC and the continued decline in MG and LG ADC between 30-minute and 60-minute time points. Our analysis included drawing large ROIs in five slices at each of the time points, whereas Elzibak et al. (2013) only evaluated one axial image at each time point. Selection of one slice for analysis reduces the number of pixels included for DTI calculations and consequently underestimates the amount of diffusivity variability within each muscle ROI. A greater number of voxels selected in a greater number of slices provides more generalizable findings in terms of representing water diffusivity within a muscle. Further, our data showed that SOL FA decreased similarly over time for young and older women. This observation was not made previously, but may be attributed to the complex architecture of the SOL and the inclusion of more slices for analysis which capture the changes in muscle fibre orientation within the five-slice ROI [32]. Fat infiltration leads to partial volume effects and affects the quantification of DTI measures [33], however the ROIs were carefully selected to exclude visible fat, especially apparent in the leg images from older women. Membrane permeability, fat infiltration, and other macromolecules are known to affect water diffusivity [33, 34]; the distribution of these morphological attributes may be less homogenous within aging skeletal muscle compared to young adult muscle. Furthermore, with less muscle area in older muscle, the influence of inhomogeneous muscle morphology on diffusion properties would be emphasized. Fat infiltration within the selected ROI influences diffusion properties by producing falsely low eigenvalues and inflated FA values, which reduce the

validity of the measurements [33, 36]. In our study, DTI was done using spectral spatial RF pulses which do not excite fat, and therefore, the degree of contamination was thought to be insignificant. Whether the differences in DTI measures over a period of supine rest are due to fluid shifts or muscle fibre morphology cannot be discerned in this study.

In contrast to age-related changes in leg muscle water diffusivity reported in men [14], the present study did not observe significant differences in leg muscle eigenvalues, ADC, or FA between young and older women. Indeed, both groups of women in our sample had higher mean λ_1 , λ_2 , and λ_3 values at the TibA, SOL, MG, and LG, compared to the previously reported sample of men [14]. This is in agreement with previous work that documented higher eigenvalues in young women compared to young men [13]. While the reasons for these sex-related differences are unknown, others have suggested that microstructural barriers, capillary density, and fibre bundle length differences affect diffusion properties [13]. There are a number of potential explanations as to why we did not observe age-related differences. First, DTI acquisition parameters can make direct comparisons between studies challenging. Although 1.5T and 3T MR systems generate comparable DTI measures, SNR decreases with increasing b -values and fewer than 12 diffusion encoding directions [35, 36]. In support of the acquisition parameter similarities, the values for all DTI measures in the young women of our study are comparable with previous DTI data for three women obtained using the same MR scanner and image acquisition settings [17, 18]. Lower λ_1 values and higher diffusion across muscle fibres and within the cross-section of a muscle fibre, represented by λ_2 and λ_3 , respectively, are believed to reflect reduced diffusivity along the long axis of the

muscle fibre and increased water diffusion perpendicular to the long axis [1]. The values for λ_2 and λ_3 observed in our sample were similar to those reported among healthy adults [18] and did not suggest a disruption in diffusivity in the leg muscles of young or older women. Next, our small sample size and the dispersion within the DTI measures in older women (Figures 2.4 and 2.5) may have masked any age-related trend. Our study highlights the importance of reporting diffusion measures separately for men and women in future studies. Continued research is warranted to validate *in vivo* DTI measures with muscle architecture.

The limitations of our study findings must be considered when interpreting our results. First, intra-rater reliability of muscle CSA segmentation and DTI analyses were not assessed, however we minimized potential variability by having one individual perform all analyses. Second, a small sample limits our confidence in the finding that muscle CSA and water diffusivity measures change similarly in young and older women. We recruited women who self-reported moderate physical activity levels because we anticipated that differences in training status would account for differences in muscle response to time spent supine. Thus, women with poor or very high physical fitness levels were excluded. However, we did not account for the duration or perceived difficulty of the commute to the imaging suite for the older participants. To reduce the influence of factors related to the commute, only healthy individuals were enrolled and persons with diagnoses that may exacerbate muscle atrophy (e.g., cardiac and pulmonary diseases) were excluded from our study. Lastly, we acknowledge the influence of thermal and hydration factors on muscle CSA and fluid shift. Although temperature and

hydration were not measured in the present study, the imaging suite temperature was maintained between 20°C and 22°C and typical hydration levels would be expected since no formal instructions were provided prior to scanning sessions.

2.6 CONCLUSIONS

We have demonstrated that MRI-based measures of CSA of the leg muscles in young and older women are not significantly changed by 30 or 60 minutes spent in a supine position. In young and older women, FA did not change with increasing time spent in supine. On the other hand, ADC in most muscles was reduced after 30 minutes, with MG and LG ADC values continuing to decrease until the 60-minute time point in young and older women. In light of our findings, we conclude that muscle CSA and DTI measures in the leg of young and older women responded similarly during 60 minutes spent in supine. Thus, it is not necessary to adjust scanning order or include different durations of time of supine rest within MRI acquisition protocols that quantify size and microstructure in the leg muscles of young and older women. Future studies evaluating structural adaptation in muscle microstructure in healthy women should standardize the MRI scanning protocol to eliminate the influence of declining ADC values in leg muscles after 30 minutes of supine rest.

2.6 ACKNOWLEDGEMENTS

The study was funded in part by a grant from The Arthritis Society. The authors thank Norm Konyer and the MRI technologists (Janet Burr, Cheryl Contant and Julie Lecomte) for their assistance throughout data collection. AL is funded in part by the Ontario Women's Health Scholar Award and the Joint Motion Program, a Canadian Institutes of Health Research Training Program in Musculoskeletal Health Research and Leadership

2.7 REFERENCES

1. Zaraiskaya T, Kumbhare D, Noseworthy MD (2006) Diffusion tensor imaging in evaluation of human skeletal muscle injury. *J Magn Reson Imaging* 24:402-408
2. Berg HE, Tedner B, Tesch PA (1993) Changes in lower limb muscle cross-sectional area and tissue fluid volume after transition from standing to supine. *Acta Physiol Scand* 148:379-385
3. Mathur S, Lott DJ, Senesac C, Germain SA, Vohra RS, Sweeney HL, Walter GA, Vandeborne K (2010) Age-related differences in lower-limb muscle cross-sectional area and torque production in boys with Duchenne muscular dystrophy. *Arch Phys Med Rehabil* 91:1051-1058
4. Schwenzer NF, Martirosian P, Machann J, Schraml C, Steidle G, Claussen CD, Schick F (2009) Aging effects on human calf muscle properties assessed by MRI at 3 Tesla. *J Magn Reson Imaging* 29:1346-1354
5. Buford TW, Lott DJ, Marzetti E, Wohlgenuth SE, Vandeborne K, Pahor M, Leeuwenburgh C, Manini TM (2012) Age-related differences in lower extremity tissue compartments and associations with physical function in older adults. *Exp Gerontol* 47:38-44 DOI 10.1016/j.exger.2011.10.001
6. Tuttle LJ, Sinacore DR, Mueller MJ (2012) Intermuscular adipose tissue is muscle specific and associated with poor functional performance. *J Aging Res* 2012:172957 DOI 10.1155/2012/172957
7. Basu R, Basu A, Nair KS (2002) Muscle changes in aging. *J Nutr Health Aging* 6:336-341
8. Kent-Braun JA, Ng AV, Young K (2000) Skeletal muscle contractile and noncontractile components in young and older women and men. *J Appl Physiol* 88:662-668
9. Murtagh KN, Hubert HB (2004) Gender differences in physical disability among an elderly cohort. *Am J Public Health* 94:1406-1411
10. Galban CJ, Maderwald S, Uffmann K, de Greiff A, Ladd ME (2004) Diffusive sensitivity to muscle architecture: a magnetic resonance diffusion tensor imaging study of the human calf. *Eur J Appl Physiol* 93:253-262
11. Hasson CJ, Caldwell GE (2012) Effects of age on mechanical properties of dorsiflexor and plantarflexor muscles. *Ann Biomed Eng* 40:1088-1101

12. Holmback AM, Porter MM, Downham D, Andersen JL, Lexell J (2003) Structure and function of the ankle dorsiflexor muscles in young and moderately active men and women. *J Appl Physiol* 95:2416-2424
13. Galban CJ, Maderwald S, Uffmann K, Ladd ME (2005) A diffusion tensor imaging analysis of gender differences in water diffusivity within human skeletal muscle. *NMR Biomed* 18:489-498
14. Galban CJ, Maderwald S, Stock F, Ladd ME (2007) Age-related changes in skeletal muscle as detected by diffusion tensor magnetic resonance imaging. *J Gerontol A Biol Sci Med Sci* 62:453-458
15. Conley MS, Foley JM, Ploutz-Snyder LL, Meyer RA, Dudley GA (1996) Effect of acute head-down tilt on skeletal muscle cross-sectional area and proton transverse relaxation time. *J Appl Physiol* (1985) 81:1572-1577
16. Maw GJ, Mackenzie IL, Taylor NA (1995) Redistribution of body fluids during postural manipulations. *Acta Physiol Scand* 155:157-163
17. Elzibak AH, Noseworthy MD (2013) Investigation of diffusion tensor imaging indices, mean BOLD signal and calf muscle cross sectional area following bed rest. In: *Proceedings of the 21st scientific meeting of the International Society for Magnetic Resonance Medicine*, Salt Lake City, p 5342
18. Elzibak AH, Noseworthy MD (2013) Assessment of diffusion tensor imaging indices in calf muscles following postural change from standing to supine position. *Magn Reson Mater Phy*. doi: 10.1007/s10334-013-0424-1
19. Lieber R (2002) *Skeletal muscle structure, function, & plasticity: The physiological basis of rehabilitation*. Lippincott Williams and Wilkins, Philadelphia, PA.
20. Andersen JL (2003) Muscle fibre type adaptation in the elderly human muscle. *Scand J Med Sci Sports* 13:40-47
21. Miwa C, Sugiyama Y, Mano T, Matsukawa T, Iwase S, Watanabe T, Kobayashi F (2000) Effects of aging on cardiovascular responses to gravity-related fluid shift in humans. *J Gerontol A Biol Sci Med Sci* 55:M329-335
22. International Society for the Advancement of Kinanthropometry (2001) *International Standards for Anthropometric Assessment*. International Society for the Advancement of Kinanthropometry, Australia.
23. Jenkinson M, Beckmann CF, Behrens TE, Woolrich MW, Smith SM (2012) FSL. *Neuroimage* 62:782-790

24. Wang R, Benner T, Sorensen A, Wedeen V (2007) Diffusion Toolkit: A software package for diffusion imaging data processing and tractography. In: Proceedings of the 16th scientific meeting of the International Society for Magnetic Resonance Medicine, Berlin, p 3720
25. Jenkinson M, Bannister P, Brady M, Smith S (2002) Improved optimization for the robust and accurate linear registration and motion correction of brain images. *Neuroimage* 17:825-841
26. Cox RW (1996) AFNI: software for analysis and visualization of functional magnetic resonance neuroimages. *Comput Biomed Res* 29:162-173
27. Le Bihan D, Mangin JF, Poupon C, Clark CA, Pappata S, Molko N, Chabriat H (2001) Diffusion tensor imaging: concepts and applications. *J Magn Reson Imaging* 13:534-546
28. Brown MD, Jeal S, Bryant J, Gamble J (2001) Modifications of microvascular filtration capacity in human limbs by training and electrical stimulation. *Acta Physiol Scand* 173:359-368
29. Charles M, Charifi N, Verney J, Pichot V, Feasson L, Costes F, Denis C (2006) Effect of endurance training on muscle microvascular filtration capacity and vascular bed morphometry in the elderly. *Acta Physiol (Oxf)* 187:399-406
30. Olsen H, Lanne T (1998) Reduced venous compliance in lower limbs of aging humans and its importance for capacitance function. *Am J Physiol* 275:H878-H886
31. Fu Q, Iwase S, Niimi Y, Kamiya A, Michikami D, Mano T (1999) Effects of aging on leg vein filling and venous compliance during low levels of lower body negative pressure in humans. *Environ Med* 43:142-145
32. Sinha S, Sinha U, Edgerton VR (2006) In vivo diffusion tensor imaging of the human calf muscle. *J Magn Reson Imaging* 24:182-190
33. Williams SE, Heemskerk AM, Welch EB, Li K, Damon BM, Park JH (2013) Quantitative effects of inclusion of fat on muscle diffusion tensor MRI measurements. *J Magn Reson Imaging* 38:1292-1297
34. Andre JB, Bammer R (2010) Advanced diffusion-weighted magnetic resonance imaging techniques of the human spinal cord. *Top Magn Reson Imaging* 21:367-378
35. Damon BM (2008) Effects of image noise in muscle diffusion tensor (DT)-MRI assessed using numerical simulations. *Magn Reson Med* 60:934-944

36. Froeling M, Nederveen AJ, Nicolay K, Strijkers GJ (2013) DTI of human skeletal muscle: the effects of diffusion encoding parameters, signal-to-noise ratio and T2 on tensor indices and fiber tracts. *NMR Biomed* 26:1339-1352

CHAPTER THREE

FEASIBILITY OF MAGNETIC RESONANCE IMAGING TO EVALUATE LEG MUSCLE MACROSTRUCTURAL AND MICROSTRUCTURAL PROPERTIES IN OLDER WOMEN

PREFACE TO CHAPTER THREE

Authors: Amanda L. Lorbergs, Michael D. Noseworthy, Norma J. MacIntyre

Publication status: This manuscript is under review in *BMC Musculoskeletal Disorders*.

Summary: In this feasibility study, magnetic resonance imaging (MRI) methods (proton density (PD)-weighted imaging, diffusion tensor imaging (DTI) and proton magnetic resonance spectroscopy ($^1\text{H-MRS}$)) were combined to evaluate macrostructural and microstructural properties of leg muscles in older women and address three specific feasibility objectives: 1) participant recruitment; 2) participant tolerance to the MRI acquisition protocol; and 3) establish acquisition and analyses protocols. The secondary objective was to report parameter estimates of muscle outcomes. Based on successful participant recruitment, tolerance, and optimal scan acquisition and analyses protocols, we have demonstrated that it is feasible to combine PD-weighted, DTI, and $^1\text{H-MRS}$ imaging techniques for characterizing skeletal muscle structure in the leg of older women

**Feasibility of magnetic resonance imaging to evaluate leg muscle macrostructural
and microstructural properties in older women**

Authors: Lorbergs, Amanda L.

School of Rehabilitation Science

McMaster University, IAHS 403

1400 Main St. W., Hamilton, ON, L8S 1C7, Canada

Tel: +1 905-525-9140 x:26410

Fax: +1 905-524-0069

Email: lorberal@mcmaster.ca

Noseworthy, Michael D.

Department of Electrical and Computer Engineering

School of Biomedical Engineering

McMaster University

MacIntyre, Norma J.

School of Rehabilitation Science

McMaster University

3.1 ABSTRACT

Objectives: The feasibility of combining magnetic resonance imaging (MRI) methods (proton density (PD)-weighted imaging, diffusion tensor imaging (DTI) and proton magnetic resonance spectroscopy ($^1\text{H-MRS}$)) to evaluate macro- and microstructural properties of leg muscles in older women was determined with respect to: 1) describe the participant recruitment rate based on three strategies, 2) determine participant tolerance to the MRI scan acquisition protocol, and 3) establish the scan acquisition and analyses protocols. The secondary objective was to report parameter estimates of muscle outcomes. **Methods:** Recruitment feasibility was based on the number of participants enrolled using various strategies. Participant tolerance was feasible if the scanning session was uninterrupted and image artifacts were absent. Optimal PD imaging, DTI, and $^1\text{H-MRS}$ acquisition and analyses protocols were established. **Results:** Nine women (mean age = 71y) were recruited over four months. The acquisition protocol was well tolerated by all participants. Adaptations were required for women with short stature and vertebral fracture risk. Analysis protocols were facilitated through application of the phased array uniformity enhancement filter to increase tissue contrast. Total muscle and intramuscular fat areas, DTI measures, and intramyocellular lipid content were determined. **Conclusions:** It is feasible to use a combination of MRI methods to evaluate muscle structure in the leg of older women.

Keywords: feasibility, magnetic resonance imaging (MRI), postmenopausal women, lower extremity, skeletal muscle

3.2 INTRODUCTION

Billions of healthcare dollars are spent annually to rehabilitate persons with functional limitations attributed to deteriorating muscle structure and function. With aging, muscle fibres become less organized¹, muscle mass decreases (with a preferential decline in the size and proportion of high-tension type II muscle fibres)², and fat increasingly infiltrates muscle tissue³. Further, neuromuscular adaptations result in an under-utilization of muscle fibres due to decreased motor unit number and activation⁴. As a result, aging muscle becomes increasingly weak and less able to produce force rapidly. With aging, both men and women lose muscle mass and accumulate intramuscular fatty deposits⁵; however, these age-related changes in muscle may be a greater public health concern for women because they live longer and generally exhibit higher rates of disability than men⁶.

Women begin to lose muscle mass in mid-adulthood. The onset of menopause coincides with decreased muscle strength⁷, increased intramuscular fat⁸, and increased oxidative stress⁹. By the time women transition through menopause, dramatic declines in muscle mass and strength are observed^{4, 10}. Older women with muscle dysfunction in the lower extremities demonstrate mobility limitations¹¹⁻¹³ and greater risk of hip fractures¹⁴.

Magnetic resonance imaging (MRI) is the gold standard non-invasive method for clinical assessment of skeletal muscle pathology. Thus, there is considerable interest in applying MRI to evaluate the association of muscle structure (e.g., size, fat infiltration) with important clinical health outcomes such as frailty, fractures, and impaired mobility^{12, 13, 15}. A recent study showed that women with osteoporotic vertebral fractures have smaller paraspinal muscles and greater intramuscular fat infiltration compared with age-

matched women without vertebral fractures¹⁶. Among women at risk for knee osteoarthritis, quadriceps muscle fat infiltration predicts physical performance and muscle force production¹⁷. In the leg, fat infiltration of ankle dorsiflexor and plantarflexor muscles is negatively associated with aerobic fitness and walking ability in adults with or at risk of diabetes^{18, 19}. Ankle dorsiflexor and plantarflexor muscles are essential for maintaining stability and balance during standing and whole body movements^{20, 21}. Continued MRI investigation of leg muscles beyond the macrostructural measures of size and fat infiltration will improve our understanding of age-related microstructural muscle and fat properties and their relationship to important health outcomes.

Diffusion tensor imaging (DTI) and proton magnetic resonance spectroscopy (¹H-MRS) are MRI scanning methods that permit analyses of muscle microstructure and composition at the tissue and cellular levels, respectively. (These techniques are reviewed elsewhere^{22, 23}.) In brief, DTI is based on the theory that water molecule diffusion in an anisotropic tissue is more likely to occur in the direction of least resistance. DTI encoding gradients provide information about muscle microstructure at the tissue level by quantifying the magnitude of water diffusivity in three orthogonal directions. The first eigenvalue (λ_1) corresponds to water diffusion along the long axis of the muscle fibres, whereas the second and third eigenvalues (λ_2, λ_3) represent water diffusivity across fibres and across muscle fascicles²⁴. DTI measures in the soleus and gastrocnemius muscles, namely the fractional anisotropy (FA), of men are reduced with advancing age²⁵. The increased disorganization of muscle fibres, represented by lower FA values in older men, may affect physical performance, but this was not evaluated. DTI has been used to study

trabecular bone tissue organization in older women²⁶, but there are no published studies reporting DTI measures of muscle tissue in this population. At the cellular level, ¹H-MRS quantifies and distinguishes lipid stored within a muscle (intramyocellular lipid, IMCL) from extramyocellular lipid stored outside of the muscle. The technique compares spectra of metabolite concentrations from a volume of interest to the reference unsuppressed water signal. Middle-aged women have greater amounts of IMCL and the amount of IMCL in the tibialis anterior muscle is negatively associated with insulin sensitivity¹⁸. Insulin sensitivity is a predictor of frailty²⁷ and may also predict clinical outcomes such as fracture and impaired mobility. Given that DTI and ¹H-MRS provide detail about muscle morphology and fatty infiltration, we propose the application of these techniques in addition to the more commonly used measures of muscle and fat tissue macrostructure will provide a comprehensive understanding of muscle structure in older women.

As a first step toward understanding the potential benefits of performing multiple MRI techniques to enhance the understanding of leg muscle status in older women, it is important to ensure that these protocols are feasible to implement in this population. Specifically, the feasibility objectives were to: 1) describe the participant recruitment rate based on three strategies, 2) determine participant tolerance to the MRI scan acquisition protocol, comprised of proton density (PD)-weighted, DTI, and ¹H-MRS scanning; and 3) establish the scan acquisition and analyses protocols. The secondary objective was to report parameter estimates for macro- and microstructural muscle outcomes that could be used to support sample size calculations in future studies²⁸.

3.3 METHODS

3.3.1 Study design

This cross-sectional study was approved by our institutional REB (Appendix B). Written informed consent was provided by participants and MRI safety screening was conducted prior to initiating the study.

3.3.2 Participant recruitment

Community-dwelling women aged 65-75 years were recruited between January and April 2013 using poster advertisements, a presentation to a community group, and mailed letter invitations to past study participants who consented to be contacted regarding future studies. Prior to enrolment, all interested volunteers were screened by telephone. Women who reported moderate physical activity levels were considered eligible. Exclusion criteria were: diabetes, chronic obstructive pulmonary disorder, stroke, cancer in the past five years, smoking cigarettes in the past two years, surgery in the past six weeks, chronic neurologic or musculoskeletal condition affecting the back or lower limbs, or MRI incompatibility.

3.3.3 Anthropometry

Height was measured in cm to the nearest 1mm using a wall-mounted stadiometer and weight was measured in kg to the nearest 0.1 kg using a calibrated scale. Body mass index (BMI; kg/m^2) was derived from height and weight as an anthropometric estimate of adiposity. Right tibia length was measured from the base of the medial malleolus to the superior margin of the medial epicondyle²⁹. Measuring proximally from the medial malleolus, the 66% site was marked with a fiducial marker.

3.3.4 Self-reported physical activity

Each participant completed the self-reported Rapid Assessment of Physical Activity (RAPA) questionnaire that consists of nine items requiring a *yes* or *no* response. Habitual physical activity was evaluated because it plays an important role in determining the extent of age-related intramuscular fat accumulation³. Validity of scores on the RAPA for assessing physical activity in adults over 50 years of age has been established by demonstrating the anticipated association with scores on the Community Health Activities Model Program for Seniors ($r = 0.54$)³⁰. RAPA scores between six and ten represent an active lifestyle, whereas scores between two and five are considered under-active³⁰.

3.3.5 Image acquisition protocols

A 3.0T MRI scanner (General Electric Healthcare, Discovery MR750) and an 8-channel phased array RF knee coil were used for all imaging. Participant positioning on the scanner bed was standardized: each woman lay supine with knees extended and both feet immobilized. A custom standardized positioning rig comprised of wooden footrests supported the ankle joints in neutral and suspended the calf muscles above the scan bed to prevent muscle distortion in the image³¹. The participant's feet were fixed to the footrests using a rubber cord with a cushion placed between the top of the foot and the rubber cord. The right leg was placed in the RF coil with the fiducial marker (66% tibial site) centered in the coil. Padding, including a large cylindrical sponge, was placed under the posterior aspect of the knees and ankles to ensure the posterior leg was not resting on the coil. Prior to advancing the participant feet first into the magnet bore, one or two pillows were

provided to support the head in a comfortable position during scanning and an emergency call bell was provided to alert the MRI technologist in the event of discomfort. Foam earplugs and noise-cancelling headphones were provided for ear protection. Blankets were provided for warmth. Subjects remained on the MRI scanner bed with their feet immobilized during the 35-minute scanning protocol. One of two accredited MRI technologists conducted all scanning. To reduce the effects of postural hypotension (i.e., dizziness), all participants sat on the scanner bed for 1 minute prior to dismounting.

PD-weighted scanning

The scanning protocol began with the acquisition of a 3-plane localizer scan (31s duration). Axial PD-weighted images were acquired with the following parameters: 30 slices (FRFSE-XL), TE/TR = 30/2344ms, field-of view (FOV) = 16cm, matrix = 320x320mm, slice thickness = 4mm (0mm skip), resolution = 0.5x0.5x4mm, total scan time = 6min 30s. The 15th slice of the series (counting inferior to superior) was centered in the middle of the fiducial marker.

Diffusion tensor imaging (DTI)

Apart from the in-plane resolution, DTI scans were acquired with the identically prescribed geometry as the PD-weighted images. DTI scans were acquired using a dual spin-echo planar imaging (EPI) pulse sequence with the following parameters: 30 slices (4mm thick, 0mm skip), 15 optimized diffusion encoding gradients³¹, one $b = 0\text{s/mm}^2$, b -value = 350s/mm^2 , TE/TR = 68.3/6000ms, number of averages (NEX) = 4, matrix size = 64x64mm, total time per average = 1min 42s, total scan time = 6min 48s. Each NEX was

collected separately to correct for eddy currents and motion prior to merging and subsequent tensor calculation.

Proton magnetic resonance spectroscopy (¹H-MRS)

A single voxel ¹H-MRS measurement of a volume of interest in the tibialis anterior muscle was obtained using a point resolved spectroscopy (PRESS) pulse sequence. The tibialis anterior was chosen because of its consistent orientation of muscle fibres parallel to the main magnetic field, which provides the greatest separation of lipid compartments³². The following parameters were used: TE/TR = 30/1500ms, averages = 128, total scan duration = 1min 18s. The 40×20×20mm (16mL) volume of interest was placed within the tibialis anterior muscle to exclude subcutaneous fat, blood vessels, and bone in an image-guided manner. Two pairs of saturation bands were manually placed to reduce the strong subcutaneous and bone marrow lipid signals. Automated shimming improved the field homogeneity. This procedure always resulted in a water peak full width half maximum (FWHM) of less than 0.231ppm.

3.3.6 Image post-processing and analyses protocols

Prior to processing and analyses, PD-weighted images were visually inspected by an accredited MRI technologist to screen for potential gross subclinical pathology.

PD-weighted images

The phased array uniformity enhancement (PURE) post-processing filter was applied to PD-weighted images to correct for image intensity non-uniformity and reduce edge blurring. On a PC workstation, SliceOmatic v4.9 image analysis software (TomoVision) was used to analyse the PURE-filtered PD-weighted images. Total muscle

and total intramuscular fat cross-sectional areas (CSA, cm²) were calculated from the 15th image of the series, corresponding to the 66% site of the tibia. The software generated a histogram of the distribution of pixel intensities within each axial image. The fat separation threshold was defined as the pixel intensities to the right of the pixel intensities for the muscle tissue peak (brighter). First, all pixels representing soft tissue below the subcutaneous fascia (except bone marrow) were tagged in blue using the morphological mode of SliceOmatic; second, all pixels representing inter- and intramuscular fat (bright pixels situated beneath the subcutaneous fascia, between the intermuscular fascia or within intramuscular fascia) were tagged in a contrasting colour using the region growing mode. Pixels representing vessels in intermuscular compartments were tagged as fat. Visual inspection determined whether manual editing for small adjustments was needed.

DTI

Eigenvalues ($\lambda_1, \lambda_2, \lambda_3$; $\times 10^{-3}$ mm²/s), apparent diffusion coefficient (ADC; $\times 10^{-3}$ mm²/s), and FA, were quantified for five regions of interest (ROIs) in four muscles: tibialis anterior, tibialis posterior, soleus, gastrocnemius medial head and lateral head. Tensor calculation and subsequent analysis were performed off-line using a combination of home-developed BASH (Bourne Again Shell) scripts, FSL³³ and Diffusion Toolkit (DTK)³⁴. To correct for eddy current distortion, the FSL *eddy_current* function was employed. This function is based on a previously developed image registration tool³⁵ and was also used for motion correction. The reference for eddy current and motion correction was the $b = 0$ s/mm² image of the first NEX. Following tensor calculation, the

15th image of the series was used to manually draw five ROIs with Analysis of Functional Neuroimaging (AFNI) software³⁶. Using the axial PD-weighted image for anatomical reference, each ROI was selected to exclude visible vessels, fat and fascia. Projection maps and the corresponding anatomical reference image are illustrated in Figure 3.1. Each ROI yielded λ_1 , λ_2 , λ_3 , ADC and FA values. ADC and FA are calculated as follows³⁷:

$$ADC = \frac{\lambda_1 + \lambda_2 + \lambda_3}{3} \quad (1)$$

$$FA = \sqrt{\frac{3}{2}} \sqrt{\frac{(\lambda_1 - (\lambda))^2 + (\lambda_2 - (\lambda))^2 + (\lambda_3 - (\lambda))^2}{\lambda_1^2 + \lambda_2^2 + \lambda_3^2}} \quad (2)$$

where λ represents the mean of the three eigenvalues.

¹H-MRS

Spectra from the tibialis anterior muscle volume of interest were analyzed using LCModel software (v6.2)³⁸. LCModel-derived lipid content is estimated by dividing the signal from a metabolite resonance area in a water suppressed spectrum by the signal from the water peak in an unsuppressed water reference signal acquired from the same voxel (see Appendix D for sample spectra). The LCModel software automatically adjusts the phase and ppm shift of the spectra, estimates the baseline, and performs eddy current correction.

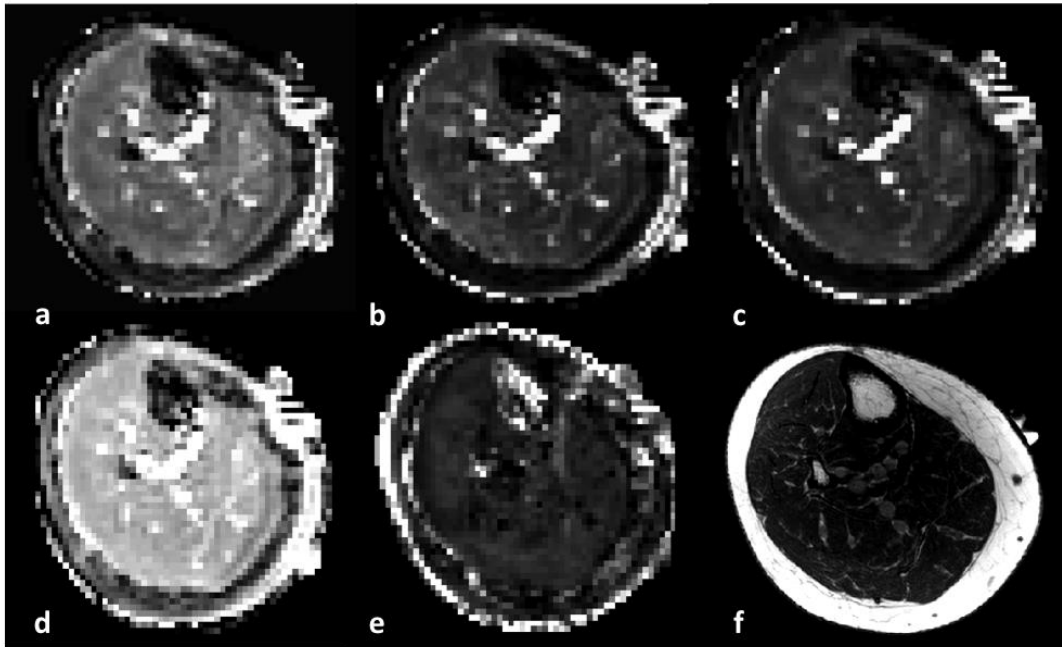


Figure 3.1: Sample diffusion tensor projection maps and proton density (PD) reference scan. The first (a), second (b), and third (c) eigenvalues, apparent diffusion coefficient (d), and fractional anisotropy (e) at the 66% site of the leg. The PD-weighted reference scan (f) is shown for the same individual.

3.3.7 Evaluation criteria for feasibility objectives

Participant recruitment aimed to evaluate the enrolment of nine healthy women into the study using three strategies: posters, a presentation, and a letter mail-out. The recruitment rate was determined by the total number of volunteers attracted, interested, and screened through each strategy in order to enrol nine participants. Criteria for feasible participant tolerance to the MRI scan acquisition protocol were uninterrupted scanning sessions for each individual and the absence of image artifacts. PD-weighted, DTI and ^1H -MRS scanning protocols were evaluated based on the optimal amount (100%) of data that could be used for analysis. The scanning acquisition and analysis protocols would be considered feasible if there were no missing data. Mean and standard

deviation (SD) values and 95% confidence intervals for all muscle and fat outcomes were generated using SPSS statistical software (v20.0: IBM Corp).

3.4 RESULTS

3.4.1 Feasibility of participant recruitment

A summary of participant recruitment, including reasons for exclusion, is illustrated in Figure 3.2. In four months, a total of 25 women expressed interest in the study. The poster advertisements and a presentation to a local community group yielded nearly all of the interested volunteers. The mailed letter invitation to past study participants yielded one interested volunteer. Five of the 25 interested volunteers were not screened for eligibility, whereas 19 were successfully contacted and screened by telephone. Ten of these women were ineligible for the study. Therefore, nine participants met the eligibility and safety criteria and were enrolled. Characteristics of the study participants are presented in Table 3.1. The overall recruitment rate was one participant every two weeks.

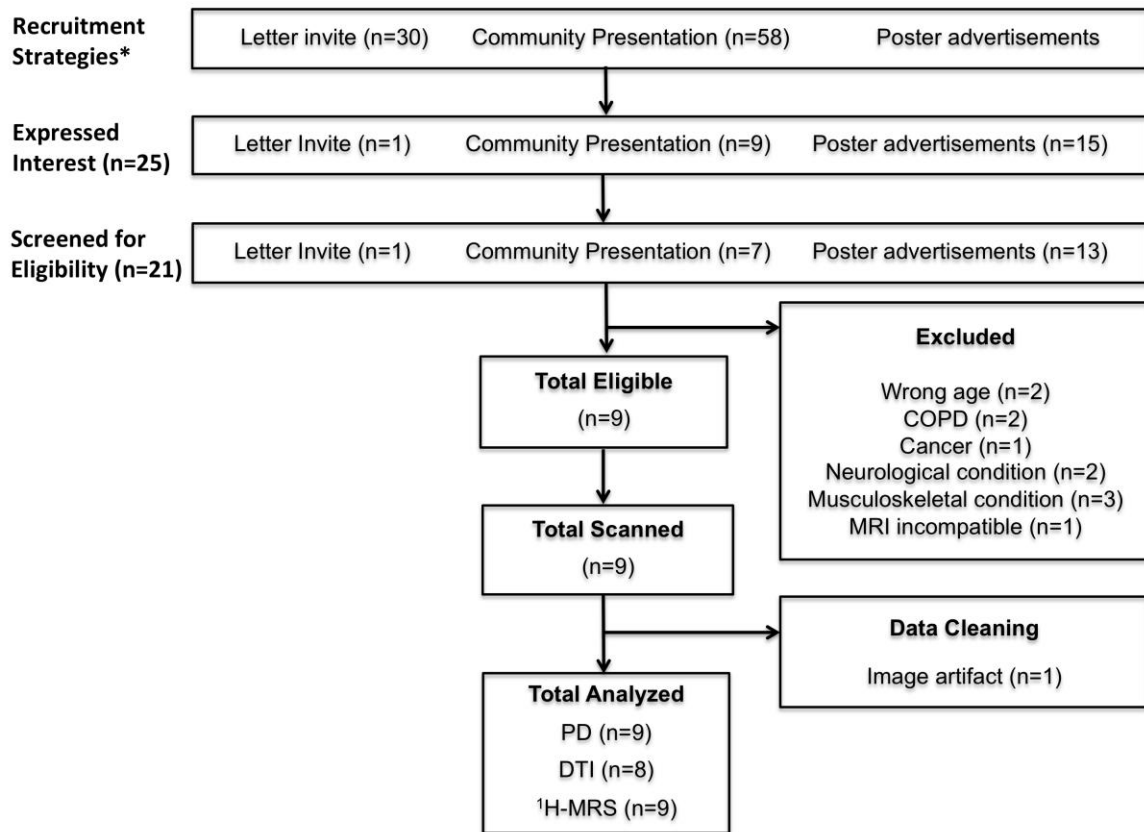


Figure 3.2: Flow chart demonstrating the number of individuals exposed, interested, and eligible for the study based on recruitment strategy. The number of volunteers excluded and the reasons for their exclusion are provided.

COPD: chronic obstructive pulmonary disorder; MRI: magnetic resonance imaging; PD: proton density; DTI: diffusion tensor imaging; ¹H-MRS: proton magnetic resonance spectroscopy.

* Since the exact number of individuals reached by poster advertisements is unknown, total number of individuals exposed to this recruitment strategy cannot be calculated

Table 3.1: Participant characteristics (N = 9)

Characteristics	Mean (SD)
Age (y)	71.0 (3.8)
Height (cm)	160.9 (5.1)
Weight (kg)	60.9 (10.0)
BMI (kg/m ²)	23.4 (3.1)
Years since menopause (y)	22.7 (3.9)
RAPA (points)	7 (1.7)

RAPA: Rapid Assessment of Physical Activity

3.4.2 Feasibility of participant tolerance to the scan acquisition protocol

The scan acquisition protocol was successful and imaging sessions were uninterrupted for all participants. Mounting the MRI scanner bed and assuming the supine position was performed with ease by most participants. Modifications to participant positioning were made for women with greater thoracic kyphosis or (risk of) vertebral fracture because the narrow scanner bed posed challenges for assuming a supine position. To assist these participants, the scan bed was lowered to allow the women to lie down on their side before slowly log-rolling over on to their back. The MRI technologist and investigator stood on either side of the bed to ensure the participant could roll on to her back safely. Care was taken to ensure that upon assuming supine posture no additional positional adjustments were required. Additional pillows were provided to support the head and neck to enhance comfort.

Accommodations were also made for participants of shorter stature with tibia lengths measuring less than 34cm. A short distance between the ankle and knee joints

was problematic for the leg being scanned because the superior surface of the foot contacted the RF coil cord connection point, which caused uncomfortable pressure on the foot. For the two participants with tibia lengths measuring less than 34cm, the RF coil was positioned on a small angle and slightly more superiorly. All efforts were made to keep the fiducial marker in the middle of the extremity coil to avoid signal loss around the 66% site. The coil diameter (13cm) was large enough to accommodate all legs, without the calf resting on the coil. Another modification to the initial positioning protocol was made upon receiving feedback from the first two participants who said that the left leg (i.e., the side not being scanned) felt like it was not completely secure and was sliding during the scanning. To address this issue and prevent potential motion during scanning, all subsequent participants had a Velcro strap fastened around the thighs.

The total duration of the scanning protocol was 35min. The amount of time spent motionless in the supine position was noted as a minor discomfort by four participants. However, the discomfort was not serious enough to require use of the call bell and there were no modifications to the acquisition protocol to address the minor discomfort.

3.4.3 Feasibility of image acquisition protocol

PD-weighted image acquisition was successful for all participants. Interim analyses were conducted after the first four participants were scanned to confirm good image quality was achieved. Bright signal intensity bands in the frequency encoding direction (right/left) in the PD-weighted images were identified with image segmentation (Figure 3.3). This type of signal resulted in segmentation pixels representing intramuscular fat that did not reflect its distribution within skeletal muscle. An example

of the false distribution of pixels representing intramuscular fat is shown in Figure 3.3(c). To provide greater tissue contrast and less edge blurring, we retrospectively applied the PURE post-processing filter to the first four participants' images and added this filter to the acquisition protocol for subsequent participants. This modification successfully removed the unwanted intensity bands, improved tissue contrast, and reduced edge blurring, as shown in Figure 3.3(d). Moreover, the PURE filter was practical because it did not increase the duration of the scan acquisition protocol or interfere with the watershed algorithm employed by the segmentation software.

DTI scanning successfully produced images that could be analyzed for all but one participant. For the participant with data excluded from analysis, DTI scans were unreadable due to image artifacts.

$^1\text{H-MRS}$ scanning and analysis was successful for all participants. The parameters remained unchanged.

3.4.4 MRI muscle and fat parameter estimates

The mean, SD, and 95% confidence interval (95% CI) values and for PD-weighted, DTI, and $^1\text{H-MRS}$ measures are reported in Table 3.2. Figure 3.4 illustrates the distribution of $^1\text{H-MRS}$ IMCL resonance areas.

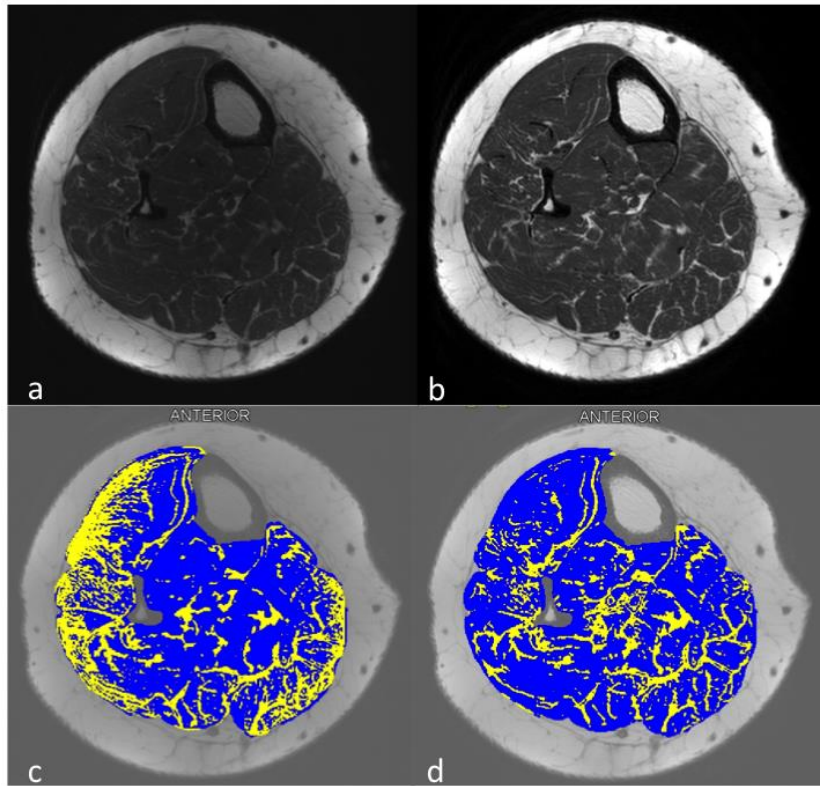


Figure 3.3: Representative axial leg images of a postmenopausal woman with and without the PURE filter application. Images without the PURE filter (a, c) and images with the filter (b, d) are presented as original (a, b) and segmented (c, d) scans. Misrepresentation of intramuscular fat (yellow) with muscle (blue) occurred as a result of signal intensity bands near the subcutaneous fat (c). The PURE post-processing filter applied to the axial PD images of the leg removed the bright signal that was falsely representing intramuscular fat (d).

Table 3.2: Variability in proton density imaging, diffusion tensor imaging, and proton magnetic resonance spectroscopy muscle and fat outcomes in the leg muscle regions of interest (ROIs). All values presented as mean (SD) with 95% confidence interval (CI)

MRI scanning technique and ROI	Mean (SD)	95% CI
PD-weighted		
Total Muscle CSA (cm ²)	46.1 (8.53)	(39.6, 52.7)
Total Intramuscular fat CSA (cm ²)	9.24 (6.18)	(4.5, 14.0)
DTI		
λ_1 (x 10 ⁻³ mm ² /s)		
Tibialis anterior	2.15 (0.12)	(2.06, 2.24)
Tibialis posterior	2.05 (0.35)	(1.78, 2.32)
Soleus	2.16 (0.11)	(2.08, 2.24)
Medial gastrocnemius	2.18 (0.21)	(2.02, 2.35)
Lateral gastrocnemius	2.13 (0.22)	(1.97, 2.30)
λ_2 (x 10 ⁻³ mm ² /s)		
Tibialis anterior	1.56 (0.16)	(1.44, 1.69)
Tibialis posterior	1.42 (0.31)	(1.18, 1.66)
Soleus	1.53 (0.10)	(1.45, 1.61)
Medial gastrocnemius	1.47 (0.11)	(1.38, 1.56)
Lateral gastrocnemius	1.54 (0.16)	(1.42, 1.66)
λ_3 (x 10 ⁻³ mm ² /s)		
Tibialis anterior	1.40 (0.12)	(1.31, 1.49)
Tibialis posterior	1.16 (0.35)	(0.89, 1.43)
Soleus	1.35 (0.09)	(1.28, 1.42)
Medial gastrocnemius	1.31 (0.13)	(1.20, 1.41)
Lateral gastrocnemius	1.25 (0.13)	(1.15, 1.34)
ADC (x 10 ⁻³ mm ² /s)		
Tibialis anterior	1.70 (0.13)	(1.60, 1.80)

Tibialis posterior	1.54 (0.33)	(1.29, 1.80)
Soleus	1.68 (0.09)	(1.61, 1.75)
Medial gastrocnemius	1.65 (0.15)	(1.54, 1.77)
Lateral gastrocnemius	1.64 (0.15)	(1.52, 1.76)
FA		
Tibialis anterior	0.23 (0.02)	(0.214, 0.250)
Tibialis posterior	0.32 (0.11)	(0.237, 0.402)
Soleus	0.25 (0.03)	(0.230, 0.269)
Medial gastrocnemius	0.28 (0.03)	(0.256, 0.296)
Lateral gastrocnemius	0.27 (0.03)	(0.246, 0.296)
¹ H-MRS		
IMCL content (mmol/kg wet weight)	0.091 (0.054)	(0.050, 0.132)

PD: proton density; DTI: diffusion tensor imaging; CSA: cross-sectional area; ADC: apparent diffusion coefficient; FA: fractional anisotropy; ¹H-MRS: proton magnetic resonance spectroscopy; IMCL: intramyocellular lipid

3.5 DISCUSSION

This study suggests that it is feasible to recruit a sample of community-dwelling, older women to perform PD-weighted, DTI, and ¹H-MRS scanning techniques for measuring muscle structure in the leg. The four-month (January thru April) recruitment strategy yielded 25 interested volunteers, of which nine met the safety and eligibility criteria. The protocol was well tolerated by all participants. Acquisition parameters were enhanced for the PD-weighted images to improve tissue contrast for segmentation analysis. Complete data were obtained and analyzed from PD-weighted and ¹H-MRS scanning protocols. This is the first study to combine three MRI techniques to assess muscle structure in the leg of older women non-invasively.

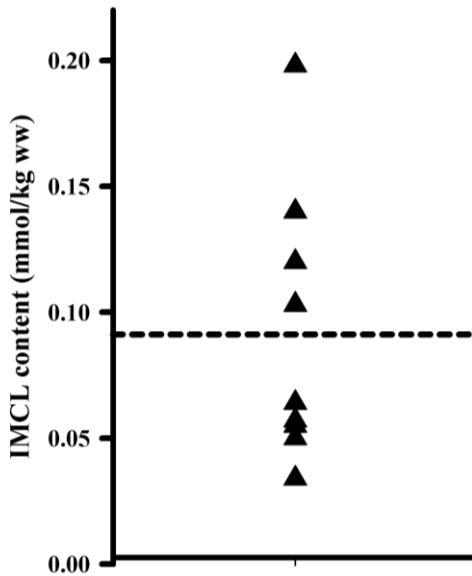


Figure 3.4: Individual values for intramyocellular lipid (IMCL) content. Relative IMCL content was quantified with ^1H -MRS in the tibialis anterior muscle of nine older women. The dotted horizontal line represents the mean value.

Posters and a brief presentation to a community group of older adults yielded all study participants. Although we cannot determine how many women viewed the poster advertising, the overall rate of recruitment was about one participant every two weeks. Recruitment of older adults for health research studies suggests that nearly three volunteers must be screened to enroll one eligible participant³⁹. Our short recruitment timeline required nearly two volunteers to be screened for every participant included. This improved rate of inclusion may be because we targeted community and seniors centers, since we expected that moderately active women between the ages of 65 and 75 would be frequenting these facilities. However, we may have missed potentially eligible women that do not frequent these centers. Presentations have been reported to yield a high number of interested volunteers and eligible participants among older adults for

health research⁴⁰. Similarly, we found that the presentation to a community group of 58 women given by the lead investigator was an efficient recruitment strategy. We speculated that putting a face to the project, up-front clarification of the study goals, and an explanation of participant exclusion criteria might have contributed to the success of this strategy. As reported previously by Adams et al (1997), mailing letters was not a successful strategy. Although the 30 letter recipients had previously participated in research conducted by the current study investigators and indicated interest in future participation, the poor response may have related to the small number of letters sent, the time of year, or changes in health status.

Physical characteristics that impacted positioning of older women on the MRI scanner bed were short stature and the presence (or risk of) vertebral fracture and kyphosis. Women with short stature were more likely to have short tibiae, and, in turn, positioning the extremity coil around the region of interest posed a challenge that we overcame while ensuring that signal was not lost. Importantly, all images acquired from women of short stature were successfully analyzed. Women with kyphosis or (a risk of) vertebral fracture must be aware of their spinal alignment during daily activities. Severe kyphosis (i.e., hyperkyphosis) modifies the forces on vertebral bodies⁴¹ and reduces trunk proprioception⁴². Therefore, movements that involve bending and twisting about the spine must be avoided⁴³. Special considerations were made for mounting and dismounting the scanner bed and finding a comfortable supine position to assume during the scanning. Future studies may elect to measure thoracic curvature to identify a kyphosis angle that may be contraindicated for longer MRI scanning protocols in the

supine position. Discomfort in the supine position could lead to movement artifact; however, all scans in our study were analyzed successfully. We suggest that future studies of older adults consider physical characteristics during the development of study design, since duration of the scanning protocol and positioning requirements could influence image quality.

Optimal image quality is essential for segmenting intramuscular fat and muscle from PD-weighted images. The PD-weighted images acquired prior to application of the PURE filter were affected by field inhomogeneity that could have resulted from variations in the magnetic field or the distance of the body segment to the receiving coil⁴⁴. Segmentation of muscle and fat was simplified with the PURE filter because the greater contrast between tissues and less edge blurring reduced the amount of manual segmentation required. We recommend that future studies interested in separating intramuscular fascia from muscle fascia or performing similar analyses employ a filter that improves tissue contrast, particularly among older adults with poorer muscle border definition and greater fat infiltration.

In our image analysis protocol, muscle was segmented as a single unit, but there may be advantages to separating certain muscles or compartments. Independent analysis of fat infiltration within individual muscles or functional muscle compartments would be valuable for ascertaining whether the size or tissue composition (fibre type distribution) of certain muscles correlates with certain disease or functional outcomes. A recent study that examined individual muscles and compartments of healthy obese and diabetic adults reported that the gastrocnemius muscle had the greatest ratio of intramuscular fat to

muscle volume in the leg¹⁹. Total calf intramuscular fat volume was inversely related to physical performance measured as the maximum distance walked in six minutes and the physical performance test, which evaluates how long it takes an individual to perform nine activities of daily living (e.g., ascending ten steps, picking up a coin off the floor)¹⁹. However, the relationships between individual muscles and physical performance measures were not tested¹⁹. One practical consideration for analyzing individual muscles is the amount of time required to perform the segmentation. Although semi-automated MR image analysis packages could reduce operator time for the measurement of certain muscles, their use is reliant upon sufficient image contrast of muscle borders to enable the software to delineate between muscles and compartments.

Missing data resulted from a substantial amount of motion artifact in one participant's DTI scan. Knee and ankle joints were stabilized with padding to restrict movement during scanning, but padding within the coil was not a viable option. Padding the leg within the coil would result in compression of the muscle fascia and lead to a change in the orientation of muscle fibres, resulting in modified diffusivity measures. A study that measured soleus IMCL concentrations in endurance trained female runners reported padding the leg within the coil⁴⁵, but the soleus is situated deep to the gastrocnemius muscle and compression would be less likely to affect the acquisition of metabolite spectra. Moving forward, it may be prudent to examine the magnitude of the effect of padding on muscle DTI measures. For studies exclusively focused on frail individuals or a population that would be challenged to remain motionless for a period of time, the development of a standardized padding strategy may be appropriate maintain

uniform effects for all participants.

We successfully quantified relative IMCL content in the tibialis anterior muscle for all participants using $^1\text{H-MRS}$. The successful acquisition and analysis of IMCL content suggests that this non-invasive alternative to muscle biopsy³² is feasible for our sample of older women. For consistency, the volume of interest was placed in the center of the tibialis anterior muscle to avoid including blood vessels and visible fat. Placement of the volume of interest was more challenging for participants with smaller muscles, since less tissue was available for moving the volume of interest to exclude blood vessels. The spectroscopic analysis was successful for all our participants, which may be attributed to methodological considerations observed in our protocol. Importantly, the separation of IMCL and from extramyocellular lipid pools is most distinct when muscle fibre alignment is parallel to the magnetic field³². Consequently, the tibialis anterior muscle provides an excellent measurement site as compared to pennate muscles, such as the soleus and gastrocnemius. Application of this technique may be important for investigating conditions related to fat infiltration of muscle, such as diabetes. Boettcher et al. (2009) demonstrated that IMCL content is moderately and positively correlated with fat distribution in other depots, yet women showed a significant negative relationship between tibialis anterior IMCL content and insulin sensitivity ($r = -0.44$, $n = 152$, 95% CI: $-0.30, -0.56$). The application of spectroscopy to evaluate metabolic muscle function associated with aging and disease has been discussed previously⁴⁶, yet this is the first time feasibility data have been presented for measuring IMCL content in the leg muscle of older women. Application of this method is recommended as a feasible non-invasive

alternative to the muscle biopsy for measuring IMCL content.

Table 3.3: Examples of sample size calculations for prospective studies to determine the effect of increased physical activity level on leg muscle structure using the apparent diffusion coefficient (ADC) in older women

Muscle ROI	Effect size*	Sample size estimate (per group)	Total N required
Tibialis anterior	2.03	5	10
Soleus	1.51	8	16
Medial gastrocnemius	0.79	27	54
Lateral gastrocnemius	1.07	15	30

All calculations are based on a two-tailed significance level set at 0.05 and a power of 0.8. ADC measures for the control group were based on literature⁵⁴

* calculated as Cohen's *d*

The final feasibility objective was to report parameter estimates of MRI muscle and fat outcomes to assist in sample size calculations. Based on the values we report, Table 3.3 summarizes the number of individuals required to detect significant between-group differences in ADC for older women with high or moderate levels of physical activity. Depending on the muscle ROI, detecting differences in ADC could require as many as 54 participants, as in the case of medial head of gastrocnemius, or as few as ten participants, as the tibialis anterior estimate suggests. Cross-sectional studies have recruited as few as 7 women⁴⁵ and as many as 249 participants¹⁸. The use of advanced MRI scanning is limited by the considerable level of expertise required for scan acquisition and analyses. With the exception of tibialis posterior, the muscle ROIs we selected were similar to those reported in previous studies employing DTI in young

adults^{47, 48}. The eigenvalues in the ankle plantarflexor muscle ROIs (medial and lateral heads of gastrocnemius, tibialis posterior, soleus) of older women (Table 3.2) were lower compared to healthy young adults reported by Galban et al. (2005) and Deux et al. (2008). Similarly, mean λ_1 in the ankle dorsiflexor muscle ROI (tibialis anterior) was lower among older women compared to young healthy adults^{47, 48}. However, mean λ_2 and λ_3 in the tibialis anterior ROI were greater than those reported in young adults^{47, 48}. The sample size estimates and cross-study comparisons should be interpreted in light of a number of factors that contribute to differences in these values, including the strength of the magnet, number of diffusion encoding directions, b value, and ROI selection. Both studies described here for comparison^{47, 48} used a 1.5T magnet and fewer diffusion encoding directions (6 and 12) than our study. Image acquisition settings used in our study were in line with recommended number of diffusion encoding directions and b value⁴⁹. Previous reports show that ROIs containing voxels contaminated with fat infiltration and blood vessels introduce partial volume artifacts, which negatively affect the validity of diffusivity rates quantified by DTI^{50, 51}. To avoid the confounding effects of fat infiltration, we selected smaller ROIs composed of at least 75% lean tissue⁵¹. We propose that future DTI studies examining elderly populations follow a similar approach to acquiring and analyzing muscle ROIs.

We have demonstrated that applying advanced MRI scanning techniques is feasible for a cross-sectional study design; however, additional methodological considerations would be essential for applying these methods prospectively. First, we acknowledge the importance of calculating the reliability of a measurement and therefore

interpret our parameter estimates with caution. We did not report reliability coefficients; however, excellent intrarater reliability is reported for lower for extremity muscle and fat segmentation^{52, 53} and DTI muscle analysis⁵⁰ using similar techniques and samples to ours. Second, important covariates of MRI measurements of muscle structure are vitamin D levels and habitual exercise levels. We did not measure serum vitamin D levels but all participants self-reported daily supplementation of 1000 to 2000IU of vitamin D. Daily activity levels were captured with a self-report questionnaire validated in older adults. Finally, hydration status was not controlled and may have affected MRI muscle measurements. We recommend that future studies consider these factors. Additional aspects to consider prior to applying these techniques to monitor disease progression or treatment effects are the feasibility of participant retention.

We recommend that future studies examine the association of muscle microstructure with clinical outcomes of physical performance. It is important to gain knowledge about the relationships between muscle structure and physical function, since findings will identify outcomes for interventions aimed at preventing, managing, or treating disease- or age-related decline in skeletal muscle function.

3.6 CONCLUSIONS

Based on successful participant recruitment, tolerance, and optimal scan acquisition and analyses protocols, we have demonstrated that it is feasible to combine PD-weighted, DTI, and ¹H-MRS imaging techniques for characterizing skeletal muscle structure in the leg of older women. We provide adjusted protocols for participant

positioning and image acquisition based on our feasibility study of older women. We recommend that the PURE filter be applied to PD-weighted images to improve tissue contrast and facilitate segmentation of muscle and intramuscular fat. We identify additional factors to consider when applying these techniques in future studies.

3.7 ACKNOWLEDGEMENTS

The authors thank Norm Konyer and the MRI technologists (Janet Burr, Cheryl Contant, Julie Lecomte) for their assistance throughout protocol development and data collection. AL is funded in part by the Ontario Women's Health Scholar Award and the Joint Motion Program, a Canadian Institutes of Health Research Training Program in Musculoskeletal Health Research and Leadership.

3.8 REFERENCES

1. Hepple RT. Muscle atrophy is not always sarcopenia. *J Appl Physiol* 2012;113(4):677-9.
2. Widrick JJ, Maddalozzo GF, Lewis D, Valentine BA, Garner DP, Stelzer JE, et al. Morphological and functional characteristics of skeletal muscle fibers from hormone-replaced and nonreplaced postmenopausal women. *J Gerontol A Biol Sci Med Sci* 2003;58(1):3-10.
3. Kent-Braun JA, Ng AV, Young K. Skeletal muscle contractile and noncontractile components in young and older women and men. *J Appl Physiol* 2000;88(2):662-8.
4. Lieber R. Skeletal muscle structure, function, & plasticity: The physiological basis of rehabilitation. Second ed. Philadelphia, PA: Lippincott Williams and Wilkins; 2002.
5. Roberts SB, Rosenberg I. Nutrition and aging: Changes in the regulation of energy metabolism with aging. *Physiol Rev* 2006;86(2):651-67.
6. Roubenoff R. Sarcopenia: A major modifiable cause of frailty in the elderly. *J Nutr Health Aging* 2000;4(3):140-2.
7. Cooper R, Mishra G, Clennell S, Guralnik J, Kuh D. Menopausal status and physical performance in midlife: Findings from a British Birth Cohort Study. *Menopause* 2008;15(6):1079-85.
8. Forsberg AM, Nilsson E, Werneman J, Bergstrom J, Hultman E. Muscle composition in relation to age and sex. *Clin Sci (Lond)* 1991;81(2):249-56.
9. Pansini F, Cervellati C, Guariento A, Stacchini MA, Castaldini C, Bernardi A, et al. Oxidative stress, body fat composition, and endocrine status in pre- and postmenopausal women. *Menopause* 2008;15(1):112-8.
10. Goodpaster BH, Park SW, Harris TB, Kritchevsky SB, Nevitt M, Schwartz AV, et al. The loss of skeletal muscle strength, mass, and quality in older adults: The health, aging and body composition study. *J Gerontol A Biol Sci Med Sci* 2006;61(10):1059-64.
11. Visser M, Goodpaster BH, Kritchevsky SB, Newman AB, Nevitt M, Rubin SM, et al. Muscle mass, muscle strength, and muscle fat infiltration as predictors of incident mobility limitations in well-functioning older persons. *J Gerontol A Biol Sci Med Sci* 2005;60(3):324-33.

12. Buford TW, Lott DJ, Marzetti E, Wohlgemuth SE, Vandenborne K, Pahor M, et al. Age-related differences in lower extremity tissue compartments and associations with physical function in older adults. *Exp Gerontol* 2012;47(1):38-44.
13. Marcus RL, Addison O, Dibble LE, Foreman KB, Morrell G, Lastayo P. Intramuscular adipose tissue, sarcopenia, and mobility function in older individuals. *J Aging Res* 2012;2012:629637.
14. Lang T, Cauley JA, Tylavsky F, Bauer D, Cummings S, Harris TB, et al. Computed tomographic measurements of thigh muscle cross-sectional area and attenuation coefficient predict hip fracture: The health, aging, and body composition study. *J Bone Miner Res* 2010;25(3):513-9.
15. Johnston JD, Liao L, Dolovich AT, Leswick DA, Kontulainen SA. Magnetic resonance imaging of bone and muscle traits at the hip: An in vivo precision study. *J Musculoskelet Neuronal Interact* 2014;14(1):104-10.
16. Kim JY, Chae SU, Kim GD, Cha MS. Changes of paraspinal muscles in postmenopausal osteoporotic spinal compression fractures: Magnetic resonance imaging study. *J Bone Metab* 2013;20(2):75-81.
17. Maly MR, Calder KM, Macintyre NJ, Beattie KA. Relationship of intermuscular fat volume in the thigh with knee extensor strength and physical performance in women at risk of or with knee osteoarthritis. *Arthritis Care Res* 2013;65(1):44-52.
18. Boettcher M, Machann J, Stefan N, Thamer C, Haring HU, Claussen CD, et al. Intermuscular adipose tissue (IMAT): Association with other adipose tissue compartments and insulin sensitivity. *J Magn Reson Imaging* 2009;29(6):1340-5.
19. Tuttle LJ, Sinacore DR, Mueller MJ. Intermuscular adipose tissue is muscle specific and associated with poor functional performance. *J Aging Res.* 2012;172957.
20. Louwerens JW, van Linge B, de Klerk LW, Mulder PG, Snijders CJ. Peroneus longus and tibialis anterior muscle activity in the stance phase. A quantified electromyographic study of 10 controls and 25 patients with chronic ankle instability. *Acta Orthop Scand* 1995;66(6):517-23.
21. Honeine JL, Schieppati M, Gagey O, Do MC. The functional role of the triceps surae muscle during human locomotion. *PLoS One* 2013;8(1):e52943.
22. Noseworthy MD, Davis AD, Elzibak AH. Advanced MR imaging techniques for skeletal muscle evaluation. *Semin Musculoskelet Radiol* 2010;14(2):257-68.
23. Boesch C. Musculoskeletal spectroscopy. *J Magn Reson Imaging* 2007;25(2):321-38.

24. Galban CJ, Maderwald S, Uffmann K, de Greiff A, Ladd ME. Diffusive sensitivity to muscle architecture: A magnetic resonance diffusion tensor imaging study of the human calf. *Eur J Appl Physiol* 2004;93(3):253-62.
25. Galban CJ, Maderwald S, Stock F, Ladd ME. Age-related changes in skeletal muscle as detected by diffusion tensor magnetic resonance imaging. *J Gerontol A Biol Sci Med Sci* 2007;62(4):453-8.
26. Manenti G, Capuani S, Fusco A, Fanucci E, Tarantino U, Simonetti G. Osteoporosis detection by 3T diffusion tensor imaging and MRI spectroscopy in women older than 60 years. *Aging Clin Exp Res* 2013;25 Suppl 1:S31-4.
27. Barzilay JI, Blaum C, Moore T, Xue QL, Hirsch CH, Walston JD, et al. Insulin resistance and inflammation as precursors of frailty: The cardiovascular health study. *Arch Intern Med* 2007;167(7):635-41.
28. Arain M, Campbell MJ, Cooper CL, Lancaster GA. What is a pilot or feasibility study? A review of current practice and editorial policy. *BMC Med Res Methodol* 2010;10:67,2288-10-67.
29. International Society for the Advancement of Kinanthropometry. International standards for anthropometric assessment. Australia: International Society for the Advancement of Kinanthropometry; 2001.
30. Topolski TD, LoGerfo J, Patrick DL, Williams B, Walwick J, Patrick MB. The rapid assessment of physical activity (RAPA) among older adults. *Prev Chronic Dis* 2006;3(4):A118.
31. Elzibak AH, Noseworthy MD. Assessment of diffusion tensor imaging indices in calf muscles following postural change from standing to supine position. *Magn Reson Mater Phy* doi: 10.1007/s10334-013-0424-1.
32. Boesch C, Slotboom J, Hoppeler H, Kreis R. In vivo determination of intramyocellular lipids in human muscle by means of localized ¹H-MR-spectroscopy. *Magn Reson Med* 1997;37(4):484-93.
33. Jenkinson M, Beckmann CF, Behrens TE, Woolrich MW, Smith SM. FSL. *Neuroimage* 2012;62(2):782-90.
34. Wang R, Benner T, Sorensen A, Wedeen V. Diffusion Toolkit: A software package for diffusion imaging data processing and tractography. In: Proceedings of the 16th scientific meeting of the International Society for Magnetic Resonance Medicine, Berlin, p 3720.

35. Jenkinson M, Bannister P, Brady M, Smith S. Improved optimization for the robust and accurate linear registration and motion correction of brain images. *Neuroimage* 2002;17(2):825-41.
36. Cox RW. AFNI: Software for analysis and visualization of functional magnetic resonance neuroimages. *Comput Biomed Res* 1996;29(3):162-73.
37. Le Bihan D, Mangin JF, Poupon C, Clark CA, Pappata S, Molko N, et al. Diffusion tensor imaging: Concepts and applications. *J Magn Reson Imaging* 2001;13(4):534-46.
38. Provencher SW. Estimation of metabolite concentrations from localized in vivo proton NMR spectra. *Magn Reson Med* 1993;30(6):672-679.
39. McMurdo ME, Roberts H, Parker S, Wyatt N, May H, Goodman C, et al. Improving recruitment of older people to research through good practice. *Age Ageing* 2011;40(6):659-65.
40. Adams J, Silverman M, Musa D, Peele P. Recruiting older adults for clinical trials. *Control Clin Trials* 1997;18(1):14-26.
41. Briggs AM, van Dieen JH, Wrigley TV, Greig AM, Phillips B, Lo SK, et al. Thoracic kyphosis affects spinal loads and trunk muscle force. *Phys Ther* 2007;87(5):595-607.
42. Granito RN, Aveiro MC, Renno AC, Oishi J, Driusso P. Comparison of thoracic kyphosis degree, trunk muscle strength and joint position sense among healthy and osteoporotic elderly women: A cross-sectional preliminary study. *Arch Gerontol Geriatr* 2012;54(2):e199-202.
43. Myers ER, Wilson SE. Biomechanics of osteoporosis and vertebral fracture. *Spine*. 1997;22(24 Suppl):25S-31S.
44. Noterdaeme O, Brady M. Correction of inhomogeneities in magnetic resonance images. *Conf Proc Eng Med Biol Soc* 2008;2221-4.
45. Larson-Meyer DE, Newcomer BR, Hunter GR. Influence of endurance running and recovery diet on intramyocellular lipid content in women: A ^1H NMR study. *Am J Physiol Endocrinol Metab* 2002;282(1):E95-E106.
46. McCully K. Magnetic resonance as a tool to study sarcopenia. *Muscle Nerve Suppl* 1997;5:S102-6.

47. Galban CJ, Maderwald S, Uffmann K, Ladd ME. A diffusion tensor imaging analysis of gender differences in water diffusivity within human skeletal muscle. *NMR Biomed* 2005;18(8):489-98.
48. Deux JF, Malzy P, Paragios N, Bassez G, Luciani A, Zerbib P, et al. Assessment of calf muscle contraction by diffusion tensor imaging. *Eur Radiol*. 2008 Oct;18(10):2303-10.
49. Froeling M, Nederveen AJ, Nicolay K, Strijkers GJ. DTI of human skeletal muscle: The effects of diffusion encoding parameters, signal-to-noise ratio and T2 on tensor indices and fiber tracts. *NMR Biomed* 2013;26(11):1339-52.
50. Damon BM. Effects of image noise in muscle diffusion tensor (DT)-MRI assessed using numerical simulations. *Magn Reson Med* 2008;60(4):934-44.
51. Williams SE, Heemskerk AM, Welch EB, Li K, Damon BM, Park JH. Quantitative effects of inclusion of fat on muscle diffusion tensor MRI measurements. *J Magn Reson Imaging* 2013;38(5):1292-7.
52. Beattie KA, MacIntyre NJ, Ramadan K, Inglis D, Maly MR. Longitudinal changes in intermuscular fat volume and quadriceps muscle volume in the thighs of women with knee osteoarthritis. *Arthritis Care Res* 2012;64(1):22-9.
53. Song MY, Ruts E, Kim J, Janumala I, Heymsfield S, Gallagher D. Sarcopenia and increased adipose tissue infiltration of muscle in elderly african american women. *Am J Clin Nutr* 2004;79(5):874-80.
54. Okamoto Y, Mori S, Kujiraoka Y, Nasu K, Hirano Y, Minami M. Diffusion property differences of the lower leg musculature between athletes and non-athletes using 1.5T MRI. *Magn Reson Mater Phy* 2012;25(4):277-84.

CHAPTER FOUR

MUSCLE AND FAT MACROSTRUCTURE AND MICROSTRUCTURE MEASURED USING MAGNETIC RESONANCE IMAGING ARE SIMILAR IN HEALTHY POSTMENOPAUSAL WOMEN WITH AND WITHOUT OSTEOPOROSIS

PREFACE TO CHAPTER FOUR

Authors: Amanda L. Lorbergs, Michael D. Noseworthy, Paul W. Stratford, David W. Holdsworth, Jonathan D. Adachi, Norma J. MacIntyre

Publication status: This manuscript has been prepared and formatted for submission to the *Journal of Bone and Mineral Research*.

Summary: Using the results from the protocol development and feasibility studies, this study compared musculoskeletal tissue structure and composition in the leg of postmenopausal women with and without osteoporosis, and determined the relationships between bone, muscle, fat, and physical performance. Compared to women without osteoporosis, women diagnosed and treated for osteoporosis have similar musculoskeletal tissue structure and composition. The study results highlight the interrelationships between muscle, bone, and fat on both macrostructural and microstructural scales. Greater fat infiltration within muscle was associated with bone that is weaker in compression loading. Gait speed was slower in women with greater fat infiltration within muscle.

Title

Muscle and fat macrostructure and microstructure measured using magnetic resonance imaging are similar in healthy postmenopausal women with and without osteoporosis

Authors

Amanda L. Lorbergs¹, Michael D. Noseworthy^{2,3}, Paul W. Stratford¹,
David W. Holdsworth⁴, Jonathan D. Adachi⁵, Norma J. MacIntyre¹

¹ School of Rehabilitation Science, McMaster University, Hamilton, ON, Canada

² Department of Electrical and Computer Engineering, McMaster University, Hamilton,
ON, Canada

³ School of Biomedical Engineering, McMaster University, Hamilton, ON, Canada

⁴ Robarts Research Institute, University of Western Ontario, London, ON, Canada

⁵ Department of Medicine, McMaster University, Hamilton, ON, Canada

Keywords: muscle, bone, physical performance, osteoporosis, pQCT, diffusion tensor imaging (DTI)

4.1 ABSTRACT

Muscle atrophy and fat infiltration predict bone loss, fractures, and declining physical performance. We aimed to compare musculoskeletal tissue structure and composition in the leg of postmenopausal women with and without osteoporosis, and to determine the relationships between bone, muscle, fat, and physical performance.

We studied 35 postmenopausal women (aged 60-75y) with similar physical activity levels, of which 18 women had osteoporosis and were taking bone-sparing medications. Peripheral quantitative computed tomography (pQCT) assessed leg muscle cross-sectional area (CSA) and density (MuD) at the 66% site and tibia bone structure (4%, 14%, 38%, 66% sites). Magnetic resonance imaging (MRI)-based measures of muscle microstructure (apparent diffusion coefficient (ADC), fractional anisotropy (FA)) were obtained for five muscle regions. Intramuscular fat volume in tibialis anterior (TibA), soleus (SOL), and gastrocnemius (GC) and total intermuscular fat were calculated from axial MRI scans. Intramyocellular lipid (IMCL) content was determined using proton magnetic resonance spectroscopy. Physical performance was assessed by gait speed and repeated chair stands. Data were analyzed using ANOVAs and Pearson correlations. Significance was set at $p \leq 0.05$ and correlation coefficients ≥ 0.40 or ≤ -0.40 .

Musculoskeletal tissue structure and composition did not differ between groups.

Intermuscular fat and bone mineral content were moderately associated ($r = 0.44-0.47$).

Bone strength at the 66% site correlated with ADC in the SOL ($r = 0.56$, 95%CI: 0.28, 0.75) and GC ($r = 0.50$, 95%CI: 0.20,0.71). Bone strength at the 4% site was inversely associated with IMCL content ($r = -0.50$, 95% CI: -0.73, -0.16). Gait speed was

associated MuD ($r = 0.50$, 95%CI: 0.20,0.71), and inversely associated with intramuscular fat in the TA ($r = -0.43$, 95%CI: -0.67,-0.11) and GC ($r = -0.41$, 95%CI: -0.65,-0.09).

Musculoskeletal tissue composition is similar in women diagnosed and treated for osteoporosis compared to women without osteoporosis. We have shown that women with more bone mineral had more fat depots between muscles. However, in women with more fat-filled muscle, the bone is weaker in compression loading. In addition, as fat depots within muscle increase, gait speed decreases. These novel measures of musculoskeletal composition may provide important insights into mechanisms by which exercise and diet may prevent osteoporotic fracture.

4.2 INTRODUCTION

Across the lifespan, bone and muscle structure and function are intricately related through genetic and lifestyle factors ^{1,2}. With aging, two conditions that have primary effects on one tissue are thought to have secondary effects on the other ³⁻⁵. The first condition is osteoporosis, characterized by loss of bone mass and microstructure that predisposes to bone fragility. The other is sarcopenia, described as the loss of skeletal muscle mass with replacement of muscle tissue with fat tissue ^{6,7}. The risk for developing these conditions is largely attributed to the menopausal transition, which results in declines in bone mineral density (BMD) and muscle mass ⁸⁻¹⁰. The personal and social burden associated with these conditions is often described by rising healthcare expenditures related to impaired mobility, increased falls risk, fractures, hospitalizations, and mortality ¹¹⁻¹⁵. To understand how we can augment physical function in postmenopausal women, the dynamic balance between age-related bone and muscle loss must be examined and, to that end, noninvasive methods for assessing the structure of these tissues over time are required.

Fat was once thought to be an inert tissue, but a surge of research has identified that not only the amount of fat, but also its distribution, is an important determinant of bone mass and structure ¹⁶⁻¹⁹. In fact, the clinical diagnosis of osteoporosis may alter the typical relationship between fat mass and BMD ^{20,21}. The interpretation of the literature is limited by the use of dual energy X-ray absorptiometry (DXA) to measure fat mass, which precludes the separation and quantification of fat located in and around muscle and other organs. Intramuscular fat, defined as the fat located within muscle and external to

the muscle cells, increases with advancing age and inactivity²²⁻²⁵. Magnetic resonance imaging (MRI) overcomes the limitations of using DXA by generating high-resolution axial images from which intramuscular fat can be visualized and quantified. MRI studies in older adults demonstrate that intramuscular fat is associated with dysfunctional muscle metabolism²⁶⁻²⁸, poor physical performance^{27,29}, and higher rates of hospitalization³⁰. As fat accumulates within muscle, the proportion of non-contractile tissue increases and the muscle generates less force and consequent adaptations to resistance training^{31,32}. Intramuscular fat may modify muscle fibre alignment and may partially explain why exercise interventions are less effective for eliciting bone adaptations in older adults³³. Fatty muscle may therefore be unable to generate physiological strains of sufficient magnitude to elicit a bone remodeling response. On the other hand, intermuscular fat (the fat situated within the fascial envelopes surrounding muscles and muscle compartments) may have a different association with muscle structure and function. Thigh intermuscular fat volume measured with MRI is associated with weaker knee extensor strength and slower performance on the timed repeated chair stand test in women with or at risk of knee osteoarthritis³⁴. Thus, the distribution and amount of fat in the lower limb may influence the force produced by skeletal muscle such that it is insufficient to elicit physiological strains on bone and perform functional tasks involving the lower extremities.

Muscle macrostructure, a term used hereafter to describe muscle cross-sectional area (CSA), density, and volume measurements, has been measured in the lower extremities with computed tomography (CT) and MRI. Measurements with CT have

demonstrated that smaller muscle CSA and lower muscle density are related to greater bone fragility³⁵⁻³⁸ and poorer physical performance³⁹⁻⁴¹. MRI measurements of muscle macrostructure are preferred to CT measures, which expose the individual to radiation and limit interpretation of fat accumulation due to limited soft tissue contrast. Despite its advantages, there is a paucity of research applying MRI to understanding the muscle-bone unit. MRI images of muscle and fat macrostructure can help determine the relationship between muscle, bone, and physical performance measures. Non-invasive assessment of muscle and fat macrostructure with MRI is an important avenue for clinicians and scientists interested in understanding the development and treatment of osteoporosis and sarcopenia.

More recently, advances in MRI facilitate non-invasive investigation of muscle microstructure through diffusion tensor imaging (DTI) and muscle composition by proton magnetic resonance spectroscopy (¹H-MRS). DTI has been applied extensively in neuroscience, but recently the technique has been utilized to measure muscle microstructure because DTI takes advantage of the anisotropic properties of skeletal muscle. The theory of DTI is described in greater detail elsewhere⁴². In brief, DTI calculates water diffusivity in three orthogonal directions⁴³. The calculated diffusion tensor provides information regarding the direction of the diffusivity of water molecules within muscle fibres from which we infer muscle fibre shape⁴⁴. Increased diffusivity is documented in aged, injured, and exercised leg muscles^{43,45,46}. Factors that alter diffusivity include membrane permeability and the interaction and size of associated macromolecules⁴⁷. Fat infiltration can be measured on a microscopic scale using ¹H-

MRS, which enables quantification of intramyocellular lipid (IMCL) content that is stored within the muscle cell⁴⁸. The relationships between DTI and IMCL content measures and bone structure and strength measures have not been examined.

Associations between bone structure and strength and muscle size and microstructure have not been investigated in postmenopausal women. Similarly, the relationship between intramuscular and intermuscular fat depots and bone strength and structure has not been reported in women with osteoporosis. Importantly, we do not know how measures of muscle structure and fat infiltration are associated with physical performance measures. Thus, the primary objective of this study was to compare bone structure and strength and muscle and fat macrostructure and microstructure in the leg of healthy postmenopausal women with and without osteoporosis. We hypothesized that there is a difference in bone, muscle, and fat measures between the two groups of women. Our secondary and tertiary objectives were to determine the associations between muscle and fat macrostructure and microstructure, tibial structure and strength, and physical performance outcomes, respectively. For our secondary and tertiary objectives, a finding of greater tissue isotropy and fat infiltration in women with inferior bone structure and poorer physical performance would support an association between muscle structure and composition with bone strength and physical functioning.

4.3 METHODS

4.3.1 Study Design and Sample

For this cross-sectional study, we recruited postmenopausal women that were classified as either: 1) diagnosed with osteoporosis, or 2) not diagnosed with osteoporosis. Women were eligible for inclusion if they were 60-75y old, had a DXA BMD test within the past three years, and reported moderate physical activity levels.

Multiple recruitment strategies were used. We posted fliers on community boards in hospitals, recreational centers, libraries, churches, pharmacies, physiotherapy clinics, residential seniors' buildings, and the university campus. Newspaper and community newsletter advertisements appeared in print and online. One investigator gave presentations to local osteoporosis support groups and recruited patients from a local osteoporosis clinic. Past study participants who consented to be contacted for future research were mailed invitations to participate in the current study.

Prior to enrolment, all interested volunteers were screened by telephone. Women were excluded if they reported any one of the following: diabetes, chronic obstructive pulmonary disorder, stroke, cancer in the past five years, smoking cigarettes in the past two years, surgery in the past six weeks, or neurologic or musculoskeletal condition affecting the back or lower limbs (e.g., knee and/or hip osteoarthritis, rheumatoid arthritis). In accordance with MRI safety standards, volunteers were also excluded if they reported MRI incompatibility. Our institutional Research Ethics Review Board approved

the study protocol (Appendix B), and all participants provided written informed consent prior to enrolling in the study.

4.3.2 Definition of participant groups

Women allocated to the osteoporosis group had a physician's diagnosis of osteoporosis (n = 18). Women who were not diagnosed with osteoporosis by their physician were allocated to the reference group (n = 17).

4.3.3 Interview

Information on the participant's current health status, years since menopause, current medication use (including vitamin and mineral supplements), and fracture history was collected in a short interview. Self-reported history of fragility fractures, defined as non-traumatic fractures occurring as the result of a fall from standing height or less, excluding any fractures of the skull, fingers and toes, was recorded. Each participant's most recent BMD test results were obtained from medical records.

4.3.4 Self-reported physical activity levels

Self-reported physical activity questionnaires were administered at the interview. The Rapid Assessment of Physical Activity (RAPA) is a nine-item questionnaire that captures the frequency and intensity of non-sports related activity with "yes" or "no" responses. RAPA scores between six and ten represent an active lifestyle, whereas scores between two and five are considered under-active ⁴⁹.

The Human Activity Profile (HAP) is a 94-item questionnaire consisting of activities listed in ascending order of metabolic energy required to complete them ⁵⁰. Response options are: "*still doing this activity*", "*stopped doing this activity*", and "*never*

did this activity". Each participant's Adjusted Activity Score (AAS) was calculated as the difference between the Maximal Activity Score (i.e., highest numeral assigned to the activity that the individual is still *doing*) and the adjustment score (i.e., number of activities an individual has *stopped doing*) to represent the range of activities the participant can perform. AAS scores are reported for each participant. Higher AAS scores (maximum score is 94) reflect better physical functioning⁵⁰.

4.3.5 Anthropometry

Height was measured to the nearest 1mm using a wall-mounted stadiometer. Body weight was measured to the nearest 0.1kg with an electronic scale. Height and weight were used to calculate body mass index (BMI, kg/m²). The length of the right tibia was measured to the nearest 1mm from the base of the medial malleolus to the superior margin of the medial epicondyle while the participant was seated with feet flat on the floor and knees bent at a 90-degree angle⁵¹. The 66% site of the tibia was calculated and marked with ink for peripheral quantitative computed tomography (pQCT) and a fiducial marker for MRI scanning.

4.3.6 pQCT scan acquisition protocol

The right leg was imaged using the Stratec XCT2000 pQCT (Pforzheim, Germany) according to the following protocol. Participants were seated on a height-adjustable chair with their leg comfortably extended through the scanner gantry. The tibia was orthogonal to the scanner gantry and the heel rested on the standard foot positioning aid. The foot was secured with a Velcro strap and a foam padded fixation

clamp secured the proximal leg to prevent movement during scanning. Care was taken to ensure that the leg was well supported and centered in the imaging field.

A 30mm coronal scout scan was obtained to allow the operator to manually place the anatomical reference line at the medial tip of the distal tibia endplate. Measuring proximally from the reference line, the scanner calculated and acquired axial images at the 4%, 14%, and 38% scan sites with an in-plane resolution of 0.4mm and 20mm/s scan speed. The image at the 66% scan site was obtained without a scout scan. The scanner was manually positioned at the ink mark that identified the 66% scan site and images were acquired with an in-plane resolution of 0.5mm scan speed of 15mm/s. All pQCT images had a slice thickness of 2.4mm. Total scan time for all four sites was about 6min. One trained operator acquired all images.

4.3.7 pQCT scan analysis protocol

Using Stratec software (Version 5.4), the following image analysis parameters were applied to 4% site images: Contour mode 2, Peel mode 1, and a threshold of 280mg/cm³ to separate bone from surrounding soft tissue. Outcomes measured at the tibial 4% site were volumetric BMD (mg/cm³) for total (ToD) and trabecular (TrD) compartments, cross-sectional area (mm²) for the total and trabecular bone compartments (ToA and TrA, respectively), bone mineral content (mg/mm) for total and trabecular bone compartments (ToC and TrC, respectively), and resistance to compression loading represented by the bone strength index (BSI, mg²/mm⁴)⁵². BSI was calculated as follows:

$$BSI = \frac{ToD^2}{1000000} \times ToA \quad (1)$$

At the 14, 38, and 66% sites we used Contour mode 3 and Peel mode 2 with thresholds set at 711mg/cm³ to separate cortical bone from soft tissue. Outcomes measured at the 14, 38, and 66% sites were cortical bone density (CoD, mg/cm³), area (CoA, mm²), and mineral content (CoC, mg/mm). We also measured the polar strength strain index (SSI, mm³), a validated estimate of bone's ability to resist bending forces along the neutral axis⁵³. SSI was calculated as follows:

$$SSI = \sum_{i=1,n} \frac{r_i^2 \times a \frac{CoD}{ND}}{r_{max}} \quad (2)$$

where r_i is the distance of a voxel from the neutral axis, r_{max} is the maximum distance of a voxel from the neutral axis, a is the area of a voxel (mm²), and ND is the assumed normal density of cortical bone (1200mg/cm³).

Total muscle CSA and density were calculated at the 66% site using methods described previously⁴¹. A square region of interest (ROI) was drawn to intersect the subcutaneous fat. Muscle filter C02 was applied and the following settings separated muscle and bone from subcutaneous fat: Contour Mode 3, Peel mode 1, and a threshold of 40mg/cm³. Bone area (tibia and fibula) was separated from muscle by an inner/outer threshold of 280mg/cm³. Muscle mass (mg/mm) was calculated by subtracting from the tibia and fibula bone mass from the total (less subcutaneous fat) mass. Bone area was subtracted from total (less subcutaneous fat) area to calculate muscle CSA. Muscle density (mg/cm³) was derived by dividing muscle mass by muscle CSA and multiplying by 0.001.

4.3.8 MRI scan acquisition protocol

The right leg was imaged with a 3.0T MRI scanner (General Electric Healthcare

Discovery MR 750, Milwaukee, WI) and an eight-channel phased array RF knee coil.

Standardized positioning ensured each participant was resting supine with knees extended and feet immobilized in a custom positioning rig as described previously^{54,55}. Prior to advancing the participant feet-first into the magnet bore, the fiducial marker identifying the 66% tibial site (located as described in section 4.3.5) was centered within the coil. Participants remained on the MRI scan bed secured to the positioning rig for the duration of the scanning protocol. One of three accredited MRI technologists performed all scanning.

The scan acquisition protocol was described previously^{55,56}. Briefly, 30 contiguous axial proton density (PD)-weighted images (slice thickness = 4mm; TE/TR = 30/2344ms, field-of view (FOV) = 16cm, matrix = 320x320mm, total scan time = 6min 30s) were acquired. The phased array uniformity enhancement (PURE) post-processing filter was applied to correct for image intensity non-uniformity and reduce edge blurring.

DTI scans were acquired with the identically prescribed geometry as the PD-weighted images. Using a dual spin-echo planar imaging (EPI) pulse sequence with the following parameters: 30 slices (4mm thick, 0mm skip), 15 optimized diffusion encoding gradients⁵⁴, one $b = 0\text{s/mm}^2$, $b\text{-value} = 350\text{s/mm}^2$, TE/TR = 68.3/6000ms, number of averages (NEX) = 4, matrix size = 64x64mm, total scan time = 6min 48s. Each NEX was collected separately to correct for eddy currents and motion prior to merging and subsequent calculation of the diffusion tensor.

A ¹H-MRS point resolved spectroscopy (PRESS) pulse sequence was used to obtain the IMCL resonance area of a single voxel within the tibialis anterior muscle. This

site was chosen because the muscle fibre orientation in this muscle permits the greatest separation of lipid compartments⁴⁸. Acquisition parameters have been described previously⁵⁵. This procedure always resulted in a water peak full width half maximum of less than 0.326ppm.

4.3.9 MRI scan processing and analyses protocols

PD images were visually inspected by an accredited technologist to screen for potential gross subclinical pathology.

On a PC workstation, SliceOmatic 4.3 image analysis software (TomoVision, Montreal, Canada) was used to segment the PD-weighted leg images and quantify tissue composition. Outcomes measured were muscle and intramuscular fat volumes (tibialis anterior, soleus, gastrocnemius, cm³) in slices 11 thru 20 in the series, counting inferior to superior. Intramuscular fat was described as a percentage of the muscle area. Total intermuscular fat volume was measured from the same segmented slices.

Segmentation involved identifying and tagging each tissue in each of the 10 image slices with a different colour, as shown in Figure 4.1. Using the histogram of pixel intensity distribution, intramuscular and intermuscular fat separation thresholds for each participant were determined by placing the lower limit of the region-growing threshold at the base of the muscle peak. In our laboratory, intramuscular fat is defined as bright pixels located beneath the muscle fascial envelope and within the epimysium and perimysium. Intermuscular fat is defined as bright pixels located within the deep fascial envelopes surrounding the muscle bellies and muscle compartments. Visual inspection determined whether manual editing of small adjustments were needed. Reliability of

manual leg muscle segmentation from MRI scans to estimate muscle volume is excellent (ICC = 0.99) if eight to ten contiguous slices are analysed⁵⁷. The average time for the segmentation of all tissues was two hours per participant.

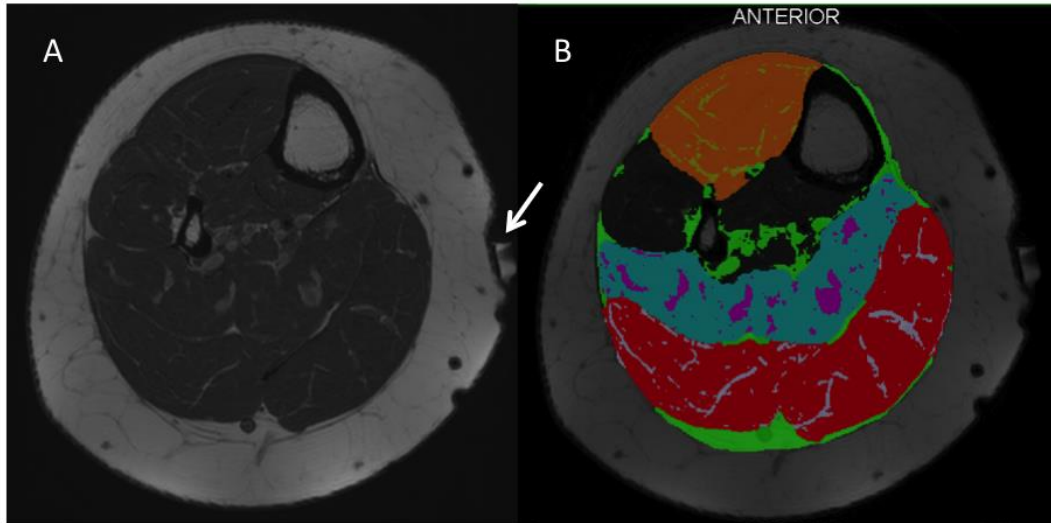


Figure 4.1: Representative proton density (PD) weighted images of the leg in a postmenopausal woman with osteoporosis (age = 65y, BMI = 29) before and after segmentation. Each PD image (A) was segmented (B). The tibialis anterior, soleus, and gastrocnemius muscles appear in orange, blue, and red, respectively. The intramuscular fat for each muscle is segmented in yellow, pink, and grey for the tibialis anterior, soleus, and gastrocnemius, respectively. Intermuscular fat (green) is located beneath the muscle fascial plane and surrounding muscle bellies or compartments. The arrow points to the fiducial marker used to visualize the 66% site.

DTI outcomes of interest were the apparent diffusion coefficient (ADC; $\times 10^{-3}$ mm²/s) and fractional anisotropy (FA). These were quantified for five leg muscle ROIs: tibialis anterior, tibialis posterior, soleus, gastrocnemius medial head and gastrocnemius lateral head. Tensor calculation and subsequent analysis were performed off-line using a combination of algorithms derived from custom-developed BASH scripts (Bourne Again Shell), FSL⁵⁸ and Diffusion Toolkit (DTK)⁵⁹. To correct for eddy current distortion the

FSL *eddy_current* function was employed. This function is based on a previously developed image registration tool ⁶⁰ and was also used for motion correction. The reference for eddy current and motion correction was the $b = 0\text{s/mm}^2$ image of the first NEX. Following tensor calculation, the five muscle ROIs were manually drawn on five images (13 thru 17, counting inferior to superior) with Analysis of Functional Neuroimaging (AFNI, National Institute of Mental Health) software ⁶¹. Using an axial PD image for anatomical reference, ROIs were chosen to encompass as much lean tissue as possible but exclude visible vessels, fat and fascia. Figure 4.2 shows representative muscle ROIs in the leg of a representative 70y old woman.

Each ROI yielded $\lambda_1, \lambda_2, \lambda_3$, ADC and FA values. Only ADC and FA are reported because they summarize the amount of overall diffusion and degree of tissue anisotropy ⁶². They are calculated as follows:

$$ADC = \frac{\lambda_1 + \lambda_2 + \lambda_3}{3} \quad (3)$$

$$FA = \sqrt{\frac{3}{2}} \sqrt{\frac{(\lambda_1 - ADC)^2 + (\lambda_2 - ADC)^2 + (\lambda_3 - ADC)^2}{\lambda_1^2 + \lambda_2^2 + \lambda_3^2}} \quad (4)$$

Spectra from the tibialis anterior muscle were analyzed using the LCModel software (v6.2) ⁶³. The LCModel-derived lipid content was determined using a two-step process. The signal from a metabolite resonance area in a water-suppressed spectrum is divided by the signal from the water peak in an unsuppressed water reference signal acquired from the same voxel. An automated spectra-fitting routine determined the IMCL methylene (CH_2) resonance area at around 1.3ppm based on algorithms that adjust

the phase and ppm shift of the spectra, estimate the baseline, and perform eddy current correction (see Appendix D for sample spectra).

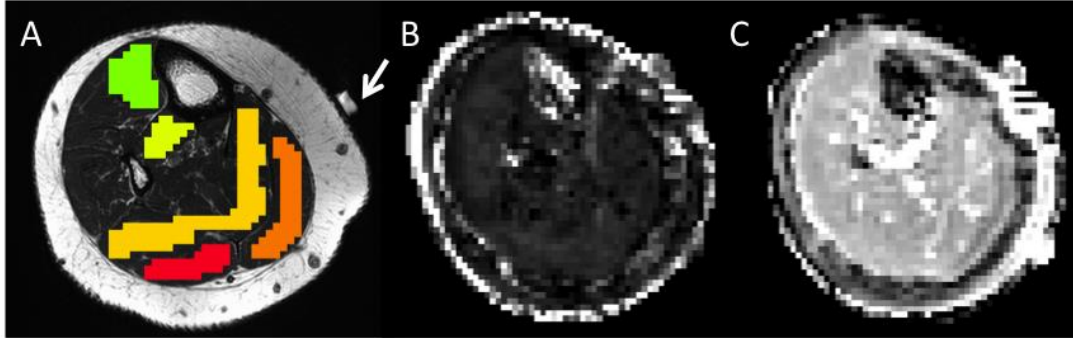


Figure 4.2: Diffusion tensor imaging muscle regions of interest (ROIs) and representative projection maps. Muscle ROIs are drawn on the axial proton density reference image of the leg of a woman with osteoporosis (A). Sample fractional anisotropy (B) and apparent diffusion coefficient (C) projection maps. The arrow is pointing to the fiducial marker that identified the 66% site of the tibia.

4.3.10 Physical performance

Using a standardized protocol⁶⁴, all participants performed the 30-second chair stand test (30-CST) twice during the study visit. With a standard chair placed against a wall, the participant began in a seated position with her arms placed across her chest with hands on the opposite shoulders and her feet flat on the floor. Upon hearing the word “go”, the participant stood up and then sat down in a continuous cycle for 30 seconds. The number of sit-stand-sit repetitions observed in 30 seconds was recorded. The highest number of repetitions of the two trials was used for analysis.

Usual gait speed (in m/s) was measured as the best performance of two trials on a 20m course in a straight uncarpeted hallway. Participants began the course 2m in front of the start line and ended 2m behind the line to account for initial acceleration and finish-

line deceleration. Time (s) to walk the 20m course was recorded using a stopwatch and the best time was divided by 20m for analysis.

4.3.11 Statistical analyses

Bone area and mineral content, muscle CSA, muscle volumes, and intramuscular fat volumes were adjusted for body size by dividing the acquired values by tibia length squared for each participant and multiplying by the mean tibia length for the sample⁶⁵. Data were inspected for normality visually by plotting histograms and statistically using the Shapiro-Wilk test. Levene's test was used to test variance equality.

Parametric data were described using means and standard deviations. Central tendency of non-parametric variables was described using the median and 25th and 75th interquartiles. Group comparisons and significant differences were determined by two-sided independent *t* tests. Group ranks were compared using the Mann Whitney test.

Based on the hypothesis that between group differences would be observed for total volumetric BMD at the 4% tibia, we calculated our sample size using a Canadian database of women (mean age 74y) with fracture and without fracture⁶⁶. Given a Cohen's *d* effect size of 1.05, it was estimated that 15 participants per group were required to detect between group differences assuming 80% power and $\alpha = 0.05$. Our group of women with osteoporosis was defined as having a physician's diagnosis and those without fracture or on bone sparing medications were not excluded. Thus, to account for these differences we increased our target sample size by 20% and aimed to enroll 19 participants per group.

Pearson correlation coefficients (*r*) (or Spearman rho (ρ) for distribution free data)

were used to test the strength and direction of associations between bone, muscle, fat, physical activity, and physical performance variables. Correlation coefficients were interpreted as follows: 0.4 - 0.6 was considered a moderate strength relationship, 0.61 - 0.8 was considered a substantial relationship, and 0.81 - 1.0 was considered an excellent relationship⁶⁷. For each correlation coefficient equal to or greater than $r = 0.4$, 95% confidence intervals (CIs) were calculated. All data management and statistical analyses were performed using PSAW software v20 (SPSS, Chicago, IL, USA). Statistical significance for all analyses was set at p less than 0.05.

4.4 RESULTS

4.4.1 Participants

Thirty-five community dwelling Caucasian women participated in the study; eighteen were diagnosed with osteoporosis and 17 were not. Participant flow is illustrated in Appendix F. Table 4.1 summarizes the demographic and clinical characteristics for each group and the entire sample. Groups were similar in all demographic characteristics. The prevalence of fragility fractures was significantly greater in the osteoporosis group (Table 4.1). Fragility fracture sites included the wrist ($n = 5$), vertebra ($n = 3$), ankle ($n = 2$), and ribs and sternum ($n = 1$). All women in the osteoporosis group reported current or recent (within past 2y) use of bone-sparing medication. Most women in the osteoporosis group were taking bisphosphonates ($n = 13$) and others were taking denosumab ($n = 4$) or parathyroid hormone ($n = 1$). Most (91%) of women responded “yes” to current daily vitamin D supplementation, whereas only

43% women said “yes” to current calcium supplementation. Supplementation was similar between groups for vitamin D ($p = 0.58$) and calcium ($p = 0.63$).

Table 4.1: Descriptive statistics of women with and without osteoporosis*

Characteristic	All <i>n</i> = 35	Osteoporosis	
		No <i>n</i> = 17	Yes <i>n</i> = 18
Age (y)	69.5 (4.3)	69.6 (4.0)	69.5 (4.8)
Height (cm)	161.4 (5.6)	161.1 (5.1)	161.8 (6.0)
Body weight (kg)	66.4 (10.6)	66.4 (12.0)	66.3 (9.5)
Body mass index (kg/m ²)	25.5 (4.3)	25.6 (4.3)	25.5 (4.4)
Years since menopause (y)	20.2 (5.6)	18.5 (4.8)	21.9 (6.3)
Tibia length (mm)	369.7 (20)	367.0 (20.2)	370.2 (25.8)
Total hip BMD (g/cm ²)	0.759 (0.113)	0.758 (0.133)	0.761 (0.095)
Total spine BMD (g/cm ²)	0.908 (0.130)	0.911 (0.149)	0.905 (0.114)
OP medication use (n, %)	18 (51%)	0	18 (100%) ^a
Fracture (n, %)	11 (31%)	1 (6%)	10 (56%) ^a

* Values are the mean (SD), unless indicated otherwise

^a Significantly different from women without osteoporosis, $p < 0.001$

BMD = bone mineral density; OP = osteoporosis

4.4.2 Bone structure and strength

All pQCT scans were analyzed; there were no failed analyses. All bone structure and strength data met the assumptions of normality and homogeneity of variance. Table 4.2 presents the bone outcomes at the 4, 14, 38, and 66% tibial sites. Women with and without osteoporosis had similar trabecular and total bone density, area, and content at the 4% tibia. CoA, CoC, and CoD at the diaphyseal tibia sites were not significantly different between groups. Similarly, groups were not significantly different in estimated bone strength at the tibial 4% site (BSI: $t(33) = 0.67, p = 0.51$) or the 66% site (SSI: $t(33) = 0.16, p = 0.88$).

4.4.3 Muscle and fat macrostructure

All PD scans were successfully acquired and analyzed. Muscle and intermuscular fat volumes and % intramuscular fat per muscle were normally distributed with equal variances. As summarized in Table 4.3, there were no statistically significant differences between groups for muscle volume or intramuscular fat content in the tibialis anterior, soleus, or gastrocnemius muscles. Women with osteoporosis had similar muscle CSA ($t(33) = -0.29, p = 0.78$) and density ($t(33) = 0.64, p = 0.53$) compared to those without (Table 4.2).

Table 4.2: pQCT bone and muscle outcomes for the total sample and groups of women with and without osteoporosis, presented as mean (SD). Bone area and content and muscle cross-sectional area measures are adjusted for tibia length

Measure	All	Osteoporosis		p
		No	Yes	
4% site				
Total density (mg/cm ³)	249 (36)	252 (37)	246 (36)	0.66
Total area (mm ²)	1081 (185)	1086 (192)	1076 (184)	0.87
Total content (mg)	265 (40)	269 (41)	262 (40)	0.61
Trabecular density	204 (35)	211 (37)	197 (32)	0.23
Trabecular area (mm ²)	487 (83)	490 (85)	484 (83)	0.83
Trabecular content (mg)	97 (15)	100 (15)	94 (15)	0.21
BSI (mg ² /mm ⁴)	67 (16)	69 (18)	63 (16)	0.51
14% site				
Cortical density (mg/cm ³)	1054 (71)	1055 (60)	1053 (82)	0.92
Cortical area (mm ²)	143 (34)	139 (32)	147 (35)	0.44
Cortical content (mg)	152 (40)	147 (39)	156 (42)	0.53
38% site				
Cortical density (mg/cm ³)	1148 (33)	1146 (30)	1151 (36)	0.66
Cortical area (mm ²)	250 (55)	257 (57)	243 (54)	0.46
Cortical content (mg)	287 (64)	296 (68)	280 (61)	0.47
66% site				
Cortical density (mg/cm ³)	1080 (40)	1076 (44)	1084 (36)	0.61
Cortical area (mm ²)	254 (53)	254 (54)	253 (54)	0.96
Cortical content (mg)	275 (61)	275 (64)	275 (60)	0.99
SSI (mm ³)	1869 (315)	1878 (352)	1861 (285)	0.88
Muscle CSA (mm ²)	6166 (1275)	6101 (1142)	6227 (1420)	0.78
Muscle density (mg/cm ³)	72 (3.4)	72 (3.4)	71 (3.5)	0.53

BSI = compressive bone strength index; SSI = polar stress strain index; CSA = cross-sectional area

Table 4.3: MRI derived muscle and fat volumes normalized to tibia length for the total sample and groups of women with and without osteoporosis, presented as mean (SD)

Measure	All	Osteoporosis		p
		No	Yes	
Tibialis anterior				
Muscle volume (cm ³)	33.1 (6.6)	33.3 (5.4)	32.9 (7.6)	0.86
Intramuscular fat (%)	8.9 (3.0)	8.4 (2.9)	9.4 (3.0)	0.29
Soleus				
Muscle volume (cm ³)	57.1 (11.3)	55.6 (9.9)	58.5 (12.6)	0.45
Intramuscular fat (%)	7.9 (3.5)	7.7 (3.5)	8.0 (3.5)	0.75
Gastrocnemius				
Muscle volume (cm ³)	69.0 (21.3)	71.3 (20.6)	66.7 (22.3)	0.53
Intramuscular fat (%)	9.0 (3.0)	7.8 (3.0)	8.3 (3.5)	0.68
Intermuscular adipose tissue volume	14.6 (45.0)	14.8 (5.0)	14.5 (5.1)	0.86

4.4.4 Muscle microstructure and IMCL content

All DTI scans were analyzed and all measures met the assumptions of normality and homogeneity of variance. DTI measures for the muscle ROIs are summarized in Table 4.4. Groups were similar for ADC and FA in all ROIs. Figure 4.3 illustrates the ADC and FA values for the entire sample.

Six IMCL data points were excluded from the analysis. Data were lost due to improper data storage prior to a hardware system malfunction (n = 3), failed analyses (n = 2), and a statistical outlier (n = 1). Therefore, Table 4.4 presents values for tibialis anterior IMCL content obtained in 29 participants. IMCL content in the tibialis anterior in women with osteoporosis (n = 15) was not different from women without osteoporosis.

Table 4.4: Microstructural measures of muscle and intramyocellular lipid (IMCL) content of the leg muscle regions of interest (ROIs) for the total sample and groups of women with and without osteoporosis, presented as mean (SD)

Muscle ROI	All	Osteoporosis		p
		No	Yes	
Tibialis anterior				
ADC ($\times 10^{-3}$ mm ² /s)	1.71 (0.10)	1.73 (0.08)	1.70 (0.11)	0.49
FA	0.23 (0.02)	0.23 (0.01)	0.23 (0.03)	0.51
IMCL (mmol/g ww) ^a	0.017 (0.01)	0.016 (0.01)	0.018 (0.01)	0.52
Tibialis posterior				
ADC ($\times 10^{-3}$ mm ² /s)	1.74 (0.13)	1.76 (0.16)	1.72 (0.11)	0.40
FA	0.25 (0.03)	0.25 (0.02)	0.24 (0.03)	0.36
Soleus				
ADC ($\times 10^{-3}$ mm ² /s)	1.77 (0.13)	1.77 (0.12)	1.76 (0.13)	0.84
FA	0.24 (0.02)	0.24 (0.03)	0.25 (0.01)	0.52
Medial gastrocnemius				
ADC ($\times 10^{-3}$ mm ² /s)	1.79 (0.13)	1.83 (0.12)	1.76 (0.13)	0.10
FA	0.28 (0.03)	0.27 (0.03)	0.28 (0.02)	0.57
Lateral gastrocnemius				
ADC ($\times 10^{-3}$ mm ² /s)	1.77 (0.11)	1.79 (0.11)	1.74 (0.10)	0.16
FA	0.26 (0.02)	0.26 (0.03)	0.27 (0.01)	0.52

^a n = 29 (n = 14 without osteoporosis)

ADC = apparent diffusion coefficient; FA = fractional anisotropy

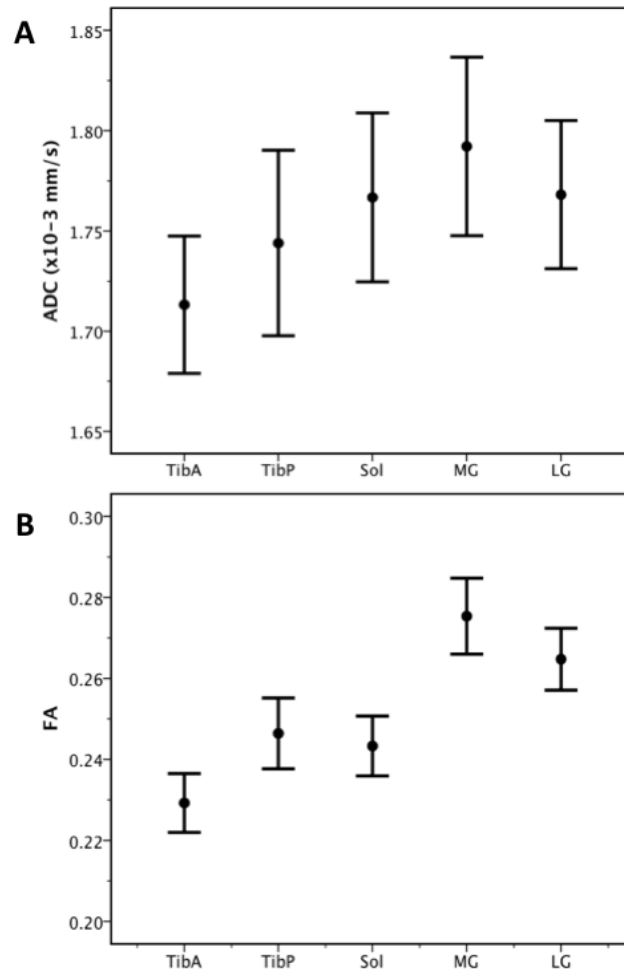


Figure 4.3: Mean values for the apparent diffusion coefficient (ADC) and fractional anisotropy (FA) in leg muscle regions of women with and without osteoporosis.

Mean (black dots) and 95% confidence intervals (bars) for (A) ADC and (B) FA in the leg muscles of 35 postmenopausal women with and without osteoporosis.

TibA = tibialis anterior, TibP = tibialis posterior, Sol = soleus, MG = medial head gastrocnemius, LG = lateral head gastrocnemius

4.4.5 Associations between bone with muscle and fat outcomes

Women with and without osteoporosis were similar for all bone, muscle, and fat outcomes. Thus, the relationships between musculoskeletal tissues were assessed for both groups combined ($n = 35$). Larger muscle CSA was associated with greater ToA (r

= 0.63, 95% CI: 0.38, 0.80) and ToC ($r = 0.62$, 95% CI: 0.36, 0.79) and TrC ($r = 0.73$, 95% CI: 0.52, 0.86) at the 4% site. Positive correlations were moderate for muscle CSA and CoA at the 14% and 38% sites ($r = 0.73$, 95% CI: 0.52, 0.86) and the 66% site ($r = 0.65$, 95% CI: 0.40, 0.81). Similarly, associations between muscle CSA and CoC were positive and moderate at the diaphyseal sites (14% site: $r = 0.63$, 95% CI: 0.38, 0.80; 38% site $r = 0.70$, 95% CI: 0.48, 0.84; 66% site: $r = 0.63$, 95% CI: 0.40, 0.81). Muscle CSA was not associated with BSI, but was moderately correlated with SSI ($r = 0.59$, 95% CI: 0.32, 0.77). None of the bone structure or strength variables correlated with muscle density (Appendix C, Table C1).

Table 4.5 shows the positive associations between bone structure and individual muscle volumes that ranged from moderate to substantial. Although muscle volumes were positively related to bone strength and structure, percent intramuscular fat in each muscle was not associated with pQCT bone outcomes (all $r \leq 0.39$; Appendix C, Table C1). Intermuscular fat volume was positively correlated with ToC at the 4% site ($r = 0.44$, 95% CI: 0.13, 0.67), CoC at the 14% $r = 0.47$, 95% CI: 0.16, 0.69) and 38% site ($r = 0.44$, 95% CI: 0.13, 0.67), and CoA at the 14% and 38% sites (both: $r = 0.46$, 95% CI: 0.15, 0.69). Correlation coefficients testing associations between intermuscular fat and bone strength were less than moderate (all $r \leq 0.20$) at the distal and diaphyseal tibia. Tibialis posterior ADC had a moderate negative association with ToD ($r = -0.51$, 95% CI: -0.72, -0.21) and TrD ($r = -0.43$, 95% CI: -0.67, -0.11) at the 4% site. Whereas ADC measures at the tibialis anterior, soleus, and medial head of gastrocnemius had moderate positive relationships with bone area and content at the 4% site ($r = 0.40$ to 0.53).

Table 4.5: Correlation coefficients for bone structure and strength outcomes with individual muscle volumes in postmenopausal women with and without osteoporosis (n = 35). Pearson correlation coefficients equal to or greater than 0.4 are presented with their 95% confidence intervals

	Measure	Muscle volume (cm ³)		
		TibA	SOL	GC
4%	Total density (mg/cm ³)	-0.15	-0.10	-0.01
	Total area (mm ²)	0.65 (0.40, 0.81)	0.51 (0.21, 0.72)	0.53 (0.24, 0.73)
	Total content (mg)	0.56 (0.28, 0.75)	0.46 (0.15, 0.69)	0.56 (0.28, 0.75)
	Trabecular density (mg/cm ³)	-0.30	-0.23	-0.13
	Trabecular area (mm ²)	0.65 (0.40, 0.81)	0.50 (0.20, 0.71)	0.53 (0.24, 0.73)
	Trabecular content (mg)	0.36	0.34	0.45 (0.14, 0.68)
	BSI (mg ² /mm ⁴)	-0.02	-0.02	0.12
14%	Cortical density (mg/cm ³)	-0.05	-0.17	-0.22
	Cortical area (mm ²)	0.73 (0.52, 0.86)	0.54 (0.25, 0.74)	0.51 (0.21, 0.72)
	Cortical content (mg)	0.63 (0.38, 0.80)	0.43 (0.11, 0.67)	0.38
38%	Cortical density (mg/cm ³)	0.02	-0.08	-0.07
	Cortical area (mm ²)	0.70 (0.48, 0.84)	0.55 (0.27, 0.75)	0.54 (0.25, 0.74)
	Cortical content (mg)	0.69 (0.46, 0.83)	0.53 (0.24, 0.73)	0.52 (0.23, 0.73)
66%	Cortical density (mg/cm ³)	0.16	0.12	0.02
	Cortical area (mm ²)	0.60 (0.33, 0.78)	0.52 (0.23, 0.73)	0.49 (0.19, 0.71)
	Cortical content (mg)	0.58 (0.31, 0.77)	0.51 (0.21, 0.72)	0.46 (0.15, 0.69)
	Strength strain index (mm ³)	0.56 (0.28, 0.75)	0.43 (0.11, 0.67)	0.47 (0.16, 0.69)

TibA = tibialis anterior; SOL = soleus; GC = gastrocnemius; BSI = Bone Strength Index

Total, trabecular, and cortical bone content and area at all tibia sites were moderately correlated with medial gastrocnemius ADC ($r = 0.42$ to 0.55). Of all muscle ROIs, only soleus and medial gastrocnemius ADC measures were positively associated with SSI (SOL: $r = 0.56$, 95% CI: 0.28, 0.75; MG: $r = 0.50$, 95% CI: 0.20, 0.71). FA was not related to bone structure and strength indices at any tibial site (Appendix C, Table C2).

Associations between IMCL and bone structure were negative and generally weak. The correlation coefficients were highest for ToD ($r = -0.39$) and ToC ($r = -0.38$) at the 4% site. As shown in Figure 4.4, BSI was moderately associated with IMCL at the 4% tibia ($r = -0.50$, 95% CI: -0.73, -0.16), but the association was weak for SSI ($r = -0.38$).

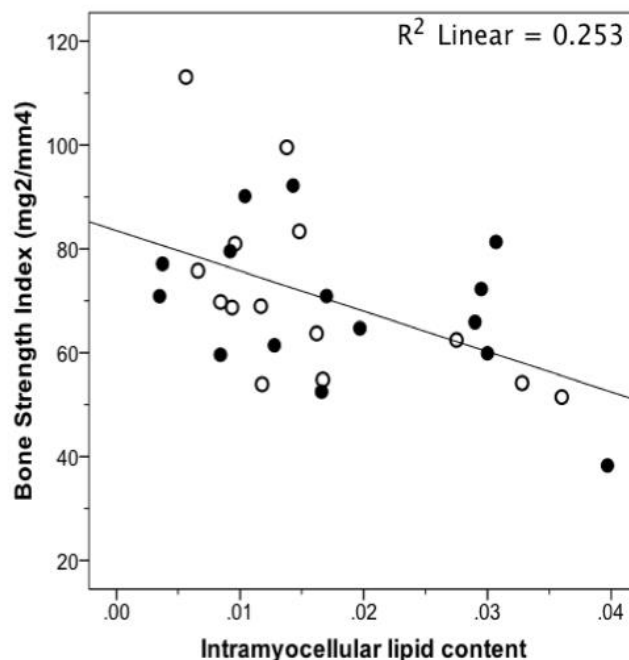


Figure 4.4: The relationship between tibialis anterior intramyocellular lipid content (mmol/kg ww) and the bone strength index at the 4% tibial site in postmenopausal women (n = 29).

Closed circles represent women with and treated for osteoporosis and open circles represent women without osteoporosis

4.4.6 Physical performance measures and physical activity levels

None of the women relied on mobility aids. Refer to Table 4.6 for a summary of physical performance and self-reported physical activity levels. The groups did not differ on the 30-CST ($t(33) = 0.81, p = 0.42$) or usual gait speed ($t(33) = 0.66, p = 0.52$). RAPA and HAP scores were similar between groups (RAPA: $t(33) = 1.55, p = 0.13$; HAP AAS: $t(33) = -0.153, p = 0.88$). The median HAP AAS score for women with and without osteoporosis correspond to swimming 25 yards (item 77) and walking 3 miles (item 75), respectively.

Table 4.6: Mean (SD) self-reported physical activity levels and performance-based physical performance for the total sample and groups of women with and without osteoporosis

Characteristic	All	Osteoporosis		p
		No	Yes	
Gait speed (m/s)	1.4 (0.1)	1.4 (0.2)	1.4 (0.1)	0.52
30-CST (reps)	15 (4)	15 (4)	14 (3)	0.42
RAPA (points) ^a	9 (3, 10)	9 (3, 10)	7 (3, 10)	0.13
HAP AAS (points) ^a	77 (55, 94)	75 (60, 89)	77 (55, 94)	0.88

^a Values are presented as median (min, max)

30-CST = 30-second chair stand test; RAPA = Rapid Assessment of Physical Activity; HAP = Human Activity Profile

Muscle density was inversely associated with gait speed ($r = -0.50, 95\% \text{ CI: } -0.71, -0.20$).

Greater intramuscular fat in the tibialis anterior and gastrocnemius was associated with slower gait speed (TibA: $r = -0.43, 95\% \text{ CI: } -0.67, -0.11$; GC: $r = -0.41, 95\% \text{ CI: } -0.65, -0.09$), however the amount of intramuscular fat volume was not associated with the 30-

CST. Despite a positive association between tibialis posterior FA and gait speed ($r = 0.45$, 95% CI: 0.14, 0.68), all other correlation coefficients for DTI measures and performance measures were less than or equal to 0.38 (medial head of gastrocnemius FA with gait speed). Self-reported physical activity was not associated with muscle or fat microstructure (Appendix C, Table C3).

4.5 DISCUSSION

The main objective of this study was to compare bone structure and strength and muscle and fat macrostructure and microstructure in the leg of healthy postmenopausal women with and without osteoporosis. It was hypothesized that the groups would be different for the primary outcome, total volumetric BMD at the distal tibia. We demonstrated that healthy postmenopausal women with and treated for osteoporosis have similar bone structure and strength, muscle macrostructure and microstructure, and distribution of fat infiltration in the leg, as compared to women of similar age and physical activity levels without osteoporosis. This is the first study to apply advanced MRI techniques to investigate macrostructural and microstructural muscle and fat measures with bone structure and strength in postmenopausal women. We were underpowered to detect significant differences in bone structure between groups; however, total leg muscle CSA and individual muscle volumes were significantly associated with bone structure and strength outcomes. While fat within the muscles was not related to bone structure or strength, intermuscular fat was moderately associated with greater bone CSA and mineral content. Microstructural evaluation of water diffusivity of muscle ROIs

demonstrated positive associations with bone variables, but FA in the same ROIs was not related to bone structure or strength. We found that the microstructural-level measure of fat infiltration in the tibialis anterior was negatively associated with estimated bone strength at the distal tibia. Of note, both pQCT and MRI methods of quantifying fat infiltration suggested that greater fat content within muscles is associated with deficits in physical performance.

The main finding of this cross-sectional study was that women with osteoporosis, all of whom reported current or recent pharmacologic osteoporosis treatment, were similar in bone structure and strength compared to women without osteoporosis. Few studies have compared differences in pQCT bone structure and strength in older women with and without osteoporosis because pharmacologic treatment is indicated for fracture risk reduction according to North American clinical practice guidelines^{68,69}. Therefore, the only way to evaluate a “true” treatment-naïve individual with osteoporosis would be upon clinical diagnosis prior to the initiation of therapy. One retrospective study reported data from initial patient visits to an osteoporosis clinic⁷⁰. Thus, women who may have indeed had osteoporosis and other indication for pharmacologic treatment were undiagnosed and untreated at the time of measurements. The women with and without osteoporosis in our sample had greater TrC, TrD, and TrA at the 4% site and increased CoC, CoD, and CoA at the 14% site of the tibia, compared to treatment-naïve women aged 60 to 80y of similar body size⁷⁰. Although we did not detect differences between groups, it is likely that measurements made prior to the initiation of treatment could have yielded bone structural values more similar to treatment naïve women reported by

Stathopoulos and colleagues (2011). Moreover, we would anticipate greater bone structure values in the treatment naïve women enrolled in our study because their medical history did not suggest to their physician that pharmacologic treatment was appropriate or necessary. For our sample as a whole, ToD at the 4% tibia was similar to values reported in similarly aged postmenopausal women in Canadian and European population-based studies using the same pQCT scanner model ^{38,66,71}. At the 38% site we found that values for CoD, CoA, and CoC for our whole sample were similar to younger ⁷² and similarly aged ³⁸ postmenopausal women. The cortical structure of the tibia diaphysis adapts to support compression during mechanical loading ¹⁸. Thus, the higher values for bone structure outcomes observed at the 14% and 38% sites may be attributed to the levels of physical activity reported by our sample. A meta-analysis reported that exercise targeting the lower extremities in healthy postmenopausal women confers small, but significant, benefits to the weight-bearing distal tibia TrD (0.87%; 95%CI: 0.37, 1.37%) and diaphyseal CoD (0.89%; 95%CI: 0.37, 1.41%) ⁷³. However, most studies do not report activity levels and exclude women on pharmacotherapy ^{66,70-72}. This study makes an important contribution to the literature due to the inclusion and evaluation of postmenopausal women with osteoporosis that are treated with bone-sparing medications. We acknowledge that pharmacologic treatments increase bone mass, however a randomized trial has documented no effect of pharmacologic therapy on tibia structure and strength in women with osteoporosis ⁷⁴. Women taking pharmacotherapy for osteoporosis are excluded from most studies and represent a growing, yet understudied population. This is a critical limitation in understanding the representative population of

otherwise healthy, postmenopausal, community-dwelling women 60-75y of age.

Including women with osteoporosis who are being treated pharmacologically will improve the generalizability of findings associated with postmenopausal bone health and identify may provide important insights into exercise strategies to prevent functional decline and osteoporotic fracture.

We found that greater fat infiltration in the leg, characterized by low muscle density and increased intramuscular fat, is related to slower gait speed in older women with and without osteoporosis. Previously, leg muscle density derived using pQCT has demonstrated strong relationships with muscle mass and peak plantarflexor concentric torque in healthy older adults⁴¹. The main disadvantages of measuring muscle density this way are its inability to discriminate between intermuscular and intramuscular fat and the inability to quantify fat depots in and around muscles and functional compartments. We were interested in measuring fat distribution because sarcopenia, characterized by decreased muscle mass and increased fat mass⁷, is more prevalent in postmenopausal women with osteoporosis^{3,75}. Our results agree with Tuttle et al. (2012) who measured calf intramuscular fat in 45 adults classified as obese, diabetic, or diabetic with peripheral neuropathy. Across all participants, the amount of intramuscular fat was associated with distance walked during a six-minute timed test²⁹. Although the six-minute walk test involves an endurance component due to the longer duration and greater distance covered, the gait speed test we used is considered a good overall predictor of physical functioning in older community-dwelling adults⁷⁶. Taken together, age-related declines in physical functioning are explained by increasing amounts of fat infiltration that are

associated with reduced muscle mass and increased muscle weakness^{29,30,40,41,77}.

Interestingly, our findings suggest that muscle density assessed by pQCT provides similar information regarding the association between fat infiltration and walking speed, as does the MRI-based measures. The segmentation method is labor intensive and is considered a feasible method for analyzing data for small samples, but could be a logistical concern for larger studies. Nevertheless, physical performance is influenced by fat accumulation and our data suggest that its general quantification within an axial image may be as sensitive as assessing the distribution of its infiltration within and between leg muscles.

We found that IMCL was inversely correlated with bone mineral content and BSI at the 4% tibia site and CoA at the tibia diaphysis. In healthy non-diabetic women with a mean age of 45y, Boettcher and colleagues (2009) reported a negative relationship between tibialis anterior IMCL content and insulin sensitivity ($r = -0.44$, 95% CI: -0.56, -0.30). Our findings of higher IMCL levels in women with reduced bone strength are in agreement with earlier reports of microstructural deterioration of trabecular and cortical bone in adults with poor insulin sensitivity^{78,79}. The screening and recruitment of our participants for our study purposely excluded women with diabetes. However, insulin resistance is considered as a precursor to frailty and women with osteoporosis and high risk of fracture may be at greater risk of developing this complex condition^{80,81}. Frailty is more prevalent in older women than older men and is characterized by physical disability and associated with bone fragility and muscle wasting^{4,82,83}. Given the limited resolution of the pQCT, the relationships between IMCL and tibial bone measured using high-resolution pQCT devices should be explored.

Our study highlights the interrelationships of muscle, bone, and fat on both macrostructural and microstructural scales. From a macrostructural perspective, our results concur with others who have demonstrated that muscle mass and density are positively associated with bone area, mineral content, and strength at the tibia^{38,41}. Interestingly, a recent study of 181 middle-aged and older men showed that CT-derived mid-femoral muscle mass was a stronger predictor of tibial bone structure than mid-tibial muscle mass⁸⁴. They hypothesized that this observation was a result of large muscle strains elicited at the tendinous quadriceps insertion site on the tibial shaft⁸⁴; however this has not been evaluated in women using the pQCT since the XCT2000 gantry is not large enough to permit thigh image acquisition. In our sample there was a positive association between tibialis anterior muscle volume and bone size and mineral content. This observation may be better understood by considering molecular crosstalk between muscle and bone, which has been applied to explaining musculoskeletal relationships that cannot be described by biomechanics alone⁸⁵. Fat infiltration in and around muscle is characteristic of sarcopenia and osteoporosis^{4,7} and should be considered an important mediator of both the biomechanical and crosstalk theories of muscle-bone interactions. Our study suggests that increased intermuscular fat, but not intramuscular fat, confers skeletal benefits at the tibia diaphysis, yet microstructural measurement of IMCL is associated with lower resistance to compression forces at the distal tibia. In contrast, only fat infiltration measured at the macrostructural level, namely intramuscular fat and muscle density, were associated with slower gait speed. Therefore, the distribution of fat in the leg appears to have a negative influence on bone structure and physical functioning when

it is located within the muscle cell and perimysium, respectively. While intermuscular fat may increase the overall fatness of an individual and subsequently result in greater habitual loads on the skeleton, intramuscular fat may negatively influence the contractile ability of muscle resulting in slower gait speed. At the microstructural level, fat infiltration in muscle is a barrier to diffusion because it is an obstacle for molecular movement⁸⁶. Elevated ADC values are documented in aging skeletal muscle⁴³. The positive relationship between soleus and medial head gastrocnemius ADC and bone structure and strength outcomes was unforeseen because it suggests that attributes of strong bones are associated with greater water diffusivity. Variation in muscle ROI fat infiltration may partially explain the unforeseen results, particularly because fat infiltration is known to vary along the length of the muscle⁸⁷ and we measured all muscle ROIs in the five slices nearest to the 66% tibial site despite differences in individual muscle CSAs. Altered muscle fibre orientation⁸⁸, cell membrane damage, or macromolecular barriers such as fat accumulation between muscle fibres could influence ADC measures. Although, fat infiltration of muscle is gradual and precedes muscle atrophy and muscle weakness⁸⁹, the temporal influence of these age-related soft tissue adaptations on bone require prospective data and is yet to be investigated.

The findings we report must be interpreted in the context of the study limitations. First, our study was cross-sectional in design and therefore causal associations cannot be construed. Second, our small sample size limits the statistical power, but we have initiated the investigation of novel non-invasive musculoskeletal outcomes in a clinically relevant population. Third, we did not collect information regarding the dose or duration

of osteoporosis pharmacologic treatments, nor did we inquire about their adherence. The women with osteoporosis were taking a variety of bone-sparing medications from different drug classes. Although the effect of bone-sparing medications on musculoskeletal tissues is an important direction for future research, our small sample size precluded controlling for drug classes in our analyses. Fourth, the generalizability of our findings may be limited to healthy, high functioning, and fairly young older women. Lastly, we only reported on imaging-based outcomes of muscle structure and did not obtain direct measurements of muscle strength.

In summary, we have demonstrated that musculoskeletal tissue composition is similar in women diagnosed and treated for osteoporosis compared to women without osteoporosis. Further, we have implicated a role for MRI-based measures of fat and muscle microstructure and macrostructure in understanding the relationships among muscle, bone and physical performance in postmenopausal women. In conjunction with genetic and basic research, these measures may provide novel targets and outcomes for pharmacologic and exercise strategies aimed at preventing functional decline and osteoporotic fracture.

4.6 ACKNOWLEDGEMENTS

The study was funded in part by a grant from The Arthritis Society. The authors appreciate the assistance and guidance from Norm Konyer and the MRI technologists (Janet Burr, Cheryl Contant, Julie Lecomte). AL is funded in part by the Ontario Women's Health Scholar Award and the Joint Motion Program, a Canadian Institutes of Health Research Training Program in Musculoskeletal Health Research and Leadership.

4.7 REFERENCES

1. Karasik, D, Kiel, DP 2010 Evidence for pleiotropic factors in genetics of the musculoskeletal system. *Bone* **46**:1226-1237.
2. Sirola, J, Kroger, H 2011 Similarities in acquired factors related to postmenopausal osteoporosis and sarcopenia. *J Osteoporos* **2011**:536735.
3. Walsh, MC, Hunter, GR, Livingstone, MB 2006 Sarcopenia in premenopausal and postmenopausal women with osteopenia, osteoporosis and normal bone mineral density. *Osteoporos Int* **17**:61-67.
4. Lang, T, Streeper, T, Cawthon, P, Baldwin, K, Taaffe, DR, Harris, TB 2010 Sarcopenia: etiology, clinical consequences, intervention, and assessment. *Osteoporos Int* **21**:543-559.
5. Kaji, H 2013 Linkage between muscle and bone: common catabolic signals resulting in osteoporosis and sarcopenia. *Curr Opin Clin Nutr Metab Care* **16**:272-277.
6. Janssen, I, Heymsfield, SB, Ross, R 2002 Low relative skeletal muscle mass (sarcopenia) in older persons is associated with functional impairment and physical disability. *J Am Geriatr Soc* **50**:889-896.
7. Fielding, RA, Vellas, B, Evans, WJ, Bhasin, S, Morley, JE, Newman, AB, Abellan van Kan, G, Andrieu, S, Bauer, J, Breuille, D, Cederholm, T, Chandler, J, De Meynard, C, Donini, L, Harris, T, Kannt, A, Keime Guibert, F, Onder, G, Papanicolaou, D, Rolland, Y, Rooks, D, Sieber, C, Souhami, E, Verlaan, S, Zamboni, M 2011 Sarcopenia: an undiagnosed condition in older adults. Current consensus definition: prevalence, etiology, and consequences. International working group on sarcopenia. *J Am Med Dir Assoc* **12**:249-256.
8. Uusi-Rasi, K, Sievanen, H, Pasanen, M, Kannus, P 2007 Age-related decline in trabecular and cortical density: a 5-year peripheral quantitative computed tomography follow-up study of pre- and postmenopausal women. *Calcif Tissue Int* **81**:249-253.
9. Greendale, GA, Sowers, M, Han, W, Huang, MH, Finkelstein, JS, Crandall, CJ, Lee, JS, Karlamangla, AS 2011 Bone mineral density loss in relation to the final menstrual period in a multi-ethnic cohort: Results from the study of women's health across the nation (SWAN). *J Bone Miner Res*.
10. Maltais, ML, Desroches, J, Dionne, IJ 2009 Changes in muscle mass and strength after menopause. *J Musculoskelet Neuronal Interact* **9**:186-197.

11. Burge, R, Dawson-Hughes, B, Solomon, DH, Wong, JB, King, A, Tosteson, A 2007 Incidence and economic burden of osteoporosis-related fractures in the United States, 2005-2025. *J Bone Miner Res* **22**:465-475.
12. Janssen, I, Shepard, DS, Katzmarzyk, PT, Roubenoff, R 2004 The healthcare costs of sarcopenia in the United States. *J Am Geriatr Soc* **52**:80-85.
13. Wiktorowicz, ME, Goeree, R, Papaioannou, A, Adachi, JD, Papadimitropoulos, E 2001 Economic implications of hip fracture: health service use, institutional care and cost in Canada. *Osteoporos Int* **12**:271-278.
14. da Silva, RB, Costa-Paiva, L, Morais, SS, Mezzalira, R, Ferreira Nde, O, Pinto-Neto, AM 2010 Predictors of falls in women with and without osteoporosis. *J Orthop Sports Phys Ther* **40**:582-588.
15. Bliuc, D, Nguyen, ND, Nguyen, TV, Eisman, JA, Center, JR 2013 Compound risk of high mortality following osteoporotic fracture and refracture in elderly women and men. *J Bone Miner Res* **28**:2317-2324.
16. Dytfeld, J, Ignaszak-Szczepaniak, M, Gowin, E, Michalak, M, Horst-Sikorska, W 2011 Influence of lean and fat mass on bone mineral density (BMD) in postmenopausal women with osteoporosis. *Arch Gerontol Geriatr* **53**:e237-42.
17. Cui, LH, Shin, MH, Kweon, SS, Park, KS, Lee, YH, Chung, EK, Nam, HS, Choi, JS 2007 Relative contribution of body composition to bone mineral density at different sites in men and women of South Korea. *J Bone Miner Metab* **25**:165-171.
18. Capozza, RF, Feldman, S, Mortarino, P, Reina, PS, Schiessl, H, Rittweger, J, Ferretti, JL, Cointy, GR 2010 Structural analysis of the human tibia by tomographic (pQCT) serial scans. *J Anat* **216**:470-481.
19. Zaidi, M, Buettner, C, Sun, L, Iqbal, J 2012 Minireview: The link between fat and bone: does mass beget mass? *Endocrinology* **153**:2070-2075.
20. Gnudi, S, Sitta, E, Fiumi, N 2007 Relationship between body composition and bone mineral density in women with and without osteoporosis: relative contribution of lean and fat mass. *J Bone Miner Metab* **25**:326-332.
21. Genaro, PS, Pereira, GA, Pinheiro, MM, Szejnfeld, VL, Martini, LA 2010 Influence of body composition on bone mass in postmenopausal osteoporotic women. *Arch Gerontol Geriatr* **51**:295-298.

22. Kent-Braun, JA, Ng, AV, Young, K 2000 Skeletal muscle contractile and noncontractile components in young and older women and men. *J Appl Physiol* **88**:662-668.
23. Schwenzer, NF, Martirosian, P, Machann, J, Schraml, C, Steidle, G, Claussen, CD, Schick, F 2009 Aging effects on human calf muscle properties assessed by MRI at 3 Tesla. *J Magn Reson Imaging* **29**:1346-1354.
24. Boettcher, M, Machann, J, Stefan, N, Thamer, C, Haring, HU, Claussen, CD, Fritsche, A, Schick, F 2009 Intermuscular adipose tissue (IMAT): association with other adipose tissue compartments and insulin sensitivity. *J Magn Reson Imaging* **29**:1340-1345.
25. Buford, TW, Lott, DJ, Marzetti, E, Wohlgemuth, SE, Vandenberg, K, Pahor, M, Leeuwenburgh, C, Manini, TM 2012 Age-related differences in lower extremity tissue compartments and associations with physical function in older adults. *Exp Gerontol* **47**:38-44.
26. Machann, J, Thamer, C, Schnoedt, B, Stefan, N, Stumvoll, M, Haring, HU, Claussen, CD, Fritsche, A, Schick, F 2005 Age and gender related effects on adipose tissue compartments of subjects with increased risk for type 2 diabetes: a whole body MRI/MRS study. *MAGMA* **18**:128-137.
27. Alizai, H, Nardo, L, Karampinos, DC, Joseph, GB, Yap, SP, Baum, T, Krug, R, Majumdar, S, Link, TM 2012 Comparison of clinical semi-quantitative assessment of muscle fat infiltration with quantitative assessment using chemical shift-based water/fat separation in MR studies of the calf of post-menopausal women. *Eur Radiol* **22**:1592-1600.
28. Karampinos, DC, Baum, T, Nardo, L, Alizai, H, Yu, H, Carballido-Gamio, J, Yap, SP, Shimakawa, A, Link, TM, Majumdar, S 2012 Characterization of the regional distribution of skeletal muscle adipose tissue in type 2 diabetes using chemical shift-based water/fat separation. *J Magn Reson Imaging* **35**:899-907.
29. Tuttle, LJ, Sinacore, DR, Mueller, MJ 2012 Intermuscular adipose tissue is muscle specific and associated with poor functional performance. *J Aging Res* **2012**:172957.
30. Cawthon, PM, Fox, KM, Gandra, SR, Delmonico, MJ, Chiou, CF, Anthony, MS, Sewall, A, Goodpaster, B, Satterfield, S, Cummings, SR, Harris, TB, Health, Aging and Body Composition Study 2009 Do muscle mass, muscle density, strength, and physical function similarly influence risk of hospitalization in older adults? *J Am Geriatr Soc* **57**:1411-1419.

31. Delmonico, MJ, Harris, TB, Visser, M, Park, SW, Conroy, MB, Velasquez-Mieyer, P, Boudreau, R, Manini, TM, Nevitt, M, Newman, AB, Goodpaster, BH, Health, A, and Body 2009 Longitudinal study of muscle strength, quality, and adipose tissue infiltration. *Am J Clin Nutr* **90**:1579-1585.
32. Marcus, RL, Addison, O, Dibble, LE, Foreman, KB, Morrell, G, Lastayo, P 2012 Intramuscular adipose tissue, sarcopenia, and mobility function in older individuals. *J Aging Res* **2012**:629637.
33. Karinkanta, S, Piirtola, M, Sievanen, H, Uusi-Rasi, K, Kannus, P 2010 Physical therapy approaches to reduce fall and fracture risk among older adults. *Nat Rev Endocrinol* **6**:396-407.
34. Maly, MR, Calder, KM, Macintyre, NJ, Beattie, KA 2013 Relationship of intermuscular fat volume in the thigh with knee extensor strength and physical performance in women at risk of or with knee osteoarthritis. *Arthritis Care Res (Hoboken)* **65**:44-52.
35. Rittweger, J, Beller, G, Ehrig, J, Jung, C, Koch, U, Ramolla, J, Schmidt, F, Newitt, D, Majumdar, S, Schiessl, H, Felsenberg, D 2000 Bone-muscle strength indices for the human lower leg. *Bone* **27**:319-326.
36. Macdonald, HM, Kontulainen, SA, Petit, M, Janssen, P, McKay, HA 2006 Bone strength and its determinants in pre- and early pubertal boys and girls. *Bone* **39**:598-608.
37. Lang, T, Cauley, JA, Tylavsky, F, Bauer, D, Cummings, S, Harris, TB, Health ABC Study 2010 Computed tomographic measurements of thigh muscle cross-sectional area and attenuation coefficient predict hip fracture: the health, aging, and body composition study. *J Bone Miner Res* **25**:513-519.
38. Edwards, MH, Gregson, CL, Patel, HP, Jameson, KA, Harvey, NC, Sayer, AA, Dennison, EM, Cooper, C 2013 Muscle size, strength, and physical performance and their associations with bone structure in the Hertfordshire Cohort Study. *J Bone Miner Res* **28**:2295-2304.
39. Visser, M, Kritchevsky, SB, Goodpaster, BH, Newman, AB, Nevitt, M, Stamm, E, Harris, TB 2002 Leg muscle mass and composition in relation to lower extremity performance in men and women aged 70 to 79: the health, aging and body composition study. *J Am Geriatr Soc* **50**:897-904.
40. Visser, M, Goodpaster, BH, Kritchevsky, SB, Newman, AB, Nevitt, M, Rubin, SM, Simonsick, EM, Harris, TB 2005 Muscle mass, muscle strength, and muscle fat infiltration as predictors of incident mobility limitations in well-functioning older persons. *J Gerontol A Biol Sci Med Sci* **60**:324-333.

41. MacIntyre, NJ, Rombough, R, Brouwer, B 2010 Relationships between calf muscle density and muscle strength, mobility and bone status in the stroke survivors with subacute and chronic lower limb hemiparesis. *J Musculoskelet Neuronal Interact* **10**:249-255.
42. Noseworthy, MD, Davis, AD, Elzibak, AH 2010 Advanced MR imaging techniques for skeletal muscle evaluation. *Semin Musculoskelet Radiol* **14**:257-268.
43. Sinha, S, Sinha, U, Edgerton, VR 2006 In vivo diffusion tensor imaging of the human calf muscle. *J Magn Reson Imaging* **24**:182-190.
44. Galban, CJ, Maderwald, S, Uffmann, K, de Greiff, A, Ladd, ME 2004 Diffusive sensitivity to muscle architecture: a magnetic resonance diffusion tensor imaging study of the human calf. *Eur J Appl Physiol* **93**:253-262.
45. Zaraiskaya, T, Kumbhare, D, Noseworthy, MD 2006 Diffusion tensor imaging in evaluation of human skeletal muscle injury. *J Magn Reson Imaging* **24**:402-408.
46. Deux, JF, Malzy, P, Paragios, N, Bassez, G, Luciani, A, Zerbib, P, Roudot-Thoraval, F, Vignaud, A, Kobeiter, H, Rahmouni, A 2008 Assessment of calf muscle contraction by diffusion tensor imaging. *Eur Radiol* **18**:2303-2310.
47. Andre, JB, Bammer, R 2010 Advanced diffusion-weighted magnetic resonance imaging techniques of the human spinal cord. *Top Magn Reson Imaging* **21**:367-378.
48. Boesch, C, Slotboom, J, Hoppeler, H, Kreis, R 1997 In vivo determination of intramyocellular lipids in human muscle by means of localized ¹H-MR-spectroscopy. *Magn Reson Med* **37**:484-493.
49. Topolski, TD, LoGerfo, J, Patrick, DL, Williams, B, Walwick, J, Patrick, MB 2006 The Rapid Assessment of Physical Activity (RAPA) among older adults. *Prev Chronic Dis* **3**:A118.
50. Daughton, DM, Fix, AJ, Kass, I, Bell, CW, Patil, KD 1982 Maximum oxygen consumption and the ADAPT quality-of-life scale. *Arch Phys Med Rehabil* **63**:620-622.
51. International Society for the Advancement of Kinanthropometry 2001 International Standards for Anthropometric Assessment International Society for the Advancement of Kinanthropometry, Australia.
52. Kontulainen, SA, Johnston, JD, Liu, D, Leung, C, Oxland, TR, McKay, HA 2008 Strength indices from pQCT imaging predict up to 85% of variance in bone failure properties at tibial epiphysis and diaphysis. *J Musculoskelet Neuronal Interact* **8**:401-409.

53. Lyritis, G (ed.) 1999 Biomechanical examinations for validation of the bone strength strain index SSI, calculated by peripheral quantitative computed tomography, vol. II. Holonome editions, Athens.
54. Elzibak, AH, Noseworthy, MD 2013 Assessment of diffusion tensor imaging indices in calf muscles following postural change from standing to supine position. *Magn Reson Mater Phy*. doi: 10.1007/s10334-013-0424-1
55. Lorbergs, AL, Noseworthy, MD, MacIntyre, NJ Submitted 2014 Feasibility of magnetic resonance imaging to evaluate leg muscle macrostructural and microstructural properties in older women. *J Musculoskelet Neuron Interact*.
56. Lorbergs, AL, Noseworthy, MD, MacIntyre, NJ Submitted 2014 Age-related differences in the response of leg muscle cross-sectional area and water diffusivity measures to a period of supine rest. *Magn Reson Mater Phy*.
57. Lund, H, Christensen, L, Savnik, A, Boesen, J, Danneskiold-Samsoe, B, Bliddal, H 2002 Volume estimation of extensor muscles of the lower leg based on MR imaging. *Eur Radiol* **12**:2982-2987.
58. Jenkinson, M, Beckmann, CF, Behrens, TE, Woolrich, MW, Smith, SM 2012 FSL. *Neuroimage* **62**:782-790.
59. Wang, R, Benner, T, Sorensen, A, Wedeen, V 2007 Diffusion Toolkit: A software package for diffusion imaging data processing and tractography. *Proceedings International Soc. Mag. Reson. Med. (ISMRM)* **15**:3720.
60. Jenkinson, M, Bannister, P, Brady, M, Smith, S 2002 Improved optimization for the robust and accurate linear registration and motion correction of brain images. *Neuroimage* **17**:825-841.
61. Cox, RW 1996 AFNI: software for analysis and visualization of functional magnetic resonance neuroimages. *Comput Biomed Res* **29**:162-173.
62. Le Bihan, D, Mangin, JF, Poupon, C, Clark, CA, Pappata, S, Molko, N, Chabriat, H 2001 Diffusion tensor imaging: concepts and applications. *J Magn Reson Imaging* **13**:534-546.
63. Provencher, SW 1993 Estimation of metabolite concentrations from localized in vivo proton NMR spectra. *Magn Reson Med* **30**:672-679.
64. Jones, CJ, Rikli, RE, Beam, WC 1999 A 30-s chair-stand test as a measure of lower body strength in community-residing older adults. *Res Q Exerc Sport* **70**:113-119.

65. Ruff, CB 1984 Allometry between length and cross-sectional dimensions of the femur and tibia in *Homo sapiens sapiens*. *Am J Phys Anthropol* **65**:347-358.
66. Wong, K 2014 A tri-modality comparison of volumetric bone measure quantification using 1.0 Tesla peripheral magnetic resonance imaging, peripheral quantitative computed tomography, and high-resolution-peripheral quantitative computed tomography. *Open Access Dissertations and Theses*. Paper 8464.
67. Cohen, J 1988 *Statistical power analysis for the behavioral sciences*, 2nd ed. Erlbaum, Hillsdale, NJ.
68. NIH Consensus Development Panel on Osteoporosis Prevention, Diagnosis, and Therapy 2001 Osteoporosis prevention, diagnosis, and therapy. *JAMA* **285**:785-795.
69. Papaioannou, A, Morin, S, Cheung, AM, Atkinson, S, Brown, JP, Feldman, S, Hanley, DA, Hodsman, A, Jamal, SA, Kaiser, SM, Kvern, B, Siminoski, K, Leslie, WD, Scientific Advisory Council of Osteoporosis Canada 2010 2010 clinical practice guidelines for the diagnosis and management of osteoporosis in Canada: summary. *CMAJ* **182**:1864-1873.
70. Stathopoulos, KD, Katsimbri, P, Atsali, E, Metania, E, Zoubos, AB, Skarantavos, G 2011 Age-related differences of bone mass, geometry, and strength in treatment-naive postmenopausal women. A tibia pQCT study. *J Clin Densitom* **14**:33-40.
71. Russo, CR, Lauretani, F, Bandinelli, S, Bartali, B, Di Iorio, A, Volpato, S, Guralnik, JM, Harris, T, Ferrucci, L 2003 Aging bone in men and women: beyond changes in bone mineral density. *Osteoporos Int* **14**:531-538.
72. Szabo, KA, Webber, CE, Gordon, C, Adachi, JD, Tozer, R, Papaioannou, A 2011 Reproducibility of peripheral quantitative computed tomography measurements at the radius and tibia in healthy pre- and postmenopausal women. *Can Assoc Radiol J* **62**:183-189.
73. Polidoulis, I, Beyene, J, Cheung, AM 2012 The effect of exercise on pQCT parameters of bone structure and strength in postmenopausal women--a systematic review and meta-analysis of randomized controlled trials. *Osteoporos Int* **23**:39-51.
74. Uusi-Rasi, K, Kannus, P, Cheng, S, SievÄrnen, H, Pasanen, M, Heinonen, A, Nenonen, A, Halleen, J, Fuerst, T, Genant, H, Vuori, I 2003 Effect of alendronate and exercise on bone and physical performance of postmenopausal women: a randomized controlled trial. *Bone* **33**:132-143.
75. Miyakoshi, N, Hongo, M, Mizutani, Y, Shimada, Y 2013 Prevalence of sarcopenia in Japanese women with osteopenia and osteoporosis. *J Bone Miner Metab* **31**:556-561.

76. Cress, ME, Schechtman, KB, Mulrow, CD, Fiatarone, MA, Gerety, MB, Buchner, DM 1995 Relationship between physical performance and self-perceived physical function. *J Am Geriatr Soc* **43**:93-101.

77. Yoshida, Y, Marcus, RL, Lastayo, PC 2012 Intramuscular adipose tissue and central activation in older adults. *Muscle Nerve* **46**:813-816.

78. Pritchard, JM, Giangregorio, LM, Atkinson, SA, Beattie, KA, Inglis, D, Ioannidis, G, Punthakee, Z, Adachi, JD, Papaioannou, A 2012 Association of larger holes in the trabecular bone at the distal radius in postmenopausal women with type 2 diabetes mellitus compared to controls. *Arthritis Care Res (Hoboken)* **64**:83-91.

79. Patsch, JM, Burghardt, AJ, Yap, SP, Baum, T, Schwartz, AV, Joseph, GB, Link, TM 2013 Increased cortical porosity in type 2 diabetic postmenopausal women with fragility fractures. *J Bone Miner Res* **28**:313-324.

80. Goodpaster, BH, Thaete, FL, Kelley, DE 2000 Thigh adipose tissue distribution is associated with insulin resistance in obesity and in type 2 diabetes mellitus. *Am J Clin Nutr* **71**:885-892.

81. Barzilay, JI, Blaum, C, Moore, T, Xue, QL, Hirsch, CH, Walston, JD, Fried, LP 2007 Insulin resistance and inflammation as precursors of frailty: the Cardiovascular Health Study. *Arch Intern Med* **167**:635-641.

82. Fried, LP, Tangen, CM, Walston, J, Newman, AB, Hirsch, C, Gottdiener, J, Seeman, T, Tracy, R, Kop, WJ, Burke, G, McBurnie, MA, Cardiovascular Health Study Collaborative Research Group 2001 Frailty in older adults: evidence for a phenotype. *J Gerontol A Biol Sci Med Sci* **56**:M146-56.

83. Ensrud, KE, Ewing, SK, Taylor, BC, Fink, HA, Stone, KL, Cauley, JA, Tracy, JK, Hochberg, MC, Rodondi, N, Cawthon, PM, Study of Osteoporotic Fractures Research Group 2007 Frailty and risk of falls, fracture, and mortality in older women: the study of osteoporotic fractures. *J Gerontol A Biol Sci Med Sci* **62**:744-751.

84. Rantalainen, T, Nikander, R, Kukuljan, S, Daly, RM 2013 Mid-femoral and mid-tibial muscle cross-sectional area as predictors of tibial bone strength in middle-aged and older men. *J Musculoskelet Neuronal Interact* **13**:273-282.

85. Brotto, M, Johnson, ML 2014 Endocrine crosstalk between muscle and bone. *Curr Osteoporos Rep* **12**:135-141.

86. Williams, SE, Heemskerk, AM, Welch, EB, Li, K, Damon, BM, Park, JH 2013 Quantitative effects of inclusion of fat on muscle diffusion tensor MRI measurements. *J Magn Reson Imaging* **38**:1292-1297.

87. Hasson, CJ, Caldwell, GE 2012 Effects of age on mechanical properties of dorsiflexor and plantarflexor muscles. *Ann Biomed Eng* **40**:1088-1101.

88. Gerber, C, Schneeberger, AG, Hoppeler, H, Meyer, DC 2007 Correlation of atrophy and fatty infiltration on strength and integrity of rotator cuff repairs: a study in thirteen patients. *J Shoulder Elbow Surg* **16**:691-696.

89. Goodpaster, BH, Park, SW, Harris, TB, Kritchevsky, SB, Nevitt, M, Schwartz, AV, Simonsick, EM, Tylavsky, FA, Visser, M, Newman, AB 2006 The loss of skeletal muscle strength, mass, and quality in older adults: the health, aging and body composition study. *J Gerontol A Biol Sci Med Sci* **61**:1059-1064.

CHAPTER FIVE

SUMMARY, CONTRIBUTIONS, LIMITATIONS, AND FUTURE DIRECTIONS OF THE THESIS RESEARCH

This chapter provides an overview of the main findings presented in this thesis, a discussion of the overall contributions of these findings to the current literature, potential limitations, and recommendations for future research directions.

5.1 SUMMARY OF THESIS RESULTS

The purpose of the first study (Chapter Two) was to evaluate the influence of a period of time spent in supine on MRI measures of muscle CSA and water diffusivity in the leg of healthy young and older women. The main finding of this study was that muscle CSA did not significantly change with 30 minutes or 60 minutes of supine rest in either age group. Similarly, neither group showed a change in FA after 30 or 60 minutes of resting supine. ADC values decreased similarly in young and older women, however young women had a greater decline in medial gastrocnemius ADC between baseline and 30 minutes. Vascular changes associated with aging were expected to demonstrate between group differences in diffusivity measures, yet the study findings did not support this notion. The implications of this study are twofold: the duration of time spent in supine should be considered when scanning women of various ages and the assessment of leg muscle with DTI should consider grouping participants by sex.

The feasibility objectives in Chapter Three were to assess the rate of participant recruitment, evaluate participant tolerance to the MRI scanning protocol, and determine optimal methods for MRI scanning and image analyses. The results of the study suggested that four months of community-based recruitment were required to enroll nine older women for a study that involved evaluating leg muscle structure using PD imaging, DTI, and ¹H-MRS. For women with greater thoracic kyphosis or (risk of) vertebral fracture there were minor modifications to the way the participant was mounted and was positioned on the MRI scan bed for scanning. Although these accommodations were minor, the strategies aimed to minimize risk of injury and maximize comfort for these participants. Overall, the scan acquisition protocol was successful because imaging sessions could be performed without interruption for all participants and all data were analyzed successfully. The successful application of the scanning and analysis protocols was important for the methods to use for MRI-based musculoskeletal evaluation in older women. Specifically, achieving satisfactory results in the evaluation of all feasibility criteria were critical for the application of the recruitment, scanning, and analysis protocols, in the final thesis study that would assess older women with OP.

The final study of the thesis applied the MRI methods that were described and evaluated in Chapter Two and Chapter Three. In this study, the primary aim was to compare bone structure and strength and muscle and fat macrostructure and microstructure in the leg of healthy postmenopausal women with and without OP. The secondary and tertiary aims were to determine the associations between muscle and fat macrostructure and microstructure, tibial structure and strength, and physical performance

outcomes, respectively. The study findings indicated that musculoskeletal tissue structure and composition were similar in women diagnosed and treated for OP compared to women without OP. Intermuscular fat content was associated with greater bone mineral content; however, fat situated within muscle had a negative relationship with distal tibia bone strength and was associated with slower gait speed. Thus, the results of this study indicate that the location of fat storage may have implications on skeletal structure and physical functioning in older women. This relationship was independent of OP diagnosis. Overall, this study implicates a role for MRI-based measures of fat and muscle microstructure and macrostructure for understanding the relationships among muscle, bone and physical performance measures in postmenopausal women. These imaging-based measures may provide novel targets for pharmacologic and exercise strategies aimed at preventing functional decline and fragility fractures.

5.2 CONTRIBUTIONS OF THE THESIS TO THE LITERATURE

The studies included within the dissertation are novel and are the first to report measures of muscle and fat microstructure in the leg of older women. Aside from opening new avenues of investigation, the research conducted as part of the thesis has made important contributions to two main areas of the literature: 1) the measurement of musculoskeletal tissues and assessment of their interrelationships and, 2) the evaluation of women with OP undergoing pharmacologic treatment.

The application of DTI and ¹H-MRS for calculating muscle fibre architecture and fat infiltration, respectively, provides a means of acquiring information at a microscopic

level without using invasive techniques, such as muscle biopsy. The results of the thesis research suggest that DTI values in the leg were not related to aging, bone structure, or physical performance. Although the similarities in DTI measures between young and old women were unexpected, they suggest that the small sample of women assessed did not demonstrate a greater degree of muscle fibre disorganization or isotropy, as had been reported previously in men [150]. Women with and without OP also had similar DTI values. Indeed, this was somewhat less surprising than the former comparison. These results were contrary to the vast body of literature supporting an inextricable relationship between muscle and bone supporting the hypothesis that compromised bone quality is associated with disruption of muscle structure. However, the implications of this finding can be viewed positively from a rehabilitation perspective, since women with OP did not demonstrate microstructural muscle alterations to suggest they may respond differently to a non-pharmacologic intervention. There were no relationships between physical functioning and muscle microstructure among the older women, which precludes any further conjectures associated with the potential effects of a training response on muscle fibre morphology. Instead, this finding supports the notion that walking and repeated chair stands are complex tasks, to which coordination, balance, and muscle power would be considered more powerful determinants.

In contrast, microstructural evaluation of fat infiltration by ^1H -MRS was inversely associated with bone strength in compressive loading in older women with and without OP. This was not the first study to document IMCL content in older women, however it was the first time noninvasive measurement of IMCL content in the TibA was

documented as having an adverse relationship with tibia bone strength. Despite the fact that IMCL content was not related to physical performance outcomes, fat infiltration measured as muscle density by pQCT was inversely associated with habitual gait speed. Further, the results demonstrated that intramuscular fat content of specific muscles (TibA and GC) was also associated with slower gait speed. To summarize, the thesis research suggests that fat infiltration in the leg muscles measured at a cellular, tissue, and organ levels is associated, to some degree, with poorer bone strength and slower gait speed. Nevertheless, the results showed that intermuscular fat had a positive relationship to tibia bone mineral content, which may support the observation that greater body weight is protective against OP. This finding adds to the importance of this thesis research to the literature. For the first time, intermuscular and intramuscular fat compartments were separated and evaluated for their independent relationships with tibia bone structure and strength in older women with OP. The research presented in the thesis has uncovered multiple methods for acquiring and quantifying the relationships between leg muscles, bone, and fat. Given the increasing prevalence of musculoskeletal conditions and the increased likelihood of physical disability in older women [156], noninvasive investigation of muscle structure and composition is warranted. The new outcomes described in the thesis may help develop novel intervention targets that could be used to optimize physical functioning in older women, particularly those at risk for falls and fractures.

A main strength of this thesis, and subsequently an important contribution of the thesis research to the literature, is the enrolment of women with OP, regardless of their

current treatment plan. Therapeutic options significantly reduce the burden of fractures. International, national, and provincial strategies are in place to close the OP care gap [52, 157, 158]. That is, to increase assessment and diagnosis of OP once a fragility fracture is reported by a patient because a large proportion of individuals who suffer fractures were being overlooked [159]. In Ontario, the main action plan in place is called the Ontario Osteoporosis Strategy, which involves the Ministry of Health and Long Term Care, the Ontario Women's Health Council, charitable organizations, health care and research professionals, and numerous other community-based stakeholders [158]. In the thesis research described in Chapter Four, many of the women with OP reported fragility fractures and all of the women diagnosed with OP reported current or recent pharmacologic treatment. As such, the thesis results suggest that the OP care gap is closing, at least in the small sample of women assessed who volunteered for this study. If the OP care gap is indeed shrinking, there can be optimism among clinicians and patients that individuals at high risk of fracture are receiving treatment as indicated. A critical next step to closing the OP care gap, as the results from Chapter Four suggest, is to understand the effect that pharmacologic treatments have on muscle structure and composition and physical functioning. As a first step in this direction, the thesis research described within the dissertation incorporates women with OP using pharmacologic therapy. The study results therefore represent, to a degree, data from a representative group of healthy, community-dwelling, high-functioning women between 60 and 75y.

5.3 POTENTIAL LIMITATIONS

The limitations of each individual study are described within each of the manuscripts. This section highlights some methodological considerations for interpreting the validity and generalizability of the dissertation as a whole, as they pertain to: imaging devices, participant characteristics, and study design.

A number of factors are known to influence microstructural and macrostructural muscle measures acquired by MRI. First, individuals who are more hydrated could present increased water diffusivity values as measured by DTI. Temperature variation could affect membrane permeability, blood viscosity and flow that influences the rate of water diffusivity in peripheral skeletal muscle. The research documented as part of the thesis did not measure hydration status or body temperature; subsequently data were not controlled or adjusted for their potential effects. Participants did not present symptoms of dehydration (e.g., cramping) and were provided blankets as needed to maintain a comfortable body temperature for the scanning protocol. Exercise elevates body temperature and is associated with greater water diffusivity in skeletal muscle [160]. To minimize the effects of exercise, young women assessed in Chapter Two were instructed to avoid engaging in vigorous physical activity on the day of their study visit.

Unfortunately, the same instruction was not provided to older women and presents a source of variability that may have affected the comparison of DTI measures in young and older women. The third consideration for DTI is the influence of muscle fibre alignment. Saupe and colleagues (2008) highlighted the importance of muscle fibre pennation angle to accurately calculate diffusivity measurements [161]. To eliminate

variability in muscle fibre alignment between individuals due to positioning, all studies in the thesis used a standardized footrest for MRI scanning. The footrest stabilized the ankles at 90 degrees. To further control for differences between individuals, the measurement site was located based on individual tibia length where the five slices nearest to the fiducial marker were analyzed for all five muscle ROIs. Muscle fibre alignment is also an important consideration for ¹H-MRS. The spectral analysis of IMCL and EMCL is dependent upon the separation of the lipid peaks, which is optimal when muscle fibre alignment is parallel and aligned with the magnetic field [162].

Accordingly, the only muscle for which relative IMCL content was quantified was TibA.

There are various participant characteristics that were not measured or reported within the thesis research, even though their associations with musculoskeletal structure and function are documented in the literature. With respect to the older women, the study was only permitted to request the physicians send patient results of the most recent BMD test scores. While this medical information was an important for patient verification of BMD T-scores, it did not provide any information about the pharmacologic treatment of women diagnosed with OP. Thus, information regarding participant exposure to other anti-osteoporosis medications and details about the duration and adherence to current pharmacotherapy were not reported. For women with fragility fractures, the anatomical site, date, and mechanism (i.e., determination of fragility versus traumatic) of fracture were based on recall that was not confirmed with patient medical records. Vitamin D levels, known to influence muscle function and bone density, independent of physical activity levels [163] were not reported in the thesis. The OP clinical practice guidelines

suggest that women aged over 50y, daily supplementation of 800-1000IU of vitamin D is recommended [52]. Despite the recognized importance of vitamin D, individual levels were not assessed due to the cost of the blood tests that are not covered by the Ontario Healthy Insurance Plan and precludes many individuals from knowing their vitamin D levels. Instead, participants provided information regarding the type and amount of daily supplementation at the study visit interview.

Interpretation of the thesis results is further limited by the cross-sectional study design employed in all three manuscripts. While there are advantages to assessing relationships between variables at a given time, there are limitations to their interpretation. Most importantly, correlations do not indicate causation. Thus, the findings documented in the dissertation are confounded by a single measurement occasion and muscle DTI measures that are largely based on the theoretical motion of water molecules in an anisotropic tissue. Despite the challenges associated with measuring muscle microstructural and macrostructural variables over time (e.g., image co-registration, reliable definition of ROIs), prospectively examining changes in muscle composition and fibre architecture noninvasively would be an important contribution to the literature.

5.4 RECOMMENDATIONS FOR FUTURE RESEARCH

Each individual manuscript within the dissertation describes specific recommendations based on study findings. This section highlights some general directions for future research based on the thesis research findings as a whole.

Bone loss is exacerbated by muscle weakness and disuse. Based on the finding that gait speed and bone strength are negatively associated with increased fat infiltration, it is recommended that future OP-related research incorporate measures of physical function with measures of musculoskeletal structure. The indicators of physical functioning applied to future studies should be clinically relevant, so that important relationships between tissue structures can be identified. The development of targeted pharmacologic and non-pharmacologic interventions will have a greater overall impact if the effectiveness translates to meaningful gains for a person's health and well-being. To further apply and improve the general understanding of the importance of the musculoskeletal imaging-based outcomes, objective measurements of physical activity levels would be beneficial. For example, accelerometry could collect data regarding the average amount of time an older woman spends participating in sedentary and non-sedentary activities. Accelerometry is particularly advantageous for capturing the habitual muscle use of the lower extremities and could provide an objective description of activity levels not captured by self-report questionnaires.

Given the enormous social and personal burden of musculoskeletal conditions, there is great potential for MRI to be applied as a tool for characterizing muscle changes at the structural level. The success of this research will depend on accruing a greater understanding of the meaning of the measures, particularly with respect to the water diffusivity coefficients calculated using DTI. Studies should aim to validate the DTI eigenvalues in human skeletal muscle so that greater meaning can be given to the measures. Further, the influence of morphological changes in muscle fibre structure

should be assessed histologically and compared with DTI measures because there is growing interest in understanding the contribution of age-related mitochondrial dysfunction and subsequent muscle fibre splitting to muscle weakness [164-166]. With the increasing prevalence of T2D and obesity, there should also be research dedicated to understanding how fat infiltration in skeletal muscle influences microstructural measures calculated by DTI. From a rehabilitation perspective, assessing the detrimental effects of excess fat storage in muscle should be evaluated so that strategies can be developed to mitigate its accumulation and negative effects. It would also be worthwhile to consider an investigation of the relationship between muscle force production and muscle structure and composition. Recent studies have begun to evaluate the relationship of DTI measures with the rate of force development [167] and fat infiltration with muscle activation [168], but this area of research remains largely unexplored.

Perhaps the most obvious recommendation for future research is to determine whether similar musculoskeletal tissue characteristics and relationships are observed in men. As the population continues to grow older, OP and fractures in men are a growing health concern [169]. OP in men is now widely recognized as an understudied area because OP was primarily considered a disease of women. A shift in clinical and scientific perspectives has resulted in a recent surge of investigation in the area of OP in men, but information in this area is lagging because men are underrepresented in the OP literature. Questions regarding sex- and age-related changes in skeletal microstructure, fat accumulation, musculoskeletal tissue relationships, and the associations of physical functioning and muscle structure and composition are yet to be elucidated in both sexes.

Comparisons and contrasts between the sexes may shed light on whether strategies for preventing OP should consider sex-dependent target outcomes to increase the overall effectiveness of a given intervention.

5.4 SUMMARY

The collection of research presented in this doctoral dissertation demonstrates the application of advanced MRI scanning methods to evaluate muscle structure and composition in older women with and without an OP diagnosis. This research was a first step to determine the utility of specific scanning methods for assessing the muscle microstructure and macrostructure in older women. The contributions of this work include the exploration of age-related differences in muscle microstructure, the determination of the feasibility of MRI scanning methods to older women, and the description of the relationships between muscle structure and composition, bone structure and strength, and physical performance in active older women with and without OP. It is anticipated that the results of the thesis stimulate continued interdisciplinary research that will ultimately lead to the development and evaluation of interventions aimed at enhancing musculoskeletal structure, maximizing mobility, and maintaining optimal physical functioning in older adults.

REFERENCES

1. Visser M, Goodpaster BH, Kritchevsky SB, Newman AB, Nevitt M, Rubin SM, Simonsick EM, Harris TB (2005) Muscle mass, muscle strength, and muscle fat infiltration as predictors of incident mobility limitations in well-functioning older persons. *J Gerontol A Biol Sci Med Sci* 60:324-33
2. Newman AB, Kupelian V, Visser M, Simonsick EM, Goodpaster BH, Kritchevsky SB, Tylavsky FA, Rubin SM, Harris TB (2006) Strength, but not muscle mass, is associated with mortality in the health, aging and body composition study cohort. *J Gerontol A Biol Sci Med Sci* 61:72-7
3. Cawthon PM, Fox KM, Gandra SR, Delmonico MJ, Chiou CF, Anthony MS, Sewall A, Goodpaster B, Satterfield S, Cummings SR, Harris TB, Health, Aging and Body Composition Study (2009) Do muscle mass, muscle density, strength, and physical function similarly influence risk of hospitalization in older adults? *J Am Geriatr Soc* 57:1411-9
4. Aoyagi Y, Shephard RJ (1992) Aging and muscle function. *Sports Med* 14:376-96
5. Calmels P, Vico L, Alexandre C, Minaire P (1995) Cross-sectional study of muscle strength and bone mineral density in a population of 106 women between the ages of 44 and 87 years: relationship with age and menopause. *Eur J Appl Physiol Occup Physiol* 70:180-6
6. Rolland YM, Perry HM, 3rd, Patrick P, Banks WA, Morley JE (2007) Loss of appendicular muscle mass and loss of muscle strength in young postmenopausal women. *J Gerontol A Biol Sci Med Sci* 62:330-5
7. Goodpaster BH, Park SW, Harris TB, Kritchevsky SB, Nevitt M, Schwartz AV, Simonsick EM, Tylavsky FA, Visser M, Newman AB (2006) The loss of skeletal muscle strength, mass, and quality in older adults: the health, aging and body composition study. *J Gerontol A Biol Sci Med Sci* 61:1059-64
8. Samson MM, Meeuwssen IB, Crowe A, Dessens JA, Duursma SA, Verhaar HJ (2000) Relationships between physical performance measures, age, height and body weight in healthy adults. *Age Ageing* 29:235-42
9. Maughan RJ, Watson JS, Weir J (1983) Strength and cross-sectional area of human skeletal muscle. *J Physiol* 338:37-49
10. Ikai M, Fukunaga T (1968) Calculation of muscle strength per unit cross-sectional area of human muscle by means of ultrasonic measurement. *Int Z Angew Physiol* 26:26-32

11. Fukunaga T, Miyatani M, Tachi M, Kouzaki M, Kawakami Y, Kanehisa H (2001) Muscle volume is a major determinant of joint torque in humans. *Acta Physiol Scand* 172:249-55
12. Frank AW, Lorbergs AL, Chilibeck PD, Farthing JP, Kontulainen SA (2010) Muscle cross sectional area and grip torque contraction types are similarly related to pQCT derived bone strength indices in the radii of older healthy adults. *J Musculoskelet Neuronal Interact* 10:136-41
13. MacIntyre NJ, Rombough R, Brouwer B (2010) Relationships between calf muscle density and muscle strength, mobility and bone status in the stroke survivors with subacute and chronic lower limb hemiparesis. *J Musculoskelet Neuronal Interact* 10:249-55
14. Lexell J, Henriksson-Larsen K, Winblad B, Sjostrom M (1983) Distribution of different fiber types in human skeletal muscles: effects of aging studied in whole muscle cross sections. *Muscle Nerve* 6:588-95
15. Lexell J, Downham D (1992) What is the effect of ageing on type 2 muscle fibres? *J Neurol Sci* 107:250-1
16. Larsson L, Sjodin B, Karlsson J (1978) Histochemical and biochemical changes in human skeletal muscle with age in sedentary males, age 22-65 years. *Acta Physiol Scand* 103:31-9
17. Lexell J, Taylor CC, Sjostrom M (1988) What is the cause of the ageing atrophy? Total number, size and proportion of different fiber types studied in whole vastus lateralis muscle from 15- to 83-year-old men. *J Neurol Sci* 84:275-94
18. Rolland Y, Czerwinski S, Abellan Van Kan G, Morley JE, Cesari M, Onder G, Woo J, Baumgartner R, Pillard F, Boirie Y, Chumlea WM, Vellas B (2008) Sarcopenia: its assessment, etiology, pathogenesis, consequences and future perspectives. *J Nutr Health Aging* 12:433-50
19. Jacob S, Machann J, Rett K, Brechtel K, Volk A, Renn W, Maerker E, Matthaei S, Schick F, Claussen CD, Haring HU (1999) Association of increased intramyocellular lipid content with insulin resistance in lean nondiabetic offspring of type 2 diabetic subjects. *Diabetes* 48:1113-9
20. Marcus RL, Addison O, Dibble LE, Foreman KB, Morrell G, Lastayo P (2012) Intramuscular adipose tissue, sarcopenia, and mobility function in older individuals. *J Aging Res* 2012:629637

21. Tuttle LJ, Sinacore DR, Mueller MJ (2012) Intermuscular adipose tissue is muscle specific and associated with poor functional performance. *J Aging Res* 2012:172957 DOI 10.1155/2012/172957
22. Ensrud KE, Palermo L, Black DM, Cauley J, Jergas M, Orwoll ES, Nevitt MC, Fox KM, Cummings SR (1995) Hip and calcaneal bone loss increase with advancing age: longitudinal results from the study of osteoporotic fractures. *J Bone Miner Res* 10:1778-87
23. Greendale GA, Sowers M, Han W, Huang MH, Finkelstein JS, Crandall CJ, Lee JS, Karlamangla AS (2011) Bone mineral density loss in relation to the final menstrual period in a multi-ethnic cohort: Results from the study of women's health across the nation (SWAN). *J Bone Miner Res* DOI 10.1002/jbmr.534
24. Recker R, Lappe J, Davies K, Heaney R (2000) Characterization of perimenopausal bone loss: a prospective study. *J Bone Miner Res* 15:1965-73
25. Khosla S, Atkinson EJ, Dunstan CR, O'Fallon WM (2002) Effect of estrogen versus testosterone on circulating osteoprotegerin and other cytokine levels in normal elderly men. *J Clin Endocrinol Metab* 87:1550-4
26. Khosla S, Bellido TM, Drezner MK, Gordon CM, Harris TB, Kiel DP, Kream BE, LeBoff MS, Lian JB, Peterson CA, Rosen CJ, Williams JP, Winer KK, Sherman SS (2011) Forum on aging and skeletal health: summary of the proceedings of an ASBMR workshop. *J Bone Miner Res* 26:2565-78
27. Uusi-Rasi K, Sievanen H, Pasanen M, Kannus P (2007) Age-related decline in trabecular and cortical density: a 5-year peripheral quantitative computed tomography follow-up study of pre- and postmenopausal women. *Calcif Tissue Int* 81:249-53
28. Zebaze RM, Ghasem-Zadeh A, Bohte A, Iuliano-Burns S, Mirams M, Price RI, Mackie EJ, Seeman E (2010) Intracortical remodelling and porosity in the distal radius and post-mortem femurs of women: a cross-sectional study. *Lancet* 375:1729-36
29. Ahlborg HG, Johnell O, Turner CH, Rannevik G, Karlsson MK (2003) Bone loss and bone size after menopause. *N Engl J Med* 349:327-34
30. Qin L, Au SK, Leung PC, Lau MC, Woo J, Choy WY, Hung WY, Dambacher MA, Leung KS (2002) Baseline BMD and bone loss at distal radius measured by peripheral quantitative computed tomography in peri- and postmenopausal Hong Kong Chinese women. *Osteoporos Int* 13:962-70
31. Sowers MR, Zheng H, Jannausch ML, McConnell D, Nan B, Harlow S, Randolph JF, Jr (2010) Amount of bone loss in relation to time around the final menstrual period and

follicle-stimulating hormone staging of the transmenopause. *J Clin Endocrinol Metab* 95:2155-62

32. Rosenberg IH (1997) Sarcopenia: origins and clinical relevance. *J Nutr* 127:990S-1S

33. Fielding RA, Vellas B, Evans WJ, Bhasin S, Morley JE, Newman AB, Abellan van Kan G, Andrieu S, Bauer J, Breuille D, Cederholm T, Chandler J, De Meynard C, Donini L, Harris T, Kannt A, Keime Guibert F, Onder G, Papanicolaou D, Rolland Y, Rooks D, Sieber C, Souhami E, Verlaan S, Zamboni M (2011) Sarcopenia: an undiagnosed condition in older adults. Current consensus definition: prevalence, etiology, and consequences. *J Am Med Dir Assoc* 12:249-56

34. Jeejeebhoy KN (2012) Malnutrition, fatigue, frailty, vulnerability, sarcopenia and cachexia: overlap of clinical features. *Curr Opin Clin Nutr Metab Care* 15:213-9

35. Conley KE, Cress ME, Jubrias SA, Esselman PC, Odderson IR (1995) From muscle properties to human performance, using magnetic resonance. *J Gerontol A Biol Sci Med Sci* 50 Spec No:35-40

36. Cree MG, Newcomer BR, Katsanos CS, Sheffield-Moore M, Chinkes D, Aarsland A, Urban R, Wolfe RR (2004) Intramuscular and liver triglycerides are increased in the elderly. *J Clin Endocrinol Metab* 89:3864-71

37. Doherty TJ (2001) The influence of aging and sex on skeletal muscle mass and strength. *Curr Opin Clin Nutr Metab Care* 4:503-8

38. Ryall JG, Schertzer JD, Lynch GS (2008) Cellular and molecular mechanisms underlying age-related skeletal muscle wasting and weakness. *Biogerontology* 9:213-28

39. Proctor DN, Melton LJ, Khosla S, Crowson CS, O'Connor MK, Riggs BL (2000) Relative influence of physical activity, muscle mass and strength on bone density. *Osteoporos Int* 11:944-52

40. Baumgartner RN, Koehler KM, Gallagher D, Romero L, Heymsfield SB, Ross RR, Garry PJ, Lindeman RD (1998) Epidemiology of sarcopenia among the elderly in New Mexico. *Am J Epidemiol* 147:755-63

41. Janssen I, Shepard DS, Katzmarzyk PT, Roubenoff R (2004) The healthcare costs of sarcopenia in the United States. *J Am Geriatr Soc* 52:80-5

42. National Institutes of Health (1993) Consensus development conference: diagnosis, prophylaxis, and treatment of osteoporosis. *Am J Med* 94:646-50

43. WHO Scientific Group on the Prevention and Management of Osteoporosis (2000 : Geneva, Switzerland) (2003) Prevention and management of osteoporosis. World Health Organ Tech Rep Ser 921:1-164

44. Lentle B, Cheung AM, Hanley DA, Leslie WD, Lyons D, Papaioannou A, Atkinson S, Brown JP, Feldman S, Hodsman AB, Jamal AS, Josse RG, Kaiser SM, Kvern B, Morin S, Siminoski K, Scientific Advisory Council of Osteoporosis Canada (2011) Osteoporosis Canada 2010 guidelines for the assessment of fracture risk. *Can Assoc Radiol J* 62:243-50

45. Osteoporosis Canada (2012) Facts and statistics about osteoporosis. http://www.osteoporosis.ca/index.php/ci_id/8867/la_id/1.htm Accessed: March 3, 2014

46. Kanis JA, Borgstrom F, De Laet C, Johansson H, Johnell O, Jonsson B, Oden A, Zethraeus N, Pflieger B, Khaltav N (2005) Assessment of fracture risk. *Osteoporos Int* 16:581-9

47. Holmberg AH, Johnell O, Nilsson PM, Nilsson J, Berglund G, Akesson K (2006) Risk factors for fragility fracture in middle age. A prospective population-based study of 33,000 men and women. *Osteoporos Int* 17:1065-77

48. Lindsay R, Silverman SL, Cooper C, Hanley DA, Barton I, Broy SB, Licata A, Benhamou L, Geusens P, Flowers K, Stracke H, Seeman E (2001) Risk of new vertebral fracture in the year following a fracture. *JAMA* 285:320-3

49. Papaioannou A, Kennedy CC, Ioannidis G, Sawka A, Hopman WM, Pickard L, Brown JP, Josse RG, Kaiser S, Anastassiades T, Goltzman D, Papadimitropoulos M, Tenenhouse A, Prior JC, Olszynski WP, Adachi JD, CaMos Study Group (2009) The impact of incident fractures on health-related quality of life: 5 years of data from the Canadian Multicentre Osteoporosis Study. *Osteoporos Int* 20:703-14

50. Ioannidis G, Papaioannou A, Hopman WM, Akhtar-Danesh N, Anastassiades T, Pickard L, Kennedy CC, Prior JC, Olszynski WP, Davison KS, Goltzman D, Thabane L, Gafni A, Papadimitropoulos EA, Brown JP, Josse RG, Hanley DA, Adachi JD (2009) Relation between fractures and mortality: results from the Canadian Multicentre Osteoporosis Study. *CMAJ* 181:265-71

51. Tarride JE, Hopkins RB, Leslie WD, Morin S, Adachi JD, Papaioannou A, Bessette L, Brown JP, Goeree R (2012) The burden of illness of osteoporosis in Canada. *Osteoporos Int* 23:2591-600

52. Papaioannou A, Morin S, Cheung AM, Atkinson S, Brown JP, Feldman S, Hanley DA, Hodsman A, Jamal SA, Kaiser SM, Kvern B, Siminoski K, Leslie WD, Scientific Advisory Council of Osteoporosis Canada (2010) 2010 clinical practice guidelines for the diagnosis and management of osteoporosis in Canada: summary. *CMAJ* 182:1864-73

53. Body JJ, Bergmann P, Boonen S, Boutsen Y, Bruyere O, Devogelaer JP, Goemaere S, Hollevoet N, Kaufman JM, Milisen K, Rozenberg S, Reginster JY (2011) Non-pharmacological management of osteoporosis: a consensus of the Belgian Bone Club. *Osteoporos Int* 22(11):2769-88
54. Boonen S, Lips P, Bouillon R, Bischoff-Ferrari HA, Vanderschueren D, Haentjens P (2007) Need for additional calcium to reduce the risk of hip fracture with vitamin d supplementation: evidence from a comparative metaanalysis of randomized controlled trials. *J Clin Endocrinol Metab* 92:1415-23
55. Tagliafico AS, Ameri P, Bovio M, Puntoni M, Capaccio E, Murialdo G, Martinoli C (2010) Relationship between fatty degeneration of thigh muscles and vitamin D status in the elderly: a preliminary MRI study. *AJR Am J Roentgenol* 194:728-34
56. Rizzoli R, Boonen S, Brandi ML, Bruyere O, Cooper C, Kanis JA, Kaufman JM, Ringe JD, Weryha G, Reginster JY (2013) Vitamin D supplementation in elderly or postmenopausal women: a 2013 update of the 2008 recommendations from the European Society for Clinical and Economic Aspects of Osteoporosis and Osteoarthritis (ESCEO). *Curr Med Res Opin* 29:305-13
57. Giangregorio LM, Papaioannou A, Macintyre NJ, Ashe MC, Heinonen A, Shipp K, Wark J, McGill S, Keller H, Jain R, Laprade J, Cheung AM (2014) Too Fit To Fracture: exercise recommendations for individuals with osteoporosis or osteoporotic vertebral fracture. *Osteoporos Int* 25:821-35
58. Howe TE, Shea B, Dawson LJ, Downie F, Murray A, Ross C, Harbour RT, Caldwell LM, Creed G (2011) Exercise for preventing and treating osteoporosis in postmenopausal women. *Cochrane Database Syst Rev* (7):CD000333 DOI 10.1002/14651858.CD000333.pub2
59. Hamilton CJ, Swan VJ, Jamal SA (2010) The effects of exercise and physical activity participation on bone mass and geometry in postmenopausal women: a systematic review of pQCT studies. *Osteoporos Int* 21:11-23
60. Gillespie LD, Robertson MC, Gillespie WJ, Lamb SE, Gates S, Cumming RG, Rowe BH (2009) Interventions for preventing falls in older people living in the community. *Cochrane Database Syst Rev* (2):CD007146. DOI 10.1002/14651858.CD007146.pub2
61. Rubin CT, Bain SD, McLeod KJ (1992) Suppression of the osteogenic response in the aging skeleton. *Calcif Tissue Int* 50:306-13

62. Papaioannou A, Kennedy CC, Dolovich L, Lau E, Adachi JD (2007) Patient adherence to osteoporosis medications: problems, consequences and management strategies. *Drugs Aging* 24:37-55
63. Sampalis JS, Adachi JD, Rampakakis E, Vaillancourt J, Karellis A, Kindundu C (2012) Long-term impact of adherence to oral bisphosphonates on osteoporotic fracture incidence. *J Bone Miner Res* 27:202-10
64. Papapoulos SE (2013; 2013) Bisphosphonates for Postmenopausal Osteoporosis, In Anonymous (2013; 2013) Primer on the Metabolic Bone Diseases and Disorders of Mineral Metabolism. John Wiley & Sons, Inc., pp 412-9.
65. Bebenek M, Kemmler W, Stengel S, Engelke K, Kalender WA (2010) Effect of exercise and *Cimicifuga racemosa* (CR BNO 1055) on bone mineral density, 10-year coronary heart disease risk, and menopausal complaints: the randomized controlled Training and *Cimicifuga racemosa* Erlangen (TRACE) study. *Menopause* 17:791-800
66. Mellstrom DD, Sorensen OH, Goemaere S, Roux C, Johnson TD, Chines AA (2004) Seven years of treatment with risedronate in women with postmenopausal osteoporosis. *Calcif Tissue Int* 75:462-8
67. Black DM, Schwartz AV, Ensrud KE, Cauley JA, Levis S, Quandt SA, Satterfield S, Wallace RB, Bauer DC, Palermo L, Wehren LE, Lombardi A, Santora AC, Cummings SR, FLEX Research Group (2006) Effects of continuing or stopping alendronate after 5 years of treatment: the Fracture Intervention Trial Long-term Extension (FLEX): a randomized trial. *JAMA* 296:2927-38
68. Black DM, Cummings SR, Karpf DB, Cauley JA, Thompson DE, Nevitt MC, Bauer DC, Genant HK, Haskell WL, Marcus R, Ott SM, Torner JC, Quandt SA, Reiss TF, Ensrud KE (1996) Randomised trial of effect of alendronate on risk of fracture in women with existing vertebral fractures. Fracture Intervention Trial Research Group. *Lancet* 348:1535-41
69. McClung MR, Geusens P, Miller PD, Zippel H, Bensen WG, Roux C, Adami S, Fogelman I, Diamond T, Eastell R, Meunier PJ, Reginster JY, Hip Intervention Program Study Group (2001) Effect of risedronate on the risk of hip fracture in elderly women. Hip Intervention Program Study Group. *N Engl J Med* 344:333-40
70. Black DM, Delmas PD, Eastell R, Reid IR, Boonen S, Cauley JA, Cosman F, Lakatos P, Leung PC, Man Z, Mautalen C, Mesenbrink P, Hu H, Caminis J, Tong K, Rosario-Jansen T, Krasnow J, Hue TF, Sellmeyer D, Eriksen EF, Cummings SR, HORIZON Pivotal Fracture Trial (2007) Once-yearly zoledronic acid for treatment of postmenopausal osteoporosis. *N Engl J Med* 356:1809-22

71. Cummings SR, Black DM, Thompson DE, Applegate WB, Barrett-Connor E, Musliner TA, Palermo L, Prineas R, Rubin SM, Scott JC, Vogt T, Wallace R, Yates AJ, LaCroix AZ (1998) Effect of alendronate on risk of fracture in women with low bone density but without vertebral fractures: results from the Fracture Intervention Trial. *JAMA* 280:2077-82
72. Harris ST, Watts NB, Genant HK, McKeever CD, Hangartner T, Keller M, Chesnut CH, 3rd, Brown J, Eriksen EF, Hoseney MS, Axelrod DW, Miller PD (1999) Effects of risedronate treatment on vertebral and nonvertebral fractures in women with postmenopausal osteoporosis: a randomized controlled trial. Vertebral Efficacy With Risedronate Therapy (VERT) Study Group. *JAMA* 282:1344-52
73. Bolognese MA (2010) SERMs and SERMs with estrogen for postmenopausal osteoporosis. *Rev Endocr Metab Disord* 11:253-9
74. Cranney A, Tugwell P, Zytaruk N, Robinson V, Weaver B, Adachi J, Wells G, Shea B, Guyatt G, Osteoporosis Methodology Group and The Osteoporosis Research Advisory Group (2002) Meta-analyses of therapies for postmenopausal osteoporosis. IV. Meta-analysis of raloxifene for the prevention and treatment of postmenopausal osteoporosis. *Endocr Rev* 23:524-8
75. Ettinger B, Black DM, Mitlak BH, Knickerbocker RK, Nickelsen T, Genant HK, Christiansen C, Delmas PD, Zanchetta JR, Stakkestad J, Gluer CC, Krueger K, Cohen FJ, Eckert S, Ensrud KE, Avioli LV, Lips P, Cummings SR (1999) Reduction of vertebral fracture risk in postmenopausal women with osteoporosis treated with raloxifene: results from a 3-year randomized clinical trial. Multiple Outcomes of Raloxifene Evaluation (MORE) Investigators. *JAMA* 282:637-45
76. Jiang Y, Zhao JJ, Mitlak BH, Wang O, Genant HK, Eriksen EF (2003) Recombinant human parathyroid hormone (1-34) [teriparatide] improves both cortical and cancellous bone structure. *J Bone Miner Res* 18:1932-41
77. Dempster DW, Cosman F, Kurland ES, Zhou H, Nieves J, Woelfert L, Shane E, Plavetic K, Muller R, Bilezikian J, Lindsay R (2001) Effects of daily treatment with parathyroid hormone on bone microarchitecture and turnover in patients with osteoporosis: a paired biopsy study. *J Bone Miner Res* 16:1846-53
78. Cosman F, Greenspan S (2013; 2013) Parathyroid Hormone Treatment for Osteoporosis, In Anonymous (2013; 2013) *Primer on the Metabolic Bone Diseases and Disorders of Mineral Metabolism*. John Wiley & Sons, Inc., pp 428-36.
79. Neer RM, Arnaud CD, Zanchetta JR, Prince R, Gaich GA, Reginster JY, Hodsmann AB, Eriksen EF, Ish-Shalom S, Genant HK, Wang O, Mitlak BH (2001) Effect of

parathyroid hormone (1-34) on fractures and bone mineral density in postmenopausal women with osteoporosis. *N Engl J Med* 344:1434-41

80. Deal C, Omizo M, Schwartz EN, Eriksen EF, Cantor P, Wang J, Glass EV, Myers SL, Krege JH (2005) Combination teriparatide and raloxifene therapy for postmenopausal osteoporosis: results from a 6-month double-blind placebo-controlled trial. *J Bone Miner Res* 20:1905-11

81. Boyce BF, Xing L (2007) The RANKL/RANK/OPG pathway. *Curr Osteoporos Rep* 5:98-104

82. Cummings SR, San Martin J, McClung MR, Siris ES, Eastell R, Reid IR, Delmas P, Zoog HB, Austin M, Wang A, Kutilek S, Adami S, Zanchetta J, Libanati C, Siddhanti S, Christiansen C, FREEDOM Trial (2009) Denosumab for prevention of fractures in postmenopausal women with osteoporosis. *N Engl J Med* 361:756-65

83. Boonen S, Adachi JD, Man Z, Cummings SR, Lippuner K, Torring O, Gallagher JC, Farrerons J, Wang A, Franchimont N, San Martin J, Grauer A, McClung M (2011) Treatment with denosumab reduces the incidence of new vertebral and hip fractures in postmenopausal women at high risk. *J Clin Endocrinol Metab* 96:1727-36

84. Miller PD, Bolognese MA, Lewiecki EM, McClung MR, Ding B, Austin M, Liu Y, San Martin J, Amg Bone Loss Study Group (2008) Effect of denosumab on bone density and turnover in postmenopausal women with low bone mass after long-term continued, discontinued, and restarting of therapy: a randomized blinded phase 2 clinical trial. *Bone* 43:222-9

85. Bone HG, Bolognese MA, Yuen CK, Kendler DL, Miller PD, Yang YC, Grazette L, San Martin J, Gallagher JC (2011) Effects of denosumab treatment and discontinuation on bone mineral density and bone turnover markers in postmenopausal women with low bone mass. *J Clin Endocrinol Metab* 96:972-80

86. Frost HM (2003) Bone's Mechanostat: A 2003 Update. *Anat Rec* 275A:1081-101

87. Kontulainen S, Sievanen H, Kannus P, Pasanen M, Vuori I (2002) Effect of long-term impact-loading on mass, size, and estimated strength of humerus and radius of female racquet-sports players: a peripheral quantitative computed tomography study between young and old starters and controls. *J Bone Miner Res* 17:2281-9

88. Nikander R, Sievanen H, Uusi-Rasi K, Heinonen A, Kannus P (2006) Loading modalities and bone structures at nonweight-bearing upper extremity and weight-bearing lower extremity: a pQCT study of adult female athletes. *Bone* 39:886-94

89. Rubin CT, Rubin J, Judex S (2013; 2013) Exercise and the Prevention of Osteoporosis, In Anonymous (2013; 2013) Primer on the Metabolic Bone Diseases and Disorders of Mineral Metabolism. John Wiley & Sons, Inc., pp 396-402.
90. Rittweger J, Felsenberg D (2009) Recovery of muscle atrophy and bone loss from 90 days bed rest: Results from a one-year follow-up RID A-4308-2009. *Bone* 44:214-24
91. Armbrecht G, Belavy DL, Backstroem M, Beller G, Alexandre C, Rizzoli R, Felsenberg D (2011) Trabecular and Cortical Bone Density and Architecture in Women After 60 Days of Bed Rest Using High-Resolution pQCT: WISE 2005. *Journal of Bone and Mineral Research* 26:2399-410
92. Shackelford LC, LeBlanc AD, Driscoll TB, Evans HJ, Rianon NJ, Smith SM, Spector E, Feedback DL, Lai D (2004) Resistance exercise as a countermeasure to disuse-induced bone loss. *J Appl Physiol* 97:119-29
93. Rittweger J, Frost HM, Schiessl H, Ohshima H, Alkner B, Tesch P, Felsenberg D (2005) Muscle atrophy and bone loss after 90 days' bed rest and the effects of flywheel resistive exercise and pamidronate: results from the LTBR study. *Bone* 36:1019-29
94. Gopal S, Majumder S, Batchelor AG, Knight SL, De Boer P, Smith RM (2000) Fix and flap: the radical orthopaedic and plastic treatment of severe open fractures of the tibia. *J Bone Joint Surg Br* 82:959-66
95. Harry LE, Sandison A, Paleolog EM, Hansen U, Pearse MF, Nanchahal J (2008) Comparison of the healing of open tibial fractures covered with either muscle or fasciocutaneous tissue in a murine model. *J Orthop Res* 26:1238-44
96. Clarke MS, Khakee R, McNeil PL (1993) Loss of cytoplasmic basic fibroblast growth factor from physiologically wounded myofibers of normal and dystrophic muscle. *J Cell Sci* 106 (Pt 1):121-33
97. Adams GR, Haddad F, Bodell PW, Tran PD, Baldwin KM (2007) Combined isometric, concentric, and eccentric resistance exercise prevents unloading-induced muscle atrophy in rats. *J Appl Physiol* (1985) 103:1644-54
98. Gilson H, Schakman O, Combaret L, Lause P, Grobet L, Attaix D, Ketelslegers JM, Thissen JP (2007) Myostatin gene deletion prevents glucocorticoid-induced muscle atrophy. *Endocrinology* 148:452-60
99. Hamrick MW (2011) A role for myokines in muscle-bone interactions. *Exerc Sport Sci Rev* 39:43-7

100. Hamrick MW, McNeil PL, Patterson SL (2010) Role of muscle-derived growth factors in bone formation. *J Musculoskelet Neuronal Interact* 10:64-70
101. World Health Organization (WHO) (2014) World Health Statistics 2014; Part III, Global health indicators
http://www.who.int/gho/publications/world_health_statistics/2014/en/ Accessed: May 8, 2014
102. Addison O, Marcus RL, Lastayo PC, Ryan AS (2014) Intermuscular Fat: A Review of the Consequences and Causes. *Int J Endocrinol* 2014:309570
103. Okazaki R, Inoue D, Shibata M, Saika M, Kido S, Ooka H, Tomiyama H, Sakamoto Y, Matsumoto T (2002) Estrogen promotes early osteoblast differentiation and inhibits adipocyte differentiation in mouse bone marrow stromal cell lines that express estrogen receptor (ER) alpha or beta. *Endocrinology* 143:2349-56
104. Goodpaster BH, Kelley DE, Thaete FL, He J, Ross R (2000) Skeletal muscle attenuation determined by computed tomography is associated with skeletal muscle lipid content. *J Appl Physiol* (1985) 89:104-10
105. Hughes VA, Frontera WR, Wood M, Evans WJ, Dallal GE, Roubenoff R, Fiatarone Singh MA (2001) Longitudinal muscle strength changes in older adults: influence of muscle mass, physical activity, and health. *J Gerontol A Biol Sci Med Sci* 56:B209-17
106. Goodpaster BH, Carlson CL, Visser M, Kelley DE, Scherzinger A, Harris TB, Stamm E, Newman AB (2001) Attenuation of skeletal muscle and strength in the elderly: The Health ABC Study. *J Appl Physiol* 90:2157-65
107. Manini TM, Clark BC, Nalls MA, Goodpaster BH, Ploutz-Snyder LL, Harris TB (2007) Reduced physical activity increases intermuscular adipose tissue in healthy young adults. *Am J Clin Nutr* 85:377-84
108. Lang T, Cauley JA, Tylavsky F, Bauer D, Cummings S, Harris TB, Health ABC Study (2010) Computed tomographic measurements of thigh muscle cross-sectional area and attenuation coefficient predict hip fracture: the health, aging, and body composition study. *J Bone Miner Res* 25:513-9
109. Karampinos DC, Baum T, Nardo L, Alizai H, Yu H, Carballido-Gamio J, Yap SP, Shimakawa A, Link TM, Majumdar S (2012) Characterization of the regional distribution of skeletal muscle adipose tissue in type 2 diabetes using chemical shift-based water/fat separation. *J Magn Reson Imaging* 35:899-907
110. Kent-Braun JA, Ng AV, Young K (2000) Skeletal muscle contractile and noncontractile components in young and older women and men. *J Appl Physiol* 88:662-8

111. Schwenzer NF, Martirosian P, Machann J, Schraml C, Steidle G, Claussen CD, Schick F (2009) Aging effects on human calf muscle properties assessed by MRI at 3 Tesla. *J Magn Reson Imaging* 29:1346-54

112. Boettcher M, Machann J, Stefan N, Thamer C, Haring HU, Claussen CD, Fritsche A, Schick F (2009) Intermuscular adipose tissue (IMAT): association with other adipose tissue compartments and insulin sensitivity. *J Magn Reson Imaging* 29:1340-5

113. Buford TW, Lott DJ, Marzetti E, Wohlgemuth SE, Vandenberg K, Pahor M, Leeuwenburgh C, Manini TM (2012) Age-related differences in lower extremity tissue compartments and associations with physical function in older adults. *Exp Gerontol* 47:38-44

114. Clark BC, Manini TM (2008) Sarcopenia \neq dynapenia. *J Gerontol A Biol Sci Med Sci* 63:829-34

115. Maly MR, Calder KM, Macintyre NJ, Beattie KA (2013) Relationship of intermuscular fat volume in the thigh with knee extensor strength and physical performance in women at risk of or with knee osteoarthritis. *Arthritis Care Res* 65:44-52

116. Macintyre NJ, Lorbergs AL (2012) Imaging-based methods for non-invasive assessment of bone properties influenced by mechanical loading. *Physiother Can* 64:202-15

117. Bonnyman AM, Webber CE, Stratford PW, MacIntyre NJ (2012) Intrarater reliability of dual-energy X-ray absorptiometry-based measures of vertebral height in postmenopausal women. *J Clin Densitom* 15:405-12

118. Shepherd JA, Fan B, Lu Y, Lewiecki EM, Miller P, Genant HK (2006) Comparison of BMD precision for Prodigy and Delphi spine and femur scans. *Osteoporos Int* 17:1303-8

119. Hounsfield GN (1980) Computed medical imaging. *Science* 210:22-8

120. Hudelmaier M, Wirth W, Himmer M, Ring-Dimitriou S, Sanger A, Eckstein F (2010) Effect of exercise intervention on thigh muscle volume and anatomical cross-sectional areas--quantitative assessment using MRI. *Magn Reson Med* 64:1713-20

121. Noseworthy MD, Davis AD, Elzibak AH (2010) Advanced MR imaging techniques for skeletal muscle evaluation. *Semin Musculoskelet Radiol* 14:257-68

122. Galban CJ, Maderwald S, Uffmann K, de Greiff A, Ladd ME (2004) Diffusive sensitivity to muscle architecture: a magnetic resonance diffusion tensor imaging study of the human calf. *Eur J Appl Physiol* 93:253-62
123. Le Bihan D, Mangin JF, Poupon C, Clark CA, Pappata S, Molko N, Chabriat H (2001) Diffusion tensor imaging: concepts and applications. *J Magn Reson Imaging* 13:534-46
124. Tseng WY, Wedeen VJ, Reese TG, Smith RN, Halpern EF (2003) Diffusion tensor MRI of myocardial fibers and sheets: correspondence with visible cut-face texture. *J Magn Reson Imaging* 17:31-42
125. Zhou Z, Delproposto Z, Wu L, Xu J, Hua J, Zhou Y, Ye Y, Zhang Z, Hu J, Haacke EM (2012) In ovo serial skeletal muscle diffusion tractography of the developing chick embryo using DTI: feasibility and correlation with histology. *BMC Dev Biol* 12:38, 213X-12-38
126. Sinha S, Sinha U, Edgerton VR (2006) In vivo diffusion tensor imaging of the human calf muscle. *J Magn Reson Imaging* 24:182-90
127. Hatakenaka M, Matsuo Y, Setoguchi T, Yabuuchi H, Okafuji T, Kamitani T, Nishikawa K, Honda H (2008) Alteration of proton diffusivity associated with passive muscle extension and contraction. *J Magn Reson Imaging* 27:932-7
128. Scheel M, von Roth P, Winkler T, Arampatzis A, Prokscha T, Hamm B, Diederichs G (2013) Fiber type characterization in skeletal muscle by diffusion tensor imaging. *NMR Biomed* 26:1220-4
129. Galban CJ, Maderwald S, Stock F, Ladd ME (2007) Age-related changes in skeletal muscle as detected by diffusion tensor magnetic resonance imaging. *J Gerontol A Biol Sci Med Sci* 62:453-8
130. Zaraiskaya T, Kumbhare D, Noseworthy MD (2006) Diffusion tensor imaging in evaluation of human skeletal muscle injury. *J Magn Reson Imaging* 24:402-8
131. Cermak NM, Noseworthy MD, Bourgeois JM, Tarnopolsky MA, Gibala MJ (2012) Diffusion tensor MRI to assess skeletal muscle disruption following eccentric exercise. *Muscle Nerve* 46:42-50
132. Schick F, Eismann B, Jung WI, Bongers H, Bunse M, Lutz O (1993) Comparison of localized proton NMR signals of skeletal muscle and fat tissue in vivo: two lipid compartments in muscle tissue. *Magn Reson Med* 29:158-67

133. Boesch C, Machann J, Vermathen P, Schick F (2006) Role of proton MR for the study of muscle lipid metabolism. *NMR Biomed* 19:968-88
134. Vermathen P, Kreis R, Boesch C (2004) Distribution of intramyocellular lipids in human calf muscles as determined by MR spectroscopic imaging. *Magn Reson Med* 51:253-62
135. Boesch C, Decombaz J, Slotboom J, Kreis R (1999) Observation of intramyocellular lipids by means of ¹H magnetic resonance spectroscopy. *Proc Nutr Soc* 58:841-50
136. Petersen KF, Befroy D, Dufour S, Dziura J, Ariyan C, Rothman DL, DiPietro L, Cline GW, Shulman GI (2003) Mitochondrial dysfunction in the elderly: possible role in insulin resistance. *Science* 300:1140-2
137. Zehnder M, Ith M, Kreis R, Saris W, Boutellier U, Boesch C (2005) Gender-specific usage of intramyocellular lipids and glycogen during exercise. *Med Sci Sports Exerc* 37:1517-24
138. Schrauwen-Hinderling VB, Schrauwen P, Hesselink MK, van Engelshoven JM, Nicolay K, Saris WH, Kessels AG, Kooi ME (2003) The increase in intramyocellular lipid content is a very early response to training. *J Clin Endocrinol Metab* 88:1610-6
139. Sinha R, Dufour S, Petersen KF, LeBon V, Enoksson S, Ma YZ, Savoye M, Rothman DL, Shulman GI, Caprio S (2002) Assessment of skeletal muscle triglyceride content by ¹H nuclear magnetic resonance spectroscopy in lean and obese adolescents: relationships to insulin sensitivity, total body fat, and central adiposity. *Diabetes* 51:1022-7
140. Bredella MA, Ghomi RH, Thomas BJ, Miller KK, Torriani M (2010) Comparison of 3.0 T proton magnetic resonance spectroscopy short and long echo-time measures of intramyocellular lipids in obese and normal-weight women. *J Magn Reson Imaging* 32:388-93
141. Boesch C (2007) Musculoskeletal spectroscopy. *J Magn Reson Imaging* 25:321-38
142. Bamman MM, Newcomer BR, Larson-Meyer DE, Weinsier RL, Hunter GR (2000) Evaluation of the strength-size relationship in vivo using various muscle size indices. *Med Sci Sports Exerc* 32:1307-13
143. Larson-Meyer DE, Newcomer BR, Hunter GR (2002) Influence of endurance running and recovery diet on intramyocellular lipid content in women: a ¹H NMR study. *Am J Physiol Endocrinol Metab* 282:E95-E106

144. Ruan XY, Gallagher D, Harris T, Albu J, Heymsfield S, Kuznia P, Heshka S (2007) Estimating whole body intermuscular adipose tissue from single cross-sectional magnetic resonance images. *J Appl Physiol* 102:748-54
145. Hasson CJ, Caldwell GE (2012) Effects of age on mechanical properties of dorsiflexor and plantarflexor muscles. *Ann Biomed Eng* 40:1088-101
146. Alizai H, Nardo L, Karampinos DC, Joseph GB, Yap SP, Baum T, Krug R, Majumdar S, Link TM (2012) Comparison of clinical semi-quantitative assessment of muscle fat infiltration with quantitative assessment using chemical shift-based water/fat separation in MR studies of the calf of post-menopausal women. *Eur Radiol* 22:1592-600
147. Fuller NJ, Hardingham CR, Graves M, Screatton N, Dixon AK, Ward LC, Elia M (1999) Assessment of limb muscle and adipose tissue by dual-energy X-ray absorptiometry using magnetic resonance imaging for comparison. *Int J Obes Relat Metab Disord* 23:1295-302
148. Holmback AM, Askaner K, Holtas S, Downham D, Lexell J (2002) Assessment of contractile and noncontractile components in human skeletal muscle by magnetic resonance imaging. *Muscle Nerve* 25:251-8
149. Holmback AM, Porter MM, Downham D, Andersen JL, Lexell J (2003) Structure and function of the ankle dorsiflexor muscles in young and moderately active men and women. *J Appl Physiol* 95:2416-24
150. Galban CJ, Maderwald S, Uffmann K, Ladd ME (2005) A diffusion tensor imaging analysis of gender differences in water diffusivity within human skeletal muscle. *NMR Biomed* 18:489-98
151. Trappe TA, Burd NA, Louis ES, Lee GA, Trappe SW (2007) Influence of concurrent exercise or nutrition countermeasures on thigh and calf muscle size and function during 60 days of bed rest in women. *Acta Physiol* 191:147-59
152. Grosset JF, Onambele-Pearson G (2008) Effect of foot and ankle immobilization on leg and thigh muscles' volume and morphology: a case study using magnetic resonance imaging. *Anat Rec* 291:1673-83
153. Deux JF, Malzy P, Paragios N, Bassez G, Luciani A, Zerbib P, Roudot-Thoraval F, Vignaud A, Kobeiter H, Rahmouni A (2008) Assessment of calf muscle contraction by diffusion tensor imaging. *Eur Radiol* 18:2303-10
154. Rana P, Varshney A, Devi MM, Kumar P, Khushu S (2008) Non-invasive assessment of oxidative capacity in young Indian men and women: a ³¹P magnetic resonance spectroscopy study. *Indian J Biochem Biophys* 45:263-8

155. Okamoto Y, Mori S, Kujiraoka Y, Nasu K, Hirano Y, Minami M (2012) Diffusion property differences of the lower leg musculature between athletes and non-athletes using 1.5T MRI. *MAGMA* 25:277-84
156. Murtagh KN, Hubert HB (2004) Gender differences in physical disability among an elderly cohort. *Am J Public Health* 94:1406-11
157. International Osteoporosis Foundation (2014) Global Policy Initiatives. <http://www.iofbonehealth.org/global-policy-initiatives> Accessed March 23, 2014
158. Jaglal SB, Hawker G, Cameron C, Canavan J, Beaton D, Bogoch E, Jain R, Papaioannou A, Osteoporosis Research, Monitoring and Evaluation Working Group (2010) The Ontario Osteoporosis Strategy: implementation of a population-based osteoporosis action plan in Canada. *Osteoporos Int* 21:903-8
159. Giangregorio L, Papaioannou A, Cranney A, Zytaruk N, Adachi JD (2006) Fragility fractures and the osteoporosis care gap: an international phenomenon. *Semin Arthritis Rheum* 35:293-305
160. Morvan D, Leroy-Willig A (1995) Simultaneous measurements of diffusion and transverse relaxation in exercising skeletal muscle. *Magn Reson Imaging* 13:943-8
161. Saupe N, White LM, Sussman MS, Kassner A, Tomlinson G, Noseworthy MD (2008) Diffusion tensor magnetic resonance imaging of the human calf: comparison between 1.5 T and 3.0 T-preliminary results. *Invest Radiol* 43:612-8
162. Boesch C, Slotboom J, Hoppeler H, Kreis R (1997) In vivo determination of intramyocellular lipids in human muscle by means of localized ¹H-MR-spectroscopy. *Magn Reson Med* 37:484-93
163. Sanders KM, Scott D, Ebeling PR (2014) Vitamin D deficiency and its role in muscle-bone interactions in the elderly. *Curr Osteoporos Rep* 12:74-81
164. Lee CM, Lopez ME, Weindruch R, Aiken JM (1998) Association of age-related mitochondrial abnormalities with skeletal muscle fiber atrophy. *Free Radic Biol Med* 25:964-72
165. Wanagat J, Cao Z, Pathare P, Aiken JM (2001) Mitochondrial DNA deletion mutations colocalize with segmental electron transport system abnormalities, muscle fiber atrophy, fiber splitting, and oxidative damage in sarcopenia. *FASEB J* 15:322-32

166. Bua E, Johnson J, Herbst A, DeLong B, McKenzie D, Salamat S, Aiken JM (2006) Mitochondrial DNA-deletion mutations accumulate intracellularly to detrimental levels in aged human skeletal muscle fibers. *Am J Hum Genet* 79:469-80

167. Scheel M, Prokscha T, von Roth P, Winkler T, Dietrich R, Bierbaum S, Arampatzis A, Diederichs G (2013) Diffusion tensor imaging of skeletal muscle--correlation of fractional anisotropy to muscle power. *Rofo* 185:857-61

168. Yoshida Y, Marcus RL, Lastayo PC (2012) Intramuscular adipose tissue and central activation in older adults. *Muscle Nerve* 46:813-6

169. Khosla S (2010) Update in male osteoporosis. *J Clin Endocrinol Metab* 95:3-10

APPENDIX A

Scoping review search strategy

Health research databases (PubMed, MEDLINE, CINAHL, Embase, Web of Science) were searched for peer-reviewed articles and conference proceedings published in the English language. No date limits were applied, but all pertinent articles published on or before August 2, 2013 were considered for inclusion.

Keywords used in various combinations included: women, female, magnetic resonance imaging, MRI, muscle, skeletal muscle, leg, lower leg, calf, dorsiflexor, plantarflexor. Animal studies were excluded. The reference lists of all pertinent articles were hand searched for articles that may have been missed in the electronic database search.

Study selection

Titles and abstracts of all articles in the database search were screened for inclusion. The focus of the investigation was identifying articles that measured leg muscle in women using MRI. Potentially relevant articles underwent full-text review. We excluded articles that examined the thigh and calf as a single leg unit. All study designs were included. Full text review confirmed key criteria for inclusion: leg skeletal muscle structure was measured with any MRI device. Participant descriptions were evaluated during full-text review to ensure that the mean age of the women in the sample was ≥ 18 years. Our primary interest was articles that reported MRI-based leg muscle structure outcomes for women separately. However, we also conducted a full-text review of articles that did not report data for women separately, but fulfilled all other criteria. This literature was thought to also contribute to refining future research inquiry.

Given the broad population criteria and the overarching goal of the literature synthesis, we excluded studies that investigated women with spinal cord injury, stroke, muscular dystrophies, and congenital muscle diseases.

APPENDIX B

Initial REB approval, October 2012



RESEARCH ETHICS BOARD



50 CHARLTON AVENUE EAST, HAMILTON, ONTARIO, CANADA L8N 4A6

Tel. (905) 522-4941 ext. 33537 Fax: (905) 521-6092

October 25, 2012

Research Ethics Board Membership

Raelene Rathbone, MB, BS, MD,
PhD, Chairperson
Peter Bielings, PhD, CPsych. –
Psychology, Vice Chair
Christine Wallace, BScPhm,
Pharmacy
Susan Goodman, BA, MA
Community
Lehana Thabane, BSc, MSc, PhD
Biostatistics
Andrew Spurgeon, BA, MA, LLB
Legal, Community
Deborah Cook, MD, FRCPC
Internal Medicine/Critical
Care
Marnie Fletcher, BA, Privacy
Margherita Cadeddu, MD, FRCSC,
General Surgery
Margaret McKinnon, BA, MA, PhD
Neuropsychology, Ethics
Mary-Lou Martin, RN, BScN,
MScN, MEd - Clinical Nurse
Specialist
Eleanor Pullenayegum, BA, PhD
Biostatistics
Helen Ramsdale, MA, BM BCh,
MRCP, FRCPC Respiriology
Debbie Macnamara, BA,
Community
Alexander Coret, MD, Diagnostic
Imaging
Giles Scofield, JD, MA Ethicist
Catherine Clase, MB BChir, MSc,
FRCPC Nephrology
Michael Kiang, MD, PhD, FRCPC
Psychiatry
David Higgins, MB, BCh, MRCPI,
FRCPC President (Ex officio)

The St. Joseph's REB operates in compliance with the Tri-Council Policy Statement: Ethical Conduct for Research Involving Humans; the Health Canada / ICH Good Clinical Practice: Consolidated Guidelines (E6); the Health Ethics Guide (CHAC); and the applicable laws and regulations of Ontario. The membership of this REB also complies with the membership requirements for REBs as defined in Canada's Food and Drug Regulations (Division 5: Drugs for Clinical Trials Involving Human Subjects).

Dr. Jonathan (Rick) Adachi
Charlton Medical Centre
Room 501
25 Charlton Ave. E.
Hamilton, ON

RE: R.P.#12-3760

Study Title: Comparing non-invasive measures of lower leg skeletal muscle structure and function in postmenopausal women with and without osteoporosis

Local Principal Investigator: Dr. Jonathan (Rick) Adachi

Received date: 24 September, 2012

Review type: Expedited

Initial Approval: 11 October, 2012

Final Approval: 25 October, 2012

All Received Enclosures:

Application Form - General Research Application
Consent Form (Main) - Participant Information/Consent Form ver: 2 22
October, 2012
Data Collection Sheet - Participant Data Collection Form ver: 1 12
September, 2012
Other - CITI GCP Certificate for Jonathan Adachi dated 12/20/11
Other - Scientific Review Committee approval dated 12 September 2012
Participant Letter - Participant Invitation Letter ver: 12 September, 2012
PI Letter - Letter dated October 22, 2012 responding to conditions
Protocol - Study Protocol ver: 2 22 October, 2012
Questionnaire - MRI Patient Safety Screen Questionnaire ver: 1 12
September, 2012
Questionnaire - Self-Report Physical Activity Questionnaire ver: 1 12
September, 2012
Recruitment Poster - Recruitment Advertisement Poster ver: 1 12
September, 2012
Telephone Script - Participant Recruitment Telephone Script ver: 2 22
October, 2012

Approved Enclosures:

Consent Form (Main) - Participant Information/Consent Form ver: 2 22
October, 2012
Data Collection Sheet - Participant Data Collection Form ver: 1 12
September, 2012
Participant Letter - Participant Invitation Letter ver: 12 September, 2012
Protocol - Study Protocol ver: 2 22 October, 2012

Dr. J.D. Adachi
RE: R.P. #12-3760

Page 2

October 25, 2012

Questionnaire - MRI Patient Safety Screen Questionnaire ver: 1 12 September, 2012
Questionnaire - Self-Report Physical Activity Questionnaire ver: 1 12 September, 2012
Recruitment Poster - Recruitment Advertisement Poster ver: 1 12 September, 2012
Telephone Script - Participant Recruitment Telephone Script ver: 2 22 October, 2012

Acknowledged Enclosures:

Application Form - General Research Application
Other - CITI GCP Certificate for Jonathan Adachi dated 12/20/11
Other - Scientific Review Committee approval dated 12 September 2012
PI Letter - Letter dated October 22, 2012 responding to conditions

Dear Dr. Adachi:

Please be advised that a member of the Research Ethics Board's Subcommittee reviewed R.P. #12-3760 on 11 October, 2012 and approved it with some conditions. Those conditions have now been met. You have final approval to commence your research.

This approval will be for a period of 12 months **ending 25 October, 2013.** We will request a progress report at that time.

If your project is terminated, it is your responsibility to notify the REB. Any changes or amendments to the protocol or consent form must be approved by the Research Ethics Board prior to implementation.

Please ensure that all study personnel are familiar with the REB requirements on the appended page.

Please reference R.P. #12-3760 in any future correspondence. Please note that all study related correspondence must be signed by the local principal investigator.

We wish you well in the completion of this research.

Sincerely yours,



Raelene Rathbone, MB, BS, MD, PhD
Chairperson, Research Ethics Board
RR:imm

cc: M. Fletcher –
Append.

REB Amendment approval, November 2012



RESEARCH ETHICS BOARD



50 CHARLTON AVENUE EAST, HAMILTON, ONTARIO, CANADA L8N 4A6

Tel. (905) 522-4941 ext. 33537 Fax: (905) 521-6092

December 05, 2012

**Research Ethics Board
Membership**

Raelene Rathbone, MB, BS, MD, PhD,
Chairperson
Peter Bieling, BSc, MA, PhD
Psychology, Vice Chair
Steve Abdool, MA, PhD
Ethicist
Margherita Cadeddu, MD, FRCSC,
General Surgery
Catherine Clase, MB BChir, MSc,
FRCPC Nephrology
Alexander Coret, MD, Diagnostic
Imaging
Deborah Cook, MD, FRCPC Internal
Medicine/Critical Care
Susan Goodman, BA, M A Community
Mark Inman, MSc, MD, PhD,
Medicine/ Respirology
Emma Kapetanovic, JD, Research
Officer/Legal
Michael Kiang, MD, PhD, FRCPC
Psychiatry
Debbie Macnamara, BA, Community
Mary-Lou Martin, RN, BScN, MScN,
MEd - Clinical Nurse Specialist
Margaret McKinnon, BA, MA, PhD
Neuropsychology, Ethics
Eleanor Pullenayegum, BA, PhD
Biostatistics
Helen Ramsdale, MA, BM BCh,
FRCPC Respirology
Andrew Spurgeon, BA, MA, LLB
Legal, Community
Lehana Thabane, BSc, MSc, PhD
Biostatistics
Christine Wallace, BscPhm, Pharmacy
David Higgins, MB, BCh, MRCPI,
FRCPC President (Ex officio)

The St. Joseph's REB operates in compliance with the Tri-Council Policy Statement: Ethical Conduct for Research Involving Humans; the Health Canada / ICH Good Clinical Practice: Consolidated Guidelines (E6); the Health Ethics Guide (CHAC); and the applicable laws and regulations of Ontario. The membership of this REB also complies with the membership requirements for REBs as defined in Canada's Food and Drug Regulations (Division 5: Drugs for Clinical Trials Involving Humans Subjects).

Dr. Jonathan (Rick) Adachi
Charlton Medical Centre
Room 501
25 Charlton Ave. E.

R.P. #12-3760: Comparing non-invasive measures of lower leg skeletal muscle structure and function in postmenopausal women with and without osteoporosis

Local Principal Investigator: Dr. Jonathan (Rick) Adachi
Amendment Request received: 29 November, 2012

Document acknowledged:

PI Letter - Letter dated November 29, 2012 clarifying amendment

Documents approved:

Protocol Amendment - Protocol Ver: 3 28 November, 2012
Consent Form Amendment - Participant Information/Consent Form
Ver: 3 28 November, 2012
Telephone Script - Participant Recruitment Telephone Script
Ver: 3 28 November, 2012
Recruitment Ad - Recruitment Advertisement Ver: 2 28 November, 2012

Dear Dr. Adachi:

A member of the Research Ethics Board Subcommittee has reviewed the Amendment Request for R.P. #12-3760 and approved it as submitted. You have approval of the amendment.

Please reference R.P. #12-3760 in any future correspondence.

Sincerely yours,

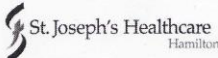
Raelene Rathbone, MB, BS, MD, PhD
Chairperson, Research Ethics Board

RR:ah

Enclosures



REB Amendment approval, April 2013

 Hamilton Health Sciences	 McMaster University <small>Inspiring Innovation and Discovery</small>	 St. Joseph's Healthcare Hamilton
---	---	--

**Hamilton Integrated Research Ethics Board
AMENDMENT REQUEST**

REB Project #: 12-3760

Principal Investigator: Dr. Jonathan (Rick) Adachi

Project Title: Comparing non-invasive measures of lower leg skeletal muscle structure and function in postmenopausal women with and without osteoporosis

Document(s) Amended with version # and date:

- Other - PI's Letter Regarding Description of Changes Dated: 22 April, 2013
- Other - Explanation of Changes Made to Study Dated: 20 April, 2013
- Administrative Change - Added Site : Hamilton Health Sciences
- Protocol - Study Protocol Ver: 4 Dated: 20 April, 2013
- Consent Form - Participant Information and Consent Form Ver: 4 Dated: 20 April, 2013
- Recruitment Poster - Study Recruitment Poster
- Telephone Script - Participant Recruitment Telephone Script Ver: 4 Dated: 20 April, 2013
- Data Collection Sheet - Participant Data Collection Form Ver: 2 Dated: 20 April, 2013
- Other - Human Activity Profile Ver: 1 Dated: 20 April, 2013
- Other - Summary of Study Measurements Ver: 1 Dated: 20 April, 2013

Research Ethics Board Review
(this box to be completed by HIREB Chair only)

Amendment approved as submitted

Amendment approved conditional on changes noted in "Conditions" section below

New enrolment suspended

Study suspended pending further review

Level of Review:

Full Research Ethics Board

Research Ethics Board Executive

Conditions:

REB #: 12-3760

The Hamilton Integrated Research Ethics Board operates in compliance with and is constituted in accordance with the requirements of: The Tri-Council Policy Statement on Ethical Conduct of Research Involving Humans; The International Conference on Harmonization of Good Clinical Practices; Part C Division 5 of the Food and Drug Regulations of Health Canada, and the provisions of the Ontario Personal Health Information Protection Act 2004 and its applicable Regulations; For studies conducted at St. Joseph's Hospital, HIREB complies with the health ethics guide of the Catholic Alliance of Canada

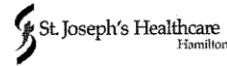

Suzette Salama PhD., Chair
Raelene Rathbone, MB BS, MD, PhD, Chair

26/04/13
Date

All Correspondence should be addressed to the HIREB Chair(s) and forwarded to:
HIREB Coordinator
293 Wellington St. N, Suite 102, Hamilton ON L8L 8E7
Tel. 905-521-2100 Ext. 42013 Fax: 905-577-8378

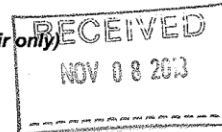
REB #: 12-3760

REB Renewal approval, November 2013



**Hamilton Integrated Research Ethics Board
RENEWAL FORM**

Review of an Active Study (to be completed by HIREB Chair only)



REB Project #: 12-3760

Principal Investigator: Dr. Jonathan (Rick) Adachi

Project Title: Comparing non-invasive measures of lower leg skeletal muscle structure and function in postmenopausal women with and without osteoporosis

Approved for Continuation

Approved conditional on changes noted in "Conditions" section below

Type of Approval:

Full Research Ethics Board

Research Ethics Board Executive

REB Approval Period: Approval period covers October 25-2013 to October 25-2014

New Enrolment Suspended

Suspended pending further review

Conditions:

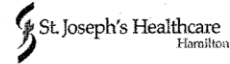
The Hamilton Integrated Research Ethics Board operates in compliance with and is constituted in accordance with the requirements of: The Tri-Council Policy Statement on Ethical Conduct of Research Involving Humans; The International Conference on Harmonization of Good Clinical Practices; Part C Division 5 of the Food and Drug Regulations of Health Canada, and the provisions of the Ontario Personal Health Information Protection Act 2004 and its applicable Regulations; for studies conducted at St. Joseph's Hospital, HIREB complies with the health ethics guide of the Catholic Alliance of Canada.

Suzette Salama PhD., Chair
Raelene Rathbone, MB BS, MD, PhD, Chair

11/6/2013
Date of REB Meeting

All Correspondence should be addressed to the HIREB Chair(s) and forwarded to:
HIREB Coordinator
293 Wellington St. N, Suite 102, Hamilton ON L8L 8E7
Tel. 905-521-2100 Ext. 42013 Fax: 905-577-8378

REB Amendment approval, March 2014



Hamilton Integrated Research Ethics Board AMENDMENT REQUEST

REB Project #: 12-3760

Principal Investigator: Dr. Jonathan (Rick) Adachi

Project Title: Comparing non-invasive measures of lower leg skeletal muscle structure and function in postmenopausal women with and without osteoporosis

Document(s) Amended with version # and date:

- Protocol Amendment - Study Protocol Ver: 6 Dated: 03 March, 2014
- Consent Form Amendment - Participant Information and Consent Form Ver: 6 Dated: 03 March, 2014
- Recruitment Material Other - Appendix M - Email to recruit young adult women Ver: 1 Dated: 03 March, 2014
- PI Letter - Letter dated March 3, 2014 re Summary of changes & including Explanation of changes

Research Ethics Board Review
(this box to be completed by HIREB Chair only)

Amendment approved as submitted

Amendment approved conditional on changes noted in "Conditions" section below

New enrolment suspended

Study suspended pending further review

Level of Review:

- Full Research Ethics Board
 Research Ethics Board Executive

The Hamilton Integrated Research Ethics Board operates in compliance with and is constituted in accordance with the requirements of: The Tri-Council Policy Statement on Ethical Conduct of Research Involving Humans; The International Conference on Harmonization of Good Clinical Practices; Part C Division 5 of the Food and Drug Regulations of Health Canada, and the provisions of the Ontario Personal Health Information Protection Act 2004 and its applicable Regulations; For studies conducted at St. Joseph's Hospital, HIREB complies with the health ethics guide of the Catholic Alliance of Canada.

Suzette Salama PhD., Chair
Raelene Rathbone, MB BS, MD, PhD, Chair

18 March, 2014
Date of REB Meeting

All Correspondence should be addressed to the HIREB Chair(s) and forwarded to:
HIREB Coordinator
293 Wellington St. N, Suite 102, Hamilton ON L8L 8E7
Tel. 905-521-2100 Ext. 42013 Fax: 905-577-8378

APPENDIX C

Table Appendix C1. Correlations between measures of leg muscle and fat macrostructure with bone structure and strength adjusted for tibia length in postmenopausal women with and without osteoporosis (n = 35)

		Muscle CSA	Muscle Density	Muscle volume			Intramuscular fat			Intermuscular fat
				TibA	SOL	GC	TibA	SOL	GC	
4%	Total density	-0.05	-0.29	-0.15	-0.10	-0.01	0.01	0.36	0.26	0.17
	Total area	0.63	0.21	0.65	0.51	0.53	-0.22	-0.19	-0.26	0.21
	Total content	0.62	-0.08	0.56	0.46	0.56	-0.21	-0.14	-0.01	0.44
	Trabecular density	-0.26	-0.17	-0.30	-0.23	-0.13	0.01	0.28	0.20	0.01
	Trabecular area	0.42	0.22	0.65	0.50	0.53	-0.22	-0.18	-0.25	0.20
	Trabecular content	0.73	-0.02	0.36	0.34	0.45	-0.18	0.07	-0.05	0.28
	Bone strength index	0.07	-0.32	-0.02	-0.02	0.12	0.02	0.39	0.24	0.19
14%	Cortical density	-0.06	-0.12	-0.05	-0.17	-0.22	0.01	0.28	0.23	0.20
	Cortical area	0.73	-0.08	0.73	0.54	0.51	-0.25	0.10	0.02	0.46
	Cortical content	0.63	-0.10	0.63	0.43	0.38	-0.22	0.18	0.09	0.47
38%	Cortical density	-0.05	-0.06	0.02	-0.08	-0.07	0.07	0.15	0.10	-0.05
	Cortical area	0.73	-0.02	0.70	0.55	0.54	-0.26	0.06	-0.03	0.46
	Cortical content	0.70	-0.02	0.69	0.53	0.52	-0.24	0.07	-0.02	0.44
66%	Cortical density	0.09	0.04	0.16	0.12	0.02	0.01	0.15	0.12	-0.11
	Cortical area	0.65	0.04	0.60	0.52	0.49	-0.24	0.03	-0.04	0.36
	Cortical content	0.63	0.05	0.58	0.51	0.46	-0.23	0.05	-0.02	0.31
	Strength strain index	0.59	-0.18	0.56	0.43	0.47	-0.15	0.18	0.04	0.20

CSA = cross sectional area; TibA = tibialis anterior, SOL = soleus; GC = gastrocnemius (both heads)

Table Appendix C2. Correlations between muscle and fat microstructure and bone structure and strength adjusted for tibia length in postmenopausal women with and without osteoporosis (n = 35)

		ADC					FA					IMCL*
		TibA	TibP	SOL	MG	LG	TibA	TibP	SOL	MG	LG	
4%	Total density	-0.30	-0.51	-0.08	-0.03	0.05	-0.08	-0.12	0.24	0.03	-0.17	-0.39
	Total area	0.44	0.33	0.40	0.42	0.16	0.08	0.05	0.05	0.13	0.17	0.04
	Total content	0.19	-0.10	0.41	0.45	0.25	-0.03	-0.08	0.30	0.17	0.02	-0.31
	Trabecular density	-0.22	-0.43	0	0.05	0.15	-0.11	-0.09	0.16	0.04	-0.30	-0.25
	Trabecular area	0.44	0.33	0.40	0.43	0.16	0.09	0.05	0.04	0.13	0.17	0.03
	Trabecular content	0.23	-0.10	0.50	0.53	0.36	-0.11	0.08	0.27	0.19	-0.16	-0.22
	Bone strength index	-0.19	-0.41	0.08	0.07	0.07	-0.16	0.03	0.21	0.11	-0.16	-0.50
14%	Cortical density	-0.01	-0.22	-0.07	0.02	0	-0.03	-0.08	0.26	0.21	0.29	-0.27
	Cortical area	0.25	-0.06	0.32	0.46	0.27	0.05	-0.03	0.13	-0.06	0.11	-0.14
	Cortical content	0.23	-0.10	0.28	0.42	0.25	0.04	0.06	0.18	0.01	0.16	-0.17
38%	Cortical density	0.10	-0.28	0.10	0.13	0.11	-0.22	-0.03	0.19	0.15	0.14	-0.23
	Cortical area	0.32	-0.02	0.40	0.54	0.31	0.06	0.00	0.20	0.06	0.10	-0.15
	Cortical content	0.33	-0.05	0.41	0.55	0.32	0.02	0.00	0.22	0.07	0.10	-0.18
66%	Cortical density	0.09	-0.21	-0.03	-0.04	-0.15	-0.20	0.06	0.33	0.28	0.30	-0.23
	Cortical area	0.28	-0.06	0.40	0.48	0.23	-0.22	0.00	0.29	0.15	0.10	-0.14
	Cortical content	0.28	-0.08	0.37	0.44	0.19	-0.05	0.01	0.32	0.18	0.14	-0.16
	Strength strain index	0.35	0.06	0.56	0.50	0.19	-0.27	-0.13	0.14	0.15	0.05	-0.38

* n = 29

ADC = apparent diffusion coefficient; FA = fractional anisotropy; TibA = tibialis anterior; TibP = tibialis posterior; MG = medial gastrocnemius; LG = lateral gastrocnemius; IMCL = intramyocellular lipid

Table Appendix C3. Correlations between muscle and fat macrostructure and microstructure and measures of physical performance and self-reported physical activity levels in postmenopausal women with and without osteoporosis (n = 35)

		Gait Speed	30-CST	RAPA score	HAP AAS score
Muscle CSA	Total	0.27	-0.05	-0.15	0.26
Muscle Density	Total	0.50	0.13	0.35	0.32
Muscle Volume	TibA	0.28	-0.14	-0.11	0.24
	SOL	0.15	-0.14	-0.19	0.12
	GC	0.31	0.04	0.03	0.23
Intermuscular fat	Total	-0.29	-0.24	-0.31	-0.21
Intramuscular fat (%)	TibA	-0.43	-0.22	-0.35	-0.21
	SOL	-0.27	-0.14	-0.16	-0.18
	GC	-0.41	-0.18	-0.25	-0.14
Apparent Diffusion Coefficient	TibA	0.16	-0.07	0.21	0.10
	TibP	0.37	0.32	0.14	0.21
	SOL	0.06	-0.08	0.16	-0.13
	MG	0.02	-0.15	0.26	-0.16
	LG	-0.32	-0.34	0.08	-0.25
Fractional Anisotropy	TibA	0.20	0.01	0.03	0.03
	TibP	0.45	0.14	0.10	0
	SOL	0.24	0.08	-0.03	-0.12
	MG	0.38	0.25	0.09	0.13
	LG	0.16	0.16	-0.07	0.15
IMCL	TibA	-0.20	-0.15	-0.25	0.09

RAPA = Rapid Assessment of Physical Activity; HAP = Human Activity Profile; 30-CST = 30 second chair stand test; CSA = cross sectional area; TibA = tibialis anterior, SOL = soleus; GC = gastrocnemius (both heads); TibP = tibialis posterior; MG = medial gastrocnemius; LG = lateral gastrocnemius; IMCL = intramyocellular lipid

APPENDIX D

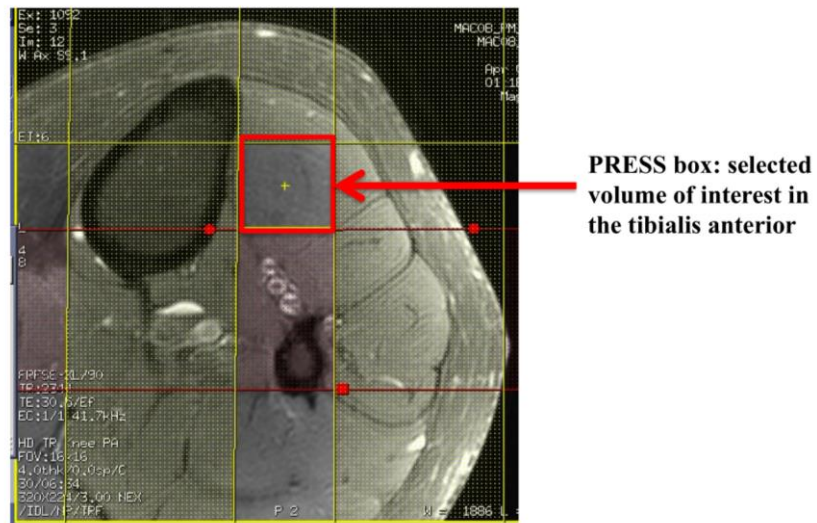
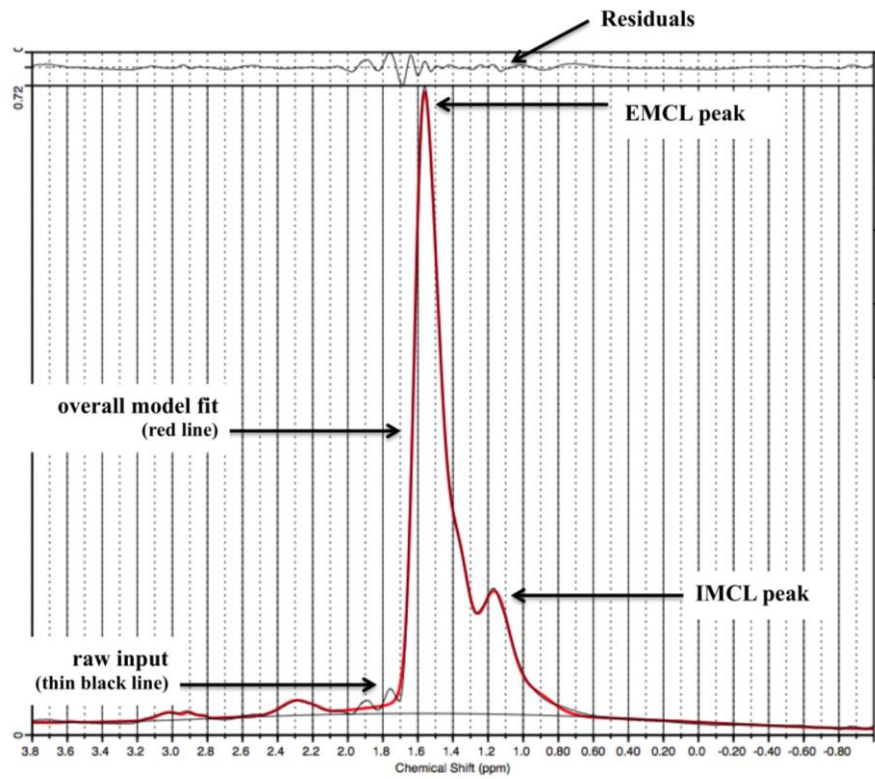


Figure Appendix D1: ^1H -MRS spectra acquisition screen image



LCModel software (v6.2, Stephen Provencher, Oakville, CAN)

Figure Appendix D2: Representative spectra fitting using LCModel software

APPENDIX E

Table Appendix E1: Reliability of Fractional Anisotropy
(3 occasions, n = 16)

	ICC_{2,1}	95% CI
Tibialis Anterior	0.919	(0.826, 0.968)
Tibialis Posterior	0.905	(0.798, 0.963)
Soleus	0.933	(0.854, 0.974)
Medial gastrocnemius	0.871	(0.732, 0.948)
Lateral gastrocnemius	0.966	(0.923, 0.987)

Table Appendix E2: Reliability of muscle cross-sectional area
(3 occasions, n = 16)

	ICC_{2,1}	95% CI
Cross-sectional area	0.992	(0.981, 0.997)
SEM = 1.01cm²		

APPENDIX F

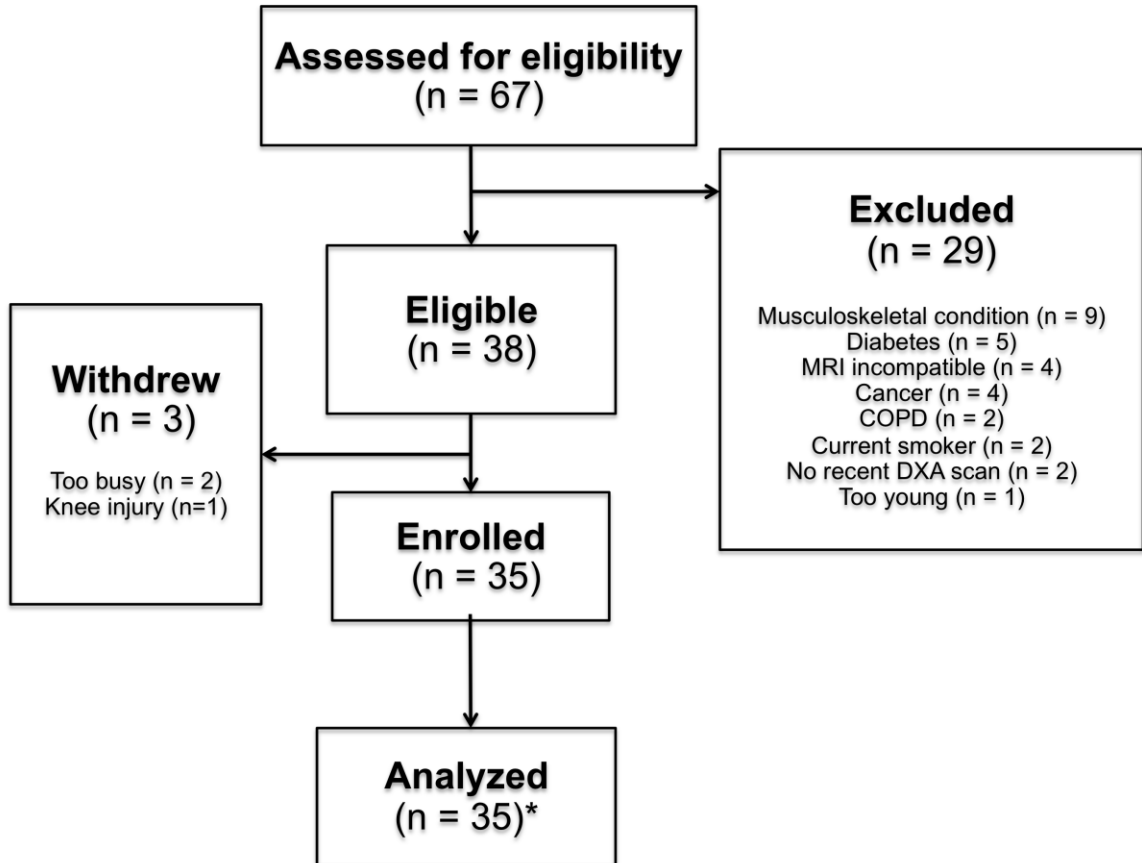


Figure Appendix E1: Flow chart demonstrating the number of individuals screened and enrolled for the study.

MRI = magnetic resonance imaging; COPD = chronic obstructive pulmonary disorder; DXA = dual energy X-ray absorptiometry